THE CONTRIBUTION OF SECONDARY MEDIATORS TO THE ETIOLOGY AND PATHOPHYSIOLOGY OF BRAIN OEDEMA: EXPERIMENTAL STUDIES USING AN INFUSION MODEL

A thesis for the degree of Doctor of Philosophy.
University of Edinburgh

by

Ian Roger Whittle
MD., MB BS., FRACS., FRCSE(SN).

Senior Lecturer and Honorary Consultant Neurosurgeon
Department of Clinical Neurosciences
University of Edinburgh
Scotland

July 1989

CONTENTS

CONTENTS (Cont)

SUMMARY

The neurological condition of patients with brain tumours often improves within 24-36 hours after corticosteroid therapy. This effect was initially attributed to the steroid effects on the peritumoural oedema. Clinical studies utilising ICP monitoring, CT and NMR neuroimaging suggest however that the effects of steroid therapy are independent of major changes in brain oedema. If the oedema has no significant pathophysiological effect how do steroids improve peritumoural brain function? The hypothesis that clinical dysfunction is not dependent on the peritumoural oedema alone but on neuro- or vasomodulating substances released by the tumour is proposed. This proposition is supported by studies which have shown that tumour products and "activated" extravasated plasma proteins possess variable neuro-, vaso- and blood-brain barrier (BBB) modulating properties. The infusion model of brain oedema was used in 40 cats and 80 rats to evaluate the relationships between brain oedema, constituents of the oedema fluid and cortical somatosensory and motor evoked potentials (SEPs and MEPs), cerebral blood flow (CBF), BBB function and both intracranial and cerebral biomechanics. Using this model the effects of focal brain oedema produced by an infusate of saline could be compared to the effects produced by infusion of putative vaso- , neuro-, and BBB modulating compounds (20% protein, bradykinin, arachidonic acid and human glioma cyst fluid) known to be released by human gliomas.

All infusates had minimal adverse effects, at normocapnia, on intracranial and cerebral biomechanics, CBF, SEPs and MEPs despite a focal increase of brain water content by 10% and the classic histological changes of brain oedema.

Except for saline all infusates caused focal BBB opening and are therefore secondary mediators of vasogenic brain oedema. The bradykinin, protein and malignant glioma cyst infusates all caused focal loss of CBF CO_2 reactivity. These results agree with clinical studies that showed no ischemia in peritumoural oedema, loss of CBF CO_2 reactivity around gliomas, and normal SEPs in peritumoural brain. These findings suggest that peritumoural brain dysfunction, in the absence of brain herniation, is independent of brain oedema but may be related to a tumour specific, biochemically mediated loss of flow reserve (CBF CO_2 reactivity). Under conditions of metabolic stress this could lead to focal peritumoural brain ischemia via an inverse steal phenomenon. Steroids could limit impairment of CBF CO_2 reactivity by inhibiting glioma protein release, extravasation of plasma protein through the "leaky" tumour capillaries, and bradykinin activation. Further studies into the etiology of this peritumoural vasoparalysis could lead to adjunctive, alternative and less toxic therapeutic options in the preoperative and chronic management of brain tumour patients.

STATEMENT

I declare that this thesis is my own composition and that it is a record of original work that I performed in the Department of Clinical Neurosciences, Western General Hospital, Edinburgh, Scotland from January 1985 to October 1988.

This thesis contains no material which has been submitted for the award of any other degree or diploma, and to the best of my knowledge contains no material previously published or written by another person except where due reference is made in the text.

The author consents to the thesis being made available for photocopying if accepted for the award of the degree.

ACKNOWLEDGEMENTS

This research was carried out under the supervision of Prof J D Miller MD PhD FRCS FRCP FACS. His foresight, helpful guidance, advice, patience and enthusiasm made possible the successful development of the project, which was supported by a project grant (8500319-NA) from the Medical Research Council (MRC).

I would also like to thank Ian Piper BSc, Alistair Lawson, Janis L Tocher, Thea Gabra-Sanders, Jim Slattery MSc, Tony Bell MD FRCS, and Mark Dearden BSc FFARCS for relevent advice and assistance during the period of laboratory research. Gillian Blundell MD FRCPath kindly performed biochemical analysis on specimens of glioma cyst fluid. Alex Gordon MD prepared brain specimens for light microscopic anlysis and commented on the finer points of neuropathology. The assistance of the librarian of the Royal Colleges of Surgeons of Edinburgh (Ms A M Stevenson) in obtaining access to archival material was also appreciated.

PUBLISHED/PRESENTED WORK

The following articles represent work from this thesis that has been published or has been presented at national or scientific meetings.

1 Whittle I R, Miller J D. Preliminary findings with a cerebral infusion oedema model. Presented at Neurosurgical Satellite Sesssion, Surgical Research Society Meeting, Guildford, January 9, 1987.

2 Whittle I R, Miller J D. Does focal brain oedema cause brain dysfunction? Presented at the 113 th Meeting of the Society of British Neurological Surgeons, Glasgow, Sept 27 , 1988. Abstract in J Neurol Neurosurg Psychiat 70; 928-929, 1989

3 Whittle I R, Miller J D. Do bradykinin and arachidonic acid contribute to the etiology and pathophysiology of brain oedema? Presented at the 115 th Meeting of the Society of British Neurological Surgeons, Newcastle, Sept 1989. Abstract J Neurol Neurosurg Psychiat (In press).

ABBREVIATIONS USED IN THESIS

BBB	Blood brain barrier
CBF	Cerebral blood flow
C_i	Craniospinal compliance
CMR	Cerebral metabolic rate
CPP	Cerebral perfusion pressure
CSF	Cerebrospinal fluid
C_t	Cerebral tissue compliance
CT	Computerized tomography
EM	Electron micrograph
H_2	Hydrogen
H & E	Hematoxylin and eosin
ICP	Intracranial pressure
IVP	Intraventricular pressure
L_p	Hydraulic conductivity of capillary
LT	Leukotriene
MEP	Motor evoked potential
MW	Molecular weight
NMR	Nuclear magnetic resonance
PET	Positron emission tomography
PG	Prostaglandin
PUFA	Polyunsaturated fatty acid
PVI	Pressure volume index
o_s	Osmotic reflection coefficient
R_o	CSF outflow resistance
SEP	Somatosensory evoked potential
SG	Specific gravity
TET	Triethyl tin
TPA	Tissue plasminogen activator

PREFACE

Neuroclinicians are familiar with the improvement in the neurological condition of patients with brain tumours that often occurs following coricosteroid therapy. Deficits in motor, sensory, language or visual function may all resolve within 24-36 hours. This amelioration was initially attributed to the steroid effects on the peritumoural oedema (Galicich et al, 1961), a mode of action that continues to be widely accepted. Clinical studies utilising ICP monitoring, CT and NMR neuroimaging suggest however that the effects of steroid therapy are independent of major changes in brain oedema (Miller et al, 1977; Meinig et al, 1976; Bell et al, 1987). The question therefore arises as to the relationship between peritumoural brain oedema and brain dysfunction. If the oedema has no significant pathophysiological role how do steroids improve peritumoural brain function? The hypothesis that clinical neural dysfunction attributed to peritumoral brain oedema is , in the absence of significant brain herniation, not dependent on the increase in brain water content alone but on vaso- or neuromodulating substances within the oedema fluid is proposed. Support for this proposition comes from clinical and radiological observations in patients with cerebral neoplasms in whom neurological dysfunction is poorly correlated to the peritumoural brain oedema (Penn, 1980) and experimental studies that have shown that oedematogenic tumour products and "activated" extravasated plasma proteins possess variable neuro- and vasomodulating properties (Baethmann et al, 1980; Wahl et al, 1988).

This thesis describes experimental work that evaluates the relationships between brain oedema, constituents of the

oedema fluid and aspects of cerebral electrophysiology, blood flow, blood brain barrier function and both craniospinal and cerebral biomechanics. The experimental models employed in this thesis are elaborations of methods described in cats and rats (Osterholm et al, 1969; Marmarou et al, 1980; Aritake et al, 1983; Chan et al, 1983; Black & Hoff, 1985), of cerebral edema produced by direct intraparenchymal infusion or microinjection. These models, which produce a pseudo-vasogenic brain oedema, are unlike cryogenic, ischemic, toxic and tumor implant brain oedema models, in that they are independent of both a primary cortical or subcortical brain insult and major disturbances in ICP dynamics. Using this model the effects of focal brain oedema produced by an infusate of saline could be compared to the effects produced by infusion of 20% plasma protein, bradykinin, arachidonic acid and human glioma cyst fluid. The effects of oedema alone could therefore be objectively studied and compared to the effects of similar volumes of putative neuromodulating and oedematogenic infusates. It was hoped that the studies would provide insights into the pathophysiology of brain oedema that could be related to mechanisms of steroid action.

1.1 BRAIN OEDEMA

1.1.i Historical aspects to modern concepts

The first descriptions of brain oedema are attributed (Bell, 1983) to Hippocrates, who described brain "swelling" following compound fractures of the skull. Many cases of cerebral softening described as "ramollisement" probably referred to brain oedema (Rostan, 1823). Ramollisement was subdivided into "jaune" and "rouge" variants depending upon the macroscopic appearance of the cut surface of the brain (Bennett, 1843; Solly, 1847). Law (1855) contributed a third variant of cerebral softening "due to serum in the (cerebral) parenchyma" that compressed the lateral ventricles. He termed this "ramollissement blanc" and added that it occurs

"in scrofulous subjects, most commonly females,... ever obscure in its symptoms, and often baffling the best directed efforts of medical skill."

By the mid 19th century there were frequent allusions in Canstatt's Jahrbericht (1856) to brain oedema and swelling, which were then regarded as synonymous (Fishman, 1976). These phenomena were recognized in conditions as diverse as cerebral tuberculoma, syphilitic gumma, cerebral arterial occlusion, catatonia, epilepsy, intracranial infection and intoxications, burns and brain tumours (Law, 1855; Reynolds, 1855; Gowers, 1893; Reichardt, 1905; Bell, 1983). Brain swelling was postulated by Andral (1838) to be due to a disturbance of cerebral blood vessels that led to ".. an exaggeration of serous fluids to the brain". Bucknill & Tuke (1874) also considered cerebral oedema as a condition "...in which the state of the tissue (brain) is permeated by water or serosity". The pivotal role of excess tissue water in brain oedema was however overlooked by most contemporary

anatomists and physicians (Law, 1855; Reynolds, 1855).

Pathological studies showed the oedema to be in the hemispheric white matter, rather than the commissural fibres, basal ganglia or cortical grey matter (Jaburek, 1936). Histological studies confirmed that the cortical architecture was generally normal (Terplan, 1937; Greenfield, 1939) whilst in the white matter there were abnormalities in the oligodendroglia (Bailey & Schaltenbrandt, 1927; Penfield & Cone, 1926), and swelling and dissolution of astrocytic processes - Alzheimers amoeboid glia (Wohlwill, 1914; Spatz, 1929). The characteristic white matter changes were dissolution or rarefaction of the extracellular space, irregular swelling of the myelin sheaths and axon cylinders, expansion of the perivascular space and degenerative changes in the white matter vasculature (Greenfield, 1939; Scheinker, 1941; 1947; Perret & Kernohan, 1943; Feigin & Popoff, 1963). The latter features led several workers to postulate abnormalities of the cerebral capillaries to be fundamental to oedema formation (Alajouanine and Hornet, 1939; Scheinker, 1941). Paradoxically the initial electron microscopic (EM) observations in oedematous brain caused some confusion since they suggested the extracellular space was only 100-200 A and that oedema was due to swelling of the glial cells (Gerschenfeld et al, 1959: Luse and Harris, 1960). These errors were later found to be related to fixation artifacts and to a failure to study the EM features of white matter (Klatzo, 1967; Cervos-Navarro and Ferszt, 1980).

In the 1966 presidential address to the American Association of Neuropathologists, Klatzo (1967) defined brain oedema as an abnormal accumulation of fluid within the brain parenchyma that produces volumetric enlargement. He proposed vasogenic and cytotoxic pathogenic mechanisms to account for the various findings concerning

Brain Oedema Type	BBB	Oedema Fluid Location	Oedema fluid	Model
Vasogenic	Damaged	Extracellular white matter	Plasma exudate	Tumour abscess, focal irradiation, cold injury
Cytotoxic	Usually normal	Intracellular cortex ¯ white myelin sheath	Plasma ultrafiltrate	Ischemia Cyanide TET
Interstitial	Normal	Periventricular white matter	CSF filtrate	Obstructive hydrocephalus (Kaolin)
Hydrostatic	Variable	Extracellular white matter	Water	Hypertension Sudden decompression
Hypo-osmotic	Normal	Intra & Extra cellular	Water	Water intoxication, Hyponatremia

Table 1: Features of the different types of brain oedema (after Klatzo, 1967; Miller, 1979)

the biochemical constituents and localisation of the oedema fluid, cerebral capillary permeability changes and cellular reactions in different models of brain oedema (Table 1). Vasogenic brain oedema was caused by increased BBB permeability, with extravasation of water and plasma protein into the white matter extracellular space. Cytotoxic oedema, in which the BBB is essentially intact, was caused by selected poisons such as triethyl tin (TET) and cyanide. Neurons and glia are swollen because cell membrane dysfunction has led to an influx of water. Vasogenic and cytotoxic mechanisms of brain oedema were later complemented by a third model termed interstitial oedema (Fishman, 1976), which occurred in the periventricular white matter due to transependymal spread of CSF in obstructive hydrocehalus. Miller (1979), in a later review, added hydrostatic and hypoosmotic mechanisms of brain oedema. Hydrostatic oedema usually occurs due to decreased cerebrovascular resistance, with accumulation of an ultrafiltrate of plasma in the extracellular space. Hypoosmotic oedema occurs due to lowering of the plasma osmolality (eg water overload) with accumulation of water in the grey and white matter. These five mechanisms of brain oedema formation (vasogenic, cytotoxic, interstitial, hydrostatic and hypoosmotic) can be invoked either alone or in combination to explain brain oedema occuring in diverse clinical settings.

1.2. PERITUMOURAL BRAIN OEDEMA

1.2.i Neuropathological and radiological studies

Cerebral "softening" and swelling around intracranial neoplasms had been noted since the early days of neuropathology (Gowers, 1893; Wohlwill, 1914). Although some German pathologists (see Scheinker, 1941) considered that this was an unusual phenomenon many others confirmed that peritumoural brain swelling was a common occurrence

(Spatz, 1929; Caspar, 1933; Jaburek, 1936; Scheinker, 1941). Peritumoural softening and swelling varied with tumour type (Gowers, 1893), being greater with malignant gliomas, metastatic carcinomas and meningiomas than well differentiated astrocytomas or oligodendrogliomas (Jaburek, 1936; Greenfield, 1939; Bonkalo, 1939; Perret & Kernohan, 1943). Peritumoural oedema was also noted to be independant of tumour size, extending irregularly around the tumour, and not significantly involving the subarcuate fibres or cortical tissues but often extending to the periventricular regions (Greenfield, 1939; Scheinker, 1947; Burger et al, 1983; Russell & Rubinstein, 1989). The oedema also accounted for the angiographic and ventriculographic findings of a large avascular mass effect in relation to some tumours (Scheinker, 1947).

The recognition that hypodense areas around brain tumours imaged using the CT scan correlated well with areas of peritumoural edema (Lanksch et al, 1976; Torack et al, 1976) provided the first method of imaging brain edema in vivo (Fig 1). The spatial distribution of CT imaged peritumoral edema in the white matter and its prominence around cerebral metastases, malignant gliomas and meningiomas (Ikeda et al, 1984; Bradac et al, 1986; Ito et al, 1986; Shinonaga et al, 1988) was very similar to that described by neuropathologists. Although with low grade astrocytomas CT definition of peritumoural edema is limited by poor imaging of the brain-tumour interface, the oedematous brain-tumour interface with anaplastic astrocytoma and glioblastoma has been shown by serial CT guided stereotactic biopsies to be the region demarcated by contrast enhancement and contiguous hypodensity (Burger et al, 1983; Daumas-Duport et al, 1987). The recent clinical introduction of nuclear magnetic resonance (NMR) imaging has shown that areas of altered T_1 and T_2 signal intensity around brain neoplasms (Fig 1b) correspond spatially and quantitatively with areas of CT imaged

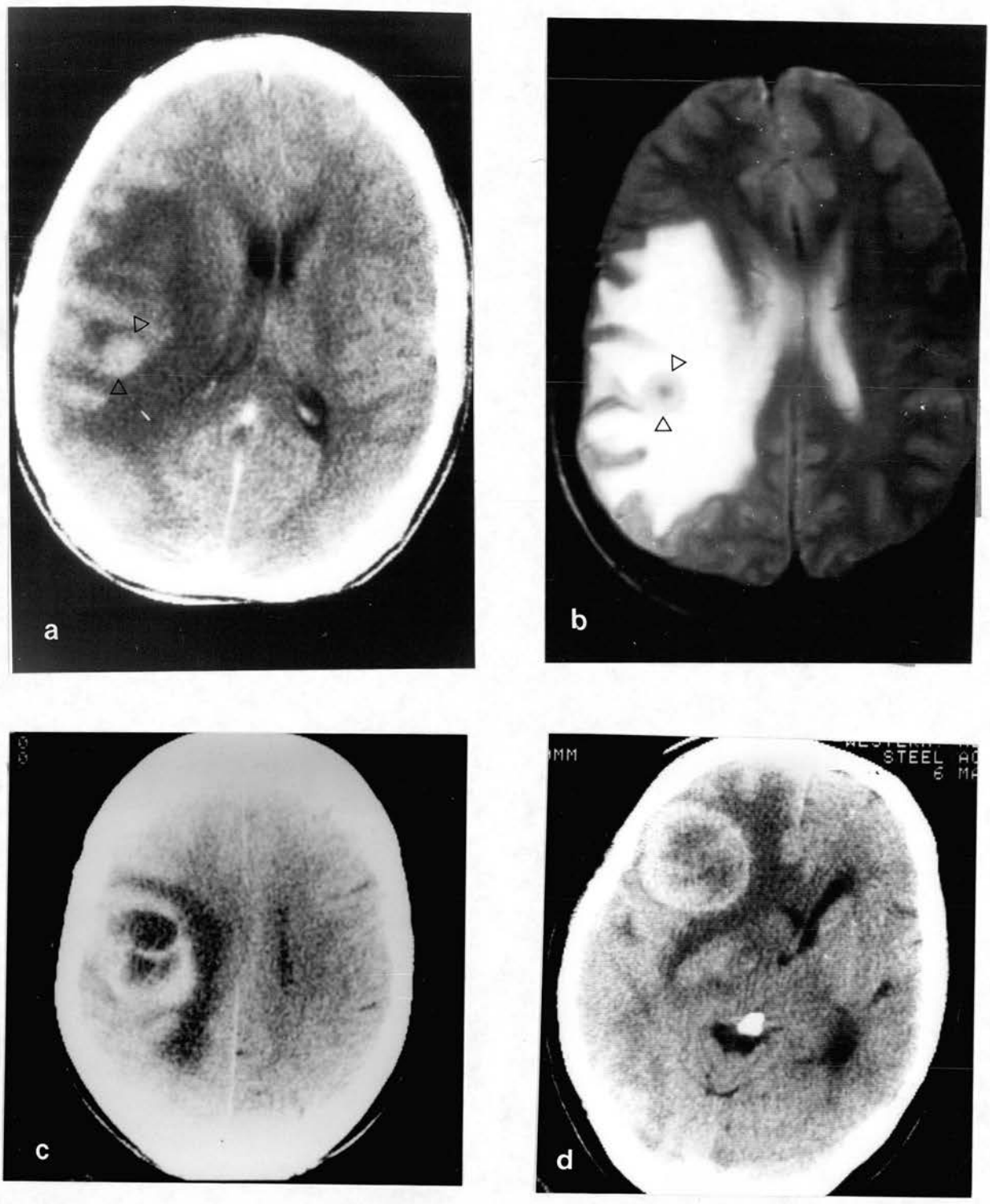

Figure 1: Neuroimaging of peritumoural oedema using CT scanning (A,C,D) and NMR (B). The spatial distribution of CT imaged oedema around a small postrolandic hemangioblastoma (arrows) (A) is very similar to that seen on a T_2 weighted NMR scan (B). Peritumoural oedema is generally maximal around glioblastomas (C) and metastases (D).

peritumoural brain oedema (MacDonald et al, 1986; Bell et al, 1987). These studies confirm experimental results that demonstrated a linear correlation between brain water content and the longitudinal relaxation time T_1 (Go and Edzes, 1975; Naruse et al, 1982). T_2 is also elevated with brain oedema but there is not a straightforward relationship with total tissue water (Kamman et al, 1988).

1.2.ii Quantitation of water content

Using a technique of drying wet tissue specimens to constant weight, Stewart-Wallace (1939) showed that oedematous deep white matter contained an average 11 g/100 g tissue more water than contralateral control samples, whilst there was only a minimal increase in peritumoural cortical water content. Subsequent studies in humans and animals have confirmed that the increase in peritumoural white matter water content are consistently in the 10-12 % range (Table 2). Although some of these studies were performed on autopsy or formalin fixed brains, there is excellent correlation between results obtained from fresh and fixed cerebral tissue (Adachi & Feigin, 1966; Torack et al, 1976).

The CT number, in Hounsfield Units, is linearly related to tissue water content, but also influenced, non-linearly, by the tissue content of lipid, protein and electrolytes, particularly those elements with high atomic weight such as calcium and iron (Torack et al, 1976; Lanksch et al, 1976). Therefore changes in tissue components caused by both the neoplasm and the reactive brain oedema will compound interpretation of the CT numbers. Despite these shortcomings estimates of brain water content from CT number in ischemic and peritumoural brain oedema suggest an increased water content ranging from 9-13 % higher in white matter directly adjacent to tumour, to a 2-4 % increase in water content in the subarcuate white matter.

Source	Brain Tissue	Water Content	Comment
Stewart-Wallace 1936	Cortex	84.3 %	
	White (centrum ovale)	70.7 - 69.6 %	Drying for 18 hours at 110°
	(corpus callosum)	75.7 %	
	Oedematous white (centrum ovale)	81.8 %	
Alexander & Looney, 1938	Cortex	82.5 - 86%	5.5 gm blocks dried to constant weight at 105°C
	white	67.2 - 80%	
Feigin & Popoff 1963	White	66 - 74%	Range of pathologies
	Oedematous white	72 - 92%	Drying at 67° x 100 hours
Adachi & Feigin 1966	Arcuate white	77.9 - 79.0 %	Drying for 144 hours at 56°
	Deep white	71.2 - 71.2 %	
	Corpus callosum	73.3 %	
	Cortex	85.3 _ 85.4 %	
Torack et al 1976	White (fresh)	70.8 ± 2.1 %	200 - 300 gm blocks dried at 100° for 72 hours
	White (fixed)	71.0 ± 3.8 %	Fixed tissue had been in 20% formalin for 1/52
	Cortex (fresh)	84.9 %	
	Cortex (fixed)	84.3 %	
	White (control)	70.5 ± 1.4 %	(36.4 ± 0.6 H units)
	Oedematous white	79.7 ± 4.77 %	(25.2 ± 5.8 H units)
Lanksch et al 1976	White	69%	(31 H units)
	Oedematous white	78.8%	(24.2 H units)

Table 2: Studies of the water content of normal and oedematous brain

The cortical and subcortical nuclear tissues were at most increased by 1-2% (Lanksch et al, 1976; Torack et al, 1976; Takagi et al, 1981; Ito et al, 1986). Similar values for peritumoural white matter water content were recorded in studies that correlated NMR T_1 values with brain water content (MacDonald et al, 1986; Bell et al, 1987). Particular T_1 values correlated with white matter water content within an error of $\pm$ 2 %, but correlation between T_1 and cortical water content was less precise.

1.3 THE ETIOLOGY AND DYNAMICS OF PERITUMOURAL BRAIN OEDEMA

1.3.i Principles of vasogenic brain oedema formation

An equation that summarizes the principal factors governing movement of fluid and solute across capillary beds has been derived from Starlings Law , and used to examine factors in vasogenic brain oedema (Fenstermacher & Patlak, 1976; Klatzo et al, 1980).

$$J_v = L_p[(P^{plasma} - P^{tissue}) - o_s(p_s^{plasma} - p_s^{tissue})]$$

where J_v = Net fluid movement into tissue bed
L_p = Hydraulic conductivity of capillary bed
o_s = Oncotic reflection coefficient of solute s
P^{plasma} = Capillary hydrostatic pressure
P^{tissue} = Interstitial tissue pressure
p_s^{plasma} = plasma oncotic pressure of solute s
p_s^{tissue} = tissue oncotic pressure of solute s

This equation states that the net flow across a capillary bed is related to the permeability of that endothelial bed to both water (L_p) and solute (o_s) and the net hydrostatic and oncotic pressures (for each solute s) acting across that capillary bed. When considering the

formation of peritumoural brain oedema factors that increase L_p and p^{plasma} and decrease p^{tissue} or o_s, which for simplicity can be considered as the inverse of capillary permeability for that particular solute, will potentiate oedema production.

1.3.ii The predominant role of neoplastic capillaries in the genesis of peritumoural oedema

Cerebral capillaries normally prevent any bulk movement of water or solute into the brain due to their low L_p and high o_s values. Comparative analysis of the L_p of different capillary beds has shown that mesenteric capillaries are 3000 x, heart capillaries 1000 x and muscle capillaries 100 x more permeable to water than cerebral capillaries (Fenstermacher & Patlak, 1976). For cerebral capillaries the o_s for Na^+ and Cl^+ is almost 1 ie they are almost totally impermeable. Simplistically these biophysical factors together with tight junctions between endothelial cells, the continuous basement membrane and relative lack of pinocytotic vesicles, under normal conditions, provide the basis of the BBB (Houthof, 1987). Few of these properties are possessed by the neoplastic endothelium of intracranial tumours. Vascular endothelial proliferation is a recognised feature of anaplastic gliomas (Russell & Rubenstein, 1989). Although some blood vessels may be reactive rather than neoplastic they have abnormalities of the tight junctions, increased interendothelial fenestrations, variable increases in pinocytotic vesicles, endothelial hyperplasia, and irregularities of both the basement membrane and its glial investiture (Long, 1970; Weller et al, 1977; Coomber et al, 1987; Stewart et al, 1987).

Experimental, clinical, CT and PET studies utilising radioactive tracers, iodinated agents and vital dyes of varying molecular weight and hydrodynamic radius have

revealed that within a particular tumour capillary permeability is highly variable and a blood tumour barrier similar to the BBB does not exist (Hossmann et al, 1980, 1983; Groothuis et al, 1982; Hawkins et al, 1984; see Brooks et al, 1986). Recognition of the "leakiness" of brain tumour capillaries was initially exploited by the use of protein bound radioactive tracers such as I^{125}Human serum albumin in the diagnosis and localization of these lesions. Different tumours demonstrate variable capillary "leakiness" that is a reflection of their level of dedifferentiation and embryological origin. Even within one tumour type there may be regional variability in capillary permeability (Groothuis et al, 1982). The "opening" of neoplastic endothelium to low but not high MW compounds is confirmed by a dissociation between electrolyte (Na+, Cl-) and protein extravasation (Bodsch et al, 1987). The importance of protein MW and hydrodynamic radius, is confirmed by immunohistochemical studies which reveal that the absolute quantity of protein extravasation and content of higher MW proteins (Ig M, transferritin, ceruloplasmin) are maximal in glioblastoma, intermediate in meningioma and metastatic neoplasia and lowest in astrocytoma and other well differentiated gliomas (Szymas & Hossmann, 1984; Seitz & Wechsler, 1987).

Mean levels of serum protein, in peritumoural oedema fluid, vary from 6 to 25% of serum level (Bodsch et al, 1987). Such levels are not considered to have a major impact on the colloid osmotic equilibrium since the oncotic effect of extracellular Na^+ is much more important (Bothe et al, 1984; Bodsch et al, 1987). Peritumoural Na+ content (range 365-624 mEq/kg dry weight) is at least double (147-169 mEq/kg dry weight) that found in normal white matter (Aleu et al, 1966; Hossman et al, 1980; Bodsch et al, 1987). Tissue oncotic pressure will also be increased by solutes and macromolecules released by tumour necrosis, tumour secretion and the activity of

tumour related proteolytic enzymes (eg tissue plasminogen activator (TPA), metalloprotease, hydrolase, acetylbeta-d-glucose-aminidase and beta-glucuronidase) on extracellular protein (McCormick and Wallace 1981; Quindlen and Bucher, 1987; Sawaya & Highsmith, 1988). These compounds may modulate the level of tumour and peritumoural brain tissue water but not principally by an oncotic effect (Bodsch et al, 1987). Clearance of extracellular proteins, some of which are phagocytosed by glia (Klatzo, 1967; Hossmann et al, 1983; Seitz & Wechsler, 1987) is thought to be contribute to clearance of the oedema fluid (Klatzo et al, 1980; Marmarou et al, 1980)

1.3.iii The contribution of BBB dysfunction in the peritumoural region, tumour blood flow and venous outflow obstruction to oedema formation

Ultrastructural studies of peritumoural brain capillaries in humans and animals have revealed a spectrum of findings ranging from the normal to the grossly abnormal. These differences seem related to whether the tumour studied has a distinctive border (eg meningioma, rat C6) or like glioblastoma, infiltrates the brain (Long, 1970; Hossmann et al, 1980; Stewart et al, 1987). Experimental studies of peritumoural capillary permeability in rats, rabbits and cats have generally shown preservation of the BBB (Herzog et al, 1965; Hossmann et al, 1980, 1983; Farrell et al, 1987). Although the implanted tumours used in these studies invariably do not infiltrate the brain they compliment human studies using contrast enhanced CT scans, supported by stereotactic biopsy and post mortem studies, that have demonstrated that extravastion of the contrast agent in malignant gliomas, and metastases, is confined to the neoplastic capillary bed (Burger et al, 1983; Dumas-Duport et al, 1987). Similarly PET studies report extravastion of tracers (^{82}Rb, ^{11}C-methyl-albumin and ^{68}Ga-EDTA) that is limited to the tumour interstitium

(Brooks et al, 1984; Hawkins et al, 1984; Brooks et al, 1986).

Tumour hypervascularity and vascular shunts visualized on angiography correlate poorly with quantification of tumour blood flow using positron emission tomography (PET) and operative surgical findings (Lammertsma et al, 1985: Bradac et al, 1986). PET studies show considerable variations in blood flow (range from 3 to 102, median 24 ml/100 g/min) within gliomas and cerebral metastases (Lammertsma et al, 1985). The mean blood flow in gliomas (35 ml/100 g/ min) is double that of metastases (18 ml/100 g/min), so tumour blood flow would not seem to be directly related to oedema formation (Brooks et al, 1986). Venous outflow obstruction caused by either tumoural invasion or thrombosis of neoplastic veins could raise intracapillary pressure and enhance oedema formation (Casanova, 1984). However analyses of the tumour blood volume in 81 patients demonstrated mean values of 2.5 to 4.0 ml/100 g wet tissue regardless of tumour type and extent of peritumoural oedema (Lammertsma et al, 1985; Bodsch et al, 1987). It would therefore seem that peritumoural oedema, which is produced at between 0.5 and 3.2 ml/hr (Ito et al, 1988), principally arises from the neoplastic endothelium with minimal contribution from peritumoural capillaries. Factors such as tumour blood flow, interstitial venous thrombosis and obstruction of major venous sinuses seem in general to be unimportant (Bonkalo, 1939; Greenfield, 1939; Perret & Kernohan, 1943; Russell & Rubinstein, 1989; Bradac et al, 1986; Quindlen & Bucher, 1987).

1.3.iv Tumour related sustances favouring oedema production and retention

The proposal that intracranial neoplasms secrete eicosanoids, peptides or enzymes that promote peritumoural oedema formation is not new (Greenfield, 1939; Scheinker,

1941) but it has recently been supported by ultrastructural, biochemical and pharmacological findings (Arenander & Vellis, 1980; 1981; Shitara et al, 1983; Phillipon et al, 1984; Black et al, 1986; Cooper et al, 1984; Stewart et al, 1987; Quindlen and Bucher, 1987; Sawaya & Highsmith, 1988). Whether tumour secreted compounds can modulate capillary permeability was speculative until a vascular permeability factor with MW 30-56,000 was isolated from cultured human astroglial cells (Bruce et al, 1987; Criscuolo et al, 1988). Production of this factor could be specifically blocked by addition of dexamethasone to the culture medium. Pretreatment of the test animal with dexamethasone also blocked the protein's permeability enhancing effects on dermal capillaries (Bruce et al, 1987). The level of TPA produced by brain tumours also correlates with the volume of peritumoural brain oedema as quantitated by CT scan (Quindlen and Bucher, 1987; Sawaya & Highsmith, 1988). Corticosteroids are potent inhibitors of TPA production. Tumour secreted polyamines and lipids may also contribute to oedematogenesis since levels of putrescine, spermidine, esterified triglycerides and steryl esters are increased in the more malignant gliomas (Smith et al, 1968; Dempsey et al, 1985; Scalabrino et al, 1985; Yamakazi et al, 1986).

The possible role of such biochemical factors released by tissue destruction, thrombosis, ischemia, immunological and inflammatory reactions, tumour secretion or "activation" of extravasated plasma protein in the pathogenesis of vasogenic brain oedema has been the subject of considerable research (see Baethmann et al, 1980; 1989; Shinonaga et al, 1988; Wahl et al, 1988). These pathological phenomena are characteristic of many gliomas and cerebral metastases (Russell & Rubenstein, 1989), and it has been proposed that a wide range of compounds (see Table 3) may increase capillary or venular

COMPOUND	SOURCE
Kinins	B_2 macroglobulin, Intrinsic brain kininogen
Arachidonic Acid Leukotrienes Prostaglandins	Cell membranes, Macrophage & leucocyte secretion, Tumour secretion, ischaemic cells
Glutamate	Damaged brain
Serotonin	Platelets, Damaged brain
Histamine	Mast cells, Damaged brain
Oxidants (O^-, HO^-) Free radicals	Activated leucocytes, PUFA metabolism, Xanthine oxidase
Proteolyic enzymes	Damaged brain, Leucocytes
C5a, C5adesAarg	Inflammed brain

Table 3: Some postulated secondary mediators of vasogenic brain oedema together with mechanisms and factors in their local production (After Baethmann et al, 1980; Allison, 1987).

permeability or alter capillary hydrostatic pressure through either arteriolar dilatation or venular constriction (Baethmann et al, 1980; Unterberg et al, 1986; Allison, 1987; Wahl et al, 1988). These factors, termed secondary mediators, may be direct acting oedematogens, have synergistic actions with each other or be leucocyte or mast cell dependent (Table 3). At present there is conflicting evidence concerning the role of these, and other, putative secondary mediator compounds in peritumoural oedematogenesis (Black et al, 1986; Ikeda et al, 1987; Unterberg et al, 1987a; 1987b). However if these

factors are important they must modulate neoplastic endothelium locally since peritumoural BBB function is preserved (see Section 1.3.ii).

1.4 PATHOPHYSIOLOGICAL ASPECTS OF PERITUMOURAL BRAIN OEDEMA

1.4.i Biomechanical effects on the brain

Peritumoural oedema aggravates the mass effect caused by an intracranial tumour (Scheinker, 1947; Klatzo, 1967). The oedematous brain may indeed be responsible for most of this mass effect since its volume effect is related to the increased brain water content and the third power of the radius of the oedematous brain (Elliot & Jaspar, 1949). The combined mass effect elevates local tissue pressure and both ICP and craniospinal elastance in an exponential fashion (Miller, 1979). These effects can lead to local impairment of cerebral perfusion pressure (CPP) and brain shifts. Cerebral herniations can cause focal brain tissue destruction and aggravate brain ischemia (Miller, 1979). The timing of these pathophysiological events will depend upon the rate of growth and the location of the tumour and secondary problems such as hydrocephalus and the balance between oedema formation and resolution (Ito et al, 1986, 1988).

As oedema worsens local brain tissue compliance rises and hydraulic resistance falls ie the ease with which water passes through the brain rises (Marmarou et al, 1980; Walstra et al, 1980; Ito et al, 1988; Hatashita and Hoff, 1988). This phenomenon, together with a favourable pressure gradient between peritumoural interstitial and intraventricular pressures, facilitates bulk diffusion of the oedema fluid away from the region of formation, at an estimated speed of 1.9 mm/hr (Ito et al, 1988), and transependymal clearance into the ventricular system

(Klatzo et al, 1980; Reulen et al, 1977; 1980). Peritumoural brain oedema, unlike most clinical and experimental models, is unique since production of oedema fluid will progressively increase and overwhelm normal clearance mechanisms.

1.4.ii Structural and cellular changes in oedematous brain

Peritumoural oedema has a predilection for the white matter of the centrum ovale with relative sparing of the commissural, capsular and subarcuate fibres (Greenfield, 1939; Scheinker, 1941: Perret and Kernohan, 1943; Hossmann et al, 1980; Szymas & Hossman, 1984; Seitz & Wechsler, 1987). The white matter extracellular space becomes sieve like or trabeculated, and often contains lakes of luxol blue-PAS or Masson trichrome positive material that is histologically and immunohistochemically identical to material contained within the congested vascular compartment (Feigin & Popoff, 1963; Szymas & Hossmann, 1984; Seitz & Wechsler, 1987). Histopathological studies, using myelin stains, showed pallor in the peritumoural brain (Perret & Kernohan, 1943; Scheinker, 1947; Burger et al, 1983). This pallor could represent either the dilutional effects of increased tissue water (Greenfield, 1939; Feigin & Popoff, 1963) or peritumoural demyelination. Quantitative studies of lipid content in the peritumoural region have shown either a normal (Hwang et al, 1986) or a 30 % reduction in lipid content (Lanksch et al, 1976), whilst qualitative studies have shown alterations in cerebrosides, cholesterol and esterified cholesterol (Yanagahara & Cummings, 1968). If peritumoural demyelination is found the toxic effects of cerebral irradiation and chemotherapy on peritumoural white matter must also be considered as etiological factors (Burger et al, 1983; Russell & Rubenstein, 1989).

Light microscopic findings in oedematous peritumoural brain reveal changes in glial cytoplasm and nuclei, congestion of blood vessels, widening of the perivascular and extracellular spaces, separation and swelling of myelin sheaths, irregular swelling of axis cylinders, loosening of the ground substance and preservation of cortical architecture (Caspar, 1933; Jaburek, 1936; Greenfield, 1939; Scheinker, 1941). The glial changes were proportional to the severity and duration of the oedema and astrocytic changes were greater than those seen in oligodendrocytes (Perret & Kernohan, 1943; Feigin & Popoff, 1962; Aleu et al, 1966; Szymas & Hossmann, 1984). Immunohistochemical and immunofluorescent studies revealed that many swollen astrocytes contain extravasated plasma protein (Klatzo, 1967; Brett & Weller, 1978; Hossmann et al, 1980; Szymas & Hossmann, 1984). Cortical neurones in lamina III were only damaged if ICP had been severely raised or local ischemia had occurred (Caspar, 1933; Greenfield, 1939).

1.4.iii The biochemical composition of oedema fluid

Peritumoural oedema fluid has Na and Cl ratios and levels (120-150 uEq/ml) similar to plasma (Stewart-Wallace, 1939; Hossman et al, 1980; Bodsch et al, 1987) and contains "lakes" of proteinaceous material histochemically similar to plasma protein (Feigin & Popoff, 1963; Aleu et al, 1966). The concentration of plasma protein in the peritumoural oedema fluid ranges from 4 to 16 mg/ml (Bothe et al, 1984; Bodsch et al, 1987). Qualitative analysis of the extravasated protein using immunofluorescent, biochemical and immunoperoxidase techniques showed that most was albumin (MW 65,000), pre-albumin (MW 61,000) and low MW immunoglobulins (Cummings, 1961; Brett & Weller, 1978; Hossman et al, 1980; Szymas & Hossman, 1984; Seitz & Wechsler, 1987). In addition a plethora of tumour related compounds (see Section 1.3.iv) will be carried by bulk

flow of the oedema fluid into the peritumoural brain.

1.4.iv A dichotomy between structural and biochemical changes and electrophysiological dysfunction

With derangement of the white matter extracellular space, glial morphology and biochemical microenvironment peritumoural axonal, neuronal and glial function would be expected to be abnormal. However although brain impedance is decreased (Go, 1980), cortical somatosensory evoked potential (SEP) waveforms are often preserved despite profound oedema induced by cortical freezing (Sutton et al, 1980), and brain tumours (Penn, 1980). When cortical SEPs ipsilateral to brain tumours have been abnormal the asymmetry is frequently in the components subsequent to the primary cortical response ie the N_{18} (median nerve) or P_{40} (tibial nerve) and it is often difficult to ascertain whether these anomalies arise because of brain destruction, cortical distortion or peritumoural oedema (Shibasaki et al, 1977; Stohr et al, 1981; Ebner et al, 1982; Whittle et al, 1987). Changes in the cortical SEP and direct cortical response have been reported in some models of brain oedema but these invariably have had superadded cortical damage or cerebral ischemia (Sutton et al, 1980; Dempsey et al, 1985; Kataoka et al, 1987; Murota et al, 1988).

Focal increases in the proportion of the slow (delta and theta waveform) components of the EEG are frequently recorded in the montages overlying brain tumours. Peritumoural oedema per se is rarely considered responsible for this polymorphic delta EEG activity (Gastaut et al, 1979; Passerini et al, 1983; Nagata et al, 1985), although others have reported a correlation between slow wave activity and the extent of peritumoural oedema (Steudel et al, 1976; Nagata et al, 1985 cases 4 and 15). Experimental work suggests the EEG changes are the result

of cerebral damage or cortical deafferentation due to tumour destruction, ischemia or secondary brain herniations rather than effects due to the peritumoural oedema (Schaul et al, 1976; Sutton et al, 1980). Experimental studies of implanted tumours in cats have utilised fast Fourier EEG analysis as a more sensitive method of detecting electrophysiological changes but only minor abnormalities were detected in 40% of animals (Hossmann et al, 1980). Although the EEG can be analysed using sophisticated mathematical techniques and microcomputer software the resultant data, whether computerized mapping or power ratio index (Nagata et al, 1985), are only as good as the initial data (Ojemann, 1985). The paucity of electrophysiological changes in the peritumoural region of many tumours correlates well with PET studies that have shown either normal, or only slightly decreased, CMR_{O2} in human peritumoural brain (Lammertsma et al, 1985; Brooks et al, 1986).

1.4.v Peritumoural brain oedema and brain dysfunction

The relationship between brain dysfunction and peritumoural oedema is complex and cannot be simply explained in terms of increased brain water content, cerebral ischemia, demyelination, expansion of the extracellular space, electrophysiological changes, or biomechanical changes in the brain. On many occasions there is no correlation between the extent of cerebral oedema as imaged by CT scan and clinical indications of focal neurological dysfunction (Penn, 1980; see Fig 1). Since the introduction of steroids for the treatment of brain tumours (Galicich et al, 1961) it has been observed that many clinical deficits resolve within 24-48 hours of treatment. The dramatic ameliorative effect of corticosteroid therapy suggests that in some patients a biochemically mediated phenomenon is causing the neural deficit. CT, NMR, ICP and quantitative experimental

studies support the contention that dysfunction is biochemically mediated rather than related to the increased tissue water content. Steroid induced resolution of CT imaged peritumoural oedema is not significant until five days after onset of methylprednisolone therapy although clinical improvement occurred earlier (Lerch and von Wild, 1983; Hatam et al, 1983). Reduction in brain water content, indirectly quantified by T_1 from NMR images, was also negligible within the first four days of therapy (Bell et al, 1987). Reductions in ICP following steroid therapy also lagged behind clinical improvement although steroids did cause some early changes in cerebral elastance (Miller et al, 1977; Miller, 1979). Experimental studies of steroid induced reduction of peritumoural brain water content have also shown that at least 3 days of therapy is necessary to significantly reduce water content (Yamada et al, 1979; Hossmann et al, 1983)

The hypothesis that a tumour secretes or releases factors that are carried by bulk flow into the peritumoural region where they impair axonal, glial or neuronal function is not new (Greenfield, 1939; Hossmann et al, 1980). Studies of tumour lines in vitro have revealed that as well as eicosanoids, polyamines, and TPAs glial and meningeal cells secrete a spectrum of proteins (Arenander and Vellis, 1980; 1981; Shitara et al, 1982). These proteins are not considered to be the products of cell lysis since they can be obtained from cultures with 99% cell viability (Shitara et al, 1982), and subfractionation reveals highly reproducible SDS-gel peaks that do not include membrane labelled proteins (Arenander & Vellis, 1980; 1981). Two dimensional gel electrophoresis studies have provided semi-quantitative data on the MW and isoelectric points of brain proteins and have shown that brain tumours contain proteins not detected in normal brain and that high and low grade gliomas also have characteristic protein profiles (Narayan et al, 1986; Sawaya & Highsmith, 1988).

If tumour specific factors do contribute to peritumoural brain dysfunction then their release or activation should be inhibited by steroids since the time course of clinical amelioration after commencement of therapy is similar to that required for steroid receptors to influence genetic expression and protein production by receptive cells (Arenander & Vellis, 1981). Steroids are known to inhibit a wide spectrum of protein synthesis by tumour cells including TPA and tumour permeability factor (Shitara et al, 1982; Arenander and Vellis, 1980, Bruce et al, 1987; Quindlen and Bucher, 1987; Criscuolo et al, 1988). Steroids also block activation of phospholipase A_2 and thereby limit arachidonic acid release from membrane phospholipids. Since arachidonic acid can modulate membrane potentials and neuronal function by altering GABA binding (Schwarz et al, 1988), inhibiting brain mitochondrial function (Hillered and Chan, 1988), modulating aspartate, GABA and glutamate uptake mechanisms in nerve terminals, neurones and astrocytes (Yu et al, 1986; Dorman et al, 1986), and by inhibiting choline uptake and acetylcholine synthesis and reaccumulation in synaptosomes (Boksa et al, 1988), the potential functional benefits of steroids due to this action alone are extremely wideranging. Steroids may also exert their beneficial effects by rectifying or restoring normal capillary transport mechanisms thereby decreasing oedema production and potential spread of neuromodulating compounds (Hossmann et al, 1983; Ito et al, 1988; Nakagawa et al, 1988). PET studies have shown that they do not have a major effect on either blood flow or metabolism in either the tumour or adjacent brain (Leenders et al, 1985).

1.4.vi Aims of thesis work

The aim of the experiments undertaken in this project was to investigate the relationships between focal brain

oedema and brain dysfunction using a model of brain oedema that avoided a primary (ie oedema producing) brain insult. The experimental design allowed an evaluation of the contribution of postulated "secondary mediators of brain oedema" to both the etiology and pathophysiology of brain oedema. It also enabled the interrelationships between brain oedema, brain biomechanics, CBF and parameters of electrophysiological function to be studied without the compounding problems of either major rises in ICP or cerebral tissue herniation.

The hypotheses to be tested were that brain oedema per se did not cause brain dysfunction and that the reversible brain dysfunction, seen in patients with malignant gliomas shortly after commencement of steroid therapy, is attributable to tumour related vaso- or neuromodulative compounds released into the oedema fluid. The compounds chosen for study (saline, 20% protein solution, bradykinin, glioma cyst fluid and arachidonic acid) enabled the effects of particular compounds in the oedema fluid to be evaluated. The contributions of these compounds to the etiology and pathophysiology of vasogenic brain oedema and brain dysfunction was therefore evaluated. The experimental findings were be related to clinical observations of peritumoural brain oedema and the known effects and actions of steroids.

METHODOLOGY

2.1 Plan of investigation

An intraparenchymal infusion model of brain oedema was designed utilising modifications of feline experimental protocols previously described (Osterholm et al, 1969; Long et al, 1980) and elaborated by Marmarou et al (1980). A similar protocol utilising modifications of previous techniques (Chan et al, 1983; Black & Hoff, 1985) was developed for the rat. This experimental design was essentially an in vivo system that enabled the effects of intraparenchymal infusion of putative mediators of brain oedema and brain dysfunction to be quantified. The infusates studied have all been implicated in the pathogenesis of brain oedema (Baethmann et al, 1980; Fishman & Chan, 1980; Wahl et al, 1988; see section 1.3.iv) but their contribution to oedematous brain dysfunction has not previously been evaluated.

Infusates studied

(1) Sham
(2) Normal saline
(3) Bradykinin 5-150 ug/ml
(4) Arachidonic acid 2-15 mg/ml
(5) 20% protein solution
(6) Human glioma cyst fluid

Selection of Neurophysiological parameters studied

The parameters that were studied before, during and after the intracerebral infusions included:

(1) CBF_g and CBF_w both ipsilateral and contralateral to the side of infusion
(2) Cortical SEPs to median nerve stimulation

(3) ICP as measured by monitoring intraventricular CSF pressure
(4) Cerebral pressure-volume index (PVI), and lumped craniospinal compliance (Ci).
(5) Dynamic CSF outflow resistance (R_o).
(6) Brain tissue hydraulic resistance (R_t) and cerebral tissue compliance (C_t).

Following the completion of the intraparenchymal infusion the following neurophysiological parameters were measured;

(1) Reactivity of the cerebral vasculature to alterations in P_aCO_2
(2) Spinal motor evoked potentials (MEP) following transcranial or focal stimulation of each hemisphere

Following sacrifice of the animal the following parameters were studied;

(1) The specific gravity, and water content, of both cerebral cortical and subcortical (white matter) tissue.
(2) The extent of blood brain barrier disruption caused by the infusion
(3) Histological analysis of the brain adjacent to and distant from the region of infusion

The measurement of these parameters during sham and saline infusions enabled acquisition of baseline data and an assessment of the validity and utility of the rodent and feline models of cerebral infusion oedema. The changes from these baseline values caused by similar volumes of different infusates could then be established. The contribution to both neurophysiological dysfunction (ie

alterations in CBF, SEPs, MEPs, ICP, PVI) and the genesis of cerebral oedema (tissue water contents, disruption of the BBB) of particular compounds could then be evaluated.

These experiments were performed by the author under licence using anaesthetic and surgical techniques approved by the Home Office under the Prevention of Cruelty to Animals Act 1876.

2.2 RODENT INFUSION MODEL

2.2.i General preparation

Male Wistar rats (Wgh 300-450 gm) were anesthetised by intraperitoneal urethane (1.2 g/kg, given as a 20% solution in distilled water). The femoral artery was cannulated with polyethelene tubing and a tracheostomy tube positioned. The animal was then placed in a stereotactic frame (Narashige Instruments, Japan) and the temperature maintained at 37°C by a thermoregulated warming blanket.

The animal was then paralysed (Gallamine 4 mg/kg) and ventilated, with an air/oxygen mixture, on a Harvard 680 Rodent respirator (Harvard Apparatus Co., Inc., South Natick, Massachusetts). Tidal volume was 3.0 $\pm$ 0.5 ml and the respiratory rate adjusted to maintain P_aCO_2 in the range 35 $\pm$ 5 mm Hg. Oxygen inflow to the ventilator was adjusted to maintain the P_aO_2 in the range 150 $\pm$ 50 mm Hg. Continuous arterial BP monitoring was done through the femoral arterial line using a Bentley transducer connected to a Rikadenki chart recorder. Blood gas analysis (P_aO_2, P_aCO_2 and PH) was done using an ILS 1302 system (Instrumentation Laboratory SpA, Milan, Italy).

2.2.ii Intracerebral infusion and brain biomechanics

A midline scalp incision was made, the periosteum diathermied and removed to expose the bregma and coronal suture. A 2 mm burrhole was then drilled 1.2 mm anterior and 3.0 mm lateral to the bregma point. Using a stereotactic manipulator a 25 G round ended needle was then placed at a depth of 3.0 mm. Using these coordinates the tip of the infusion needle would be placed deep to the junction of the caudatoputamen nucleus and the subcortical white matter (Paxinos & Watson, 1982; Fig 2). The frontopolar and precentral cortical areas overlie this infusion locus (Krieg, 1946) and which functionally includes the anterior limit of the primary somatosensory cortex for the forelimb (Hall & Lindholm, 1974). The dura was then covered with fragments of chopped surgicel (Johnson & Johnson, Slough, England) and the burrhole sealed with methylmethacrylate. In all the experiments the burrholes were drilled, and extradural and intracerebral electrodes or needles placed using either surgical loupes (x4 magnification) or the operating microscope.

The infusate, contained in a 1 ml syringe, was connected to the 25 G needle by polyethylene tubing. The rate of infusion was regulated by a Vickers Treonic IP4 infusion pump (Vickers Medical, Priestley Rd, Basingstoke, Hants, England) the barrel of which had been modified to seat a 1 ml syringe. Using this modification a metered infusion rate of 3.4 ml/hr delivered 0.1 ml fluid/hr. The flow rate of the Infusion pump had previously been checked, and was found to be accurate, against resistant pressures ranging from 10-100 mmHg. A Bell and Howell 4/422 transducer was connected in parallel with the infusion line so that infusion pressure (P_{inf}) could be monitored continuously

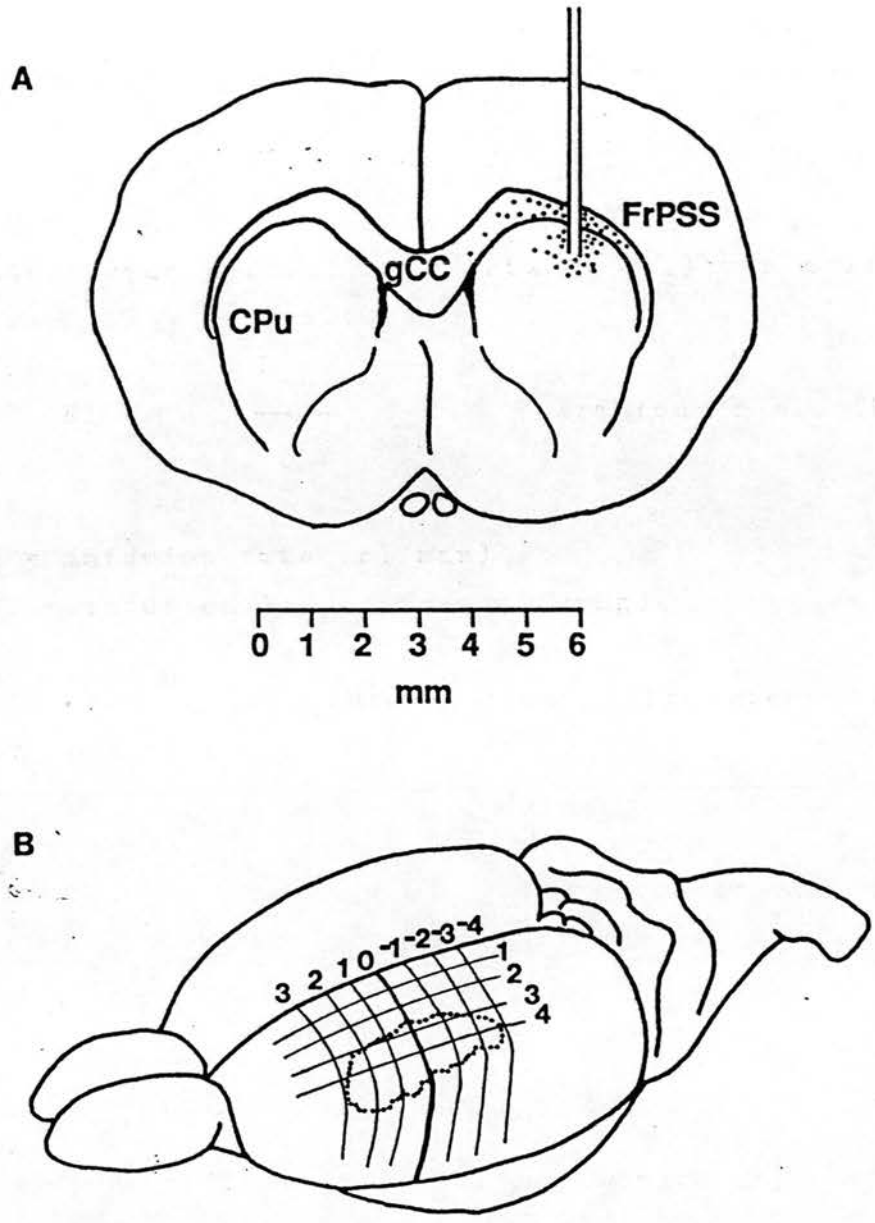

Figure 2:A Coronal section of the rodent brain (+1.2 mm from bregma) outlining the infusion locus and dissipation of the fluid. Abbreviations gCC genu of corpus callosum; FrPSS frontoparietal somatosensory cortex; CPu caudatoputamen nucleus (After Paxinos & Watson, 1982). **Figure 2B** shows a surface view of the rodent brain outlining the forelimb primary somatosensory cortex in relation to topographic stereotaxic coordinates (After Hall & Lindholm, 1974).

on a Rikadenki chart recorder.

The brain tissue hydraulic resistance (R_t) was calculated using the following equation :-

$$R_t = \frac{P_{inf}}{Q} \qquad \text{(Marmarou et al, 1980)}$$

where Q = infusion rate (ml/min)
and P_{inf} = infusion line pressure (mmHg)

The brain tissue compliance (C_t) was calculated using the following equation:-

$$C_t = \frac{V}{P_{inf}} \qquad \text{(Marmarou et al, 1980)}$$

where V = volume of fluid infused
and P_{inf} = infusion pressure

2.2.iii Intraventricular CSF pressure monitoring

A 2 mm burrhole was centred 1.0 mm posterior and 1.5 mm lateral to the bregma point on the calvarium contraleral to the site of placement of the infusion needle. The ventricle was then cannulated with a round ended 25 G needle fixed in a stereotactic manipulator at a depth of 2.6 mm. Placement in the ventricle was confirmed by the recording of respiratory regulated pressure changes and an increase in ICP following manual compression of the abdomen. The burrhole was then lined with chopped surgicel and sealed with methylmethacrylate.

The ICP was recorded in mm Hg via a Bentley transducer onto a Rikadenki chart recorder, with the zero reference point being at the level of the ear bars of the sterotactic frame.

2.2.iv Regional cerebral blood flow (rCBF)

Regional CBF was measured by the hydrogen (H_2) clearance technique (Pasztor et al, 1973). Two 2mm burrholes were drilled bilaterally 4 mm from the midline at the anterior and posterior ends of the parietal bone. The dura was opened under magnified vision using a 23 G needle with a bent tip. Teflon coated 90% platinum/ 10% iridium electrodes (250 micron diameter) with the distal 1 mm bared were then placed 1.5 mm into the cortex using a stereotactic manipulator. The burrholes were then filled with surgicel and sealed with methlymethacrylate. A reference electrode, polarised at -400 mV was positioned in a subcutaneous thoracic pouch.

H_2 was administered at a concentration of 6-10 % by a sidearm to the ventilatory tubing. H_2 clearance curves were obtained by pen recording the current output from the polarised electrode system onto a Rikadenki chart recorder with chart speed set at 2 cm/min. The initial 30 seconds of the clearance curve was discarded, with the CBF being obtained by analysis of the curve over the ensuing two minutes. Five points (30 s apart) from each curve were fed into a computer programme that calculated the CBF in ml/100 gm brain/ min.

After completion of the intracerebral infusion the rodent ventilator tidal volume and rate of respiration were altered so that the arterial CO_2 level was sequentially

increased from 25 mm Hg to 60 mm Hg. H_2 clearance curves were obtained at various values within this range. At least twenty minutes elapsed between recording of CBF, and usually CBF was recorded at four different CO_2 levels for each rat. Reactivity was analysed by plotting CBF against CO_2. Linear regression analysis of CBF and CO_2 data and correlation coeeficients were calculated using the commercial statistics computer programme MINITAB (Ryan et al, 1985).

2.2.v Cortical somatosensory evoked potential (SEP)

Burrholes of 2mm diameter were drilled bilaterally in the midparietal region 3mm behind the bregma and 4 mm lateral to the midline. This location overlies the cortical area postcentralis caudalis which represents the posterior extent of the primaru somatosensory cortex for the forelimb (Krieg, 1946; Hall and Lindholm, 1974; Fig 2.1). The dura was exposed but not opened. The burrhole was then filled with conduction paste (Dracard Electrode Gel, Maidstone, Kent). Platinum alloy ball electrodes were then placed epidurally using a stereotactic manipulator. A reference needle electrode was placed subcutaneously over the nasal ridge, and an earth plate electrode subcutaneously over the thorax. These electrodes were connected to a PA 89 peamplifier, which was in turn connected to a Medelec MS92a signal averaging unit. Stimulating electrodes (Stainless steel 26 G needle electrodes were positioned on the dorsal and volar aspects of both forepaws.

Stimuli of 6 - 10 mA (square wave shocks of 0.1 ms duration) were delivered from a Medelec S10II at 5 Hz across the stimulating electrodes. Epochs of 20 -50 ms

were studied and 128-512 stimuli averaged. The frequency bandpass was set at 20-2000 Hz, with amplifier sensitivity at 20 or 50 uV. All records were duplicated and copied onto an inbuilt chart recorder that documented voltage and timescale. Peak latencies were displayed by cursor readout and documented with each set of recordings.

2.2.vi Brain water and Specific gravimetric (SG)

One hour after the conclusion of the infusion the rat was decapitated, the calvarium removed with bone rongeurs and the dura removed from the underlying brain. The cerebrum was removed by sections at the level of the rhinal sulcus and the mesencephalon (at the plane between the cerebellum and occipital region). Each hemisphere was then weighed, and placed in a drying oven at 80^{o}C until a constant weight was attained (usually 48 hrs). The % tissue water content was calculated from estimation of the wet/dry weighting of the cerebrum;

$$\%\text{water} = \frac{\text{Wet weight - dry weight}}{\text{Wet weight}} \times 100$$

In other rats local brain tissue SG was measured to obtain data on water content in small cortical and subcortical tissue samples. The technique of gravimetry employed (Marmarou et al, 1978,1982) required rapid removal of the cerebrum after termination of the experiment. Cortical and subcortical brain tissue samples measuring 2-4 mm^3 were then obtained and dropped into a layered kerosene/bromobenzene column. The isogravimetric point was the depth in mm to which the tissue particles had sedimented at 2 minutes. The SG was obtained by reference to a linear regression equation derived from the depths to which standard droplets from five samples of potassium

sulphate (5 uL) of varying SG (1.021, 1.025, 1.035, 1.040, 1.045) had sedimented.

2.3 FELINE INFUSION MODEL

2.3.i General preparation

Mongrel cats weighing between 2.9 and 4.5 kg were anaesthetised by intraperitoneal injection of Pentobarbital 45 mg/kg. A tracheostomy was performed and the animal intubated with a noncuffed Size 9 Portex endotracheal tube. The femoral artery and vein were cannulated with polyethelene tubing. The animal was placed in a stereotactic frame (Narashige Instruments, Japan) in the sphinx position. Following paralysis with pancuronium (0.05 mg/Kg) ventilation was commenced with a 66% N_2O; 33% O_2 mixture administered through a Harvard Cat ventilator. Tidal volume was 30 $\pm$ 5 ml and respiratory rate was adjusted to maintain arterial CO_2 in the range 33 $\pm$ 3 mm Hg and P_aO_2 greater than 100 mm Hg. A continuous infusion of lactated Ringers solution was delivered intravenously at a rate of 1 ml/kg/hr. The animal was placed on a thermoregulated (via rectal thermometer) warming blanket so that body temperature was maintained at 37.5°C. Blood pressure and arterial blood gases were measured as described in the Rodent model (See Section 2.2.i).

2.3.ii Intracerebral infusion and brain tissue hydraulic resistance

A 2 mm burrhole was drilled 9.5 mm lateral and 19 mm anterior to the zero reference point. The tip of a 23 G needle was then placed at a depth of 9 mm using a stereotactic manipulator (Fig 3). These coordinates

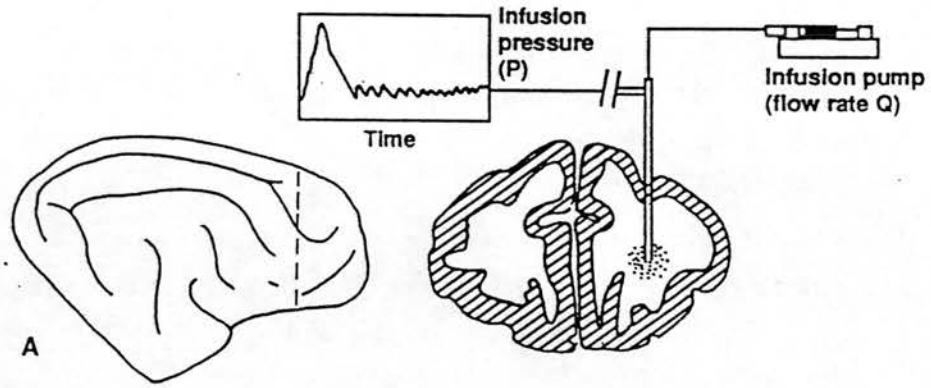

Figure 3A: Lateral view of the feline brain showing coronal level of infusion, and outlining the infusion locus deep in the forebrain white matter.

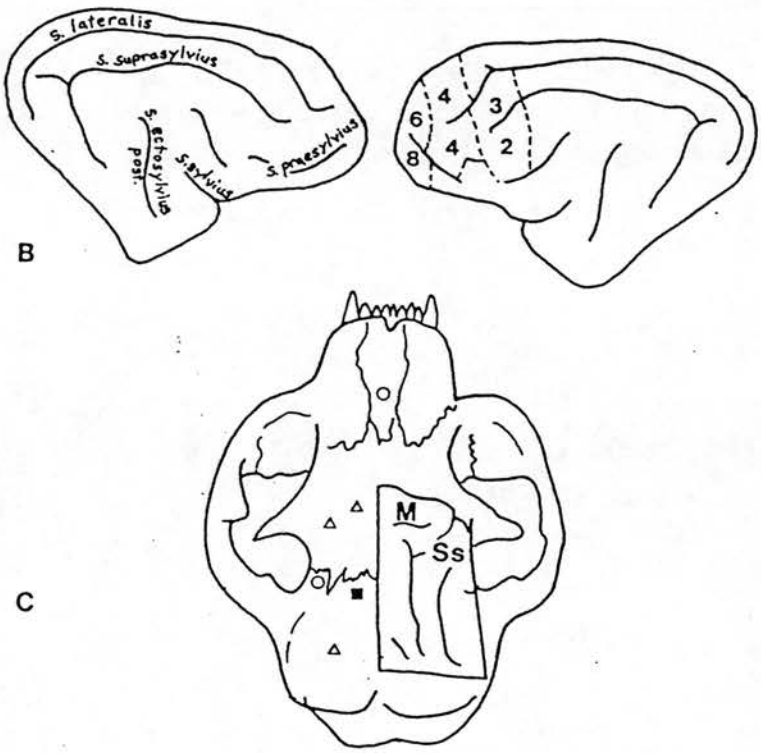

Figures 3B: Lateral view of feline brain (after Guldin & Markowitsch, 1984) outling the major sulci and Brodmann areas corresponding to the primary somatosensory (Area 2,3) and motor cortex (Area 4,6,8). **Figure 3C** Superior aspect of the feline cranium outlining placement of electrodes and monitoring lines and their relationship to the motor (M) and somatosensory (Ss) cortex (after Dong et al, 1982). Key o = Ag/AgCl electrode (SEP); Δ = platinum/iridium electrode (CBF); ■ = Intraventricular needle (ICP).

would place the tip of the infusion needle in the white matter of the anterior centrum ovale in direct proximity to the primary somatosensory thalamocortical and corticospinal fibres (Snider & Niemer, 1962; Guldin et al, 1984). The burrhole was then lined with surgicel and sealed with methylmethacrylate. The infusion rate (0.2 ml/hr) was controlled and infusion pressure, from which the R_t was calculated, measured as described in section 2.2.ii. The period of infusion was three hours.

2.3.iii ICP, Pressure-volume index (PVI), intracranial compliance (C_i) and CSF outflow resistance (R_o)

A 2 mm burrhole was drilled at a position 3.5 lateral and 14 mm anterior to the zero reference plane on the calvarium contralateral to the side of infusion (Fig 3). A 23 G spinal needle connected via saline filled tubing to a Bentley transducer was positioned in the lateral ventricle which was usually encountered at a depth of 13 $\pm$ 1 mm. Correct position was confirmed by obtaining a pulsatile ICP waveform on a Rikadenki chart recorder, and by observation of an increase in ICP with manual compression of the abdomen. The range of ICP monitoring was 0-90 mm Hg. The zero reference point for the Bentley transducer was at the level of the ear bars.

PVI, Ci and Ro were calculated following intraventricular bolus injections of 0.1ml saline by use of the following equations (Marmarou et al, 1975).

$$PVI = \frac{V}{\log\left(\frac{P_p}{P_o}\right)} \qquad (1)$$

$$C_i = \frac{.4343 \times PVI}{P_o} \qquad (2)$$

$$R_o = \frac{\frac{T_2 \cdot P_o}{PVI}}{\log\left(\frac{P_2(P_p - P_o)}{P_p(P_2 - P_o)}\right)} \qquad (3)$$

where V = Volume of bolus injection

P_o = Baseline ICP prior to bolus injection

P_p = Peak ICP after bolus injection

P_2= ICP at time T_2 after bolus intraventricular injection

T_2 = Time after intraventricular injection

These parameters were calculated as baseline values and then every hour during the period of infusion and three hours after completion of the infusion.

2.3.iv rCBF

CBF was measured in four brain areas every 30 minutes during the period of infusion using the hydrogen clearance technique as described in section 2.2.iv. Two electrodes were positioned bilaterally into the sigmoid and coronalis gyri following craniectomy through the frontal sinus and dural opening with an 11 Blade and hooked 21 G needle (Fig 3). A parietal electrode was similarly positioned in both posterior suprasylvian gyri. Once positioned the exposed dura was covered with surgicel and the electrodes cemented in position and cranium sealed using methylmethacrylate. The anterior electrodes were positioned approximately 5 mm

anterior, and the parietal electrodes approximately 10 mm posterior to the infusion site. A Ag/AgCl reference electrode was placed in a subcutaneous neck pouch and polarised to -400 mV. Hydrogen (6-10%) was administered to the animal through a side arm on the inspiratory limb of the ventilatory circuit. CBF was calculated from the clearance curves in a similar method as described in section 2.2.iv.

After completion of the intracerebral infusion the ventilator tidal volume and rate of respiration were altered so that the arterial CO_2 levels was increased from 25 mm Hg to 60 mm Hg. CBF measurements were obtained at various values within this range. At least 25 minutes elapsed between recording of CBF, and usually CBF was recorded at five different CO_2 levels for each cat. Reactivity data was analysed as described in section 2.2.iv.

2.3.v Cortical SEP recording

Cortical SEPs were recorded from the skull surface overlying the anterior ectosylvian gyrus using Ag/AgCl disc electrodes referenced to an electrode placed subcutaneously in the region of the nasion (Fig 3). An earth electrode plate was positioned subcutaneosly over the lumbosacral region. The earth, recording and reference electrodes were connected via a PA89 Medelec preamplifier to a MS92a signal averaging unit. Stimulating electrodes (26 G stainless steel) were placed subcutaneously in the dorsal and volar aspects of the radial side of each forepaw. Accurate placement of the latter electrodes in relation to the median nerve was confirmed by rythmical forepaw twitching following electrical stimulation (5-8

mA, 0.1 ms duration, 5 Hz). Epochs of 20-100 ms were studied with parameters of signal averaging which were as described in section 2.2.v.

2.3.vi Motor Evoked potentials (MEP)

Spinal motor evoked potentials (Levy et al, 1984) were recorded subdurally from the low thoracic region two and one half to three hours after termination of the intraparenchymal infusion. The spinal MEP was generated by either transcranial or direct cortical stimulation with the anode being either the Ag/AgCl electrode overlying the respective anterior ectosylvian gyrus or the platinum-iridium electrodes in the sigmoid or coronalis gyri. In both cases the cathode was a Ag/AgCl electrode attached to the hard palate. Parameters were 5-20 mA stimulus of 0.3 ms duration delivered at 20Hz. The spinal MEP was recorded subdurally using a platinum alloy ball electrode referenced to a paraspinal needle electrode. These electrodes were connected to a Medelec PA 89 preamplifier and an MS 92A signal averaging unit. Between 28 and 256 stimuli were averaged. Epochs of 10 ms were analysed with bandpass set at 20-2000 Hz. All recordings were obtained at normocapnia and normotension.

2.3.vii Brain water and specific gravity

Following the completion of the experiment all monitoring lines were removed from the skull and the calvarium removed with bone rongeurs. A lethal intravenous dose of pentobarbital (60 mg/kg) was administered. The animal was then decapitated and a total craniectomy performed. The calvarial dura which was initially left intact was then opened coronally in a plane 1 mm anterior to the infusion

needle entry point. Small blocks of cortex (2-4 mm^3) were removed from locations 3 mm lateral and medial to the infusion needle and from similar locations from the contralateral hemisphere. Specific gravity measurements were made in a layered kerosene-bromobenzene column as described in section 2.2.vii. The hemisphere was then incised by coronal section through the plane 1 mm anterior to the intracerebral infusion. Specimens (2-4 mm^3) of white matter were then removed from the locus of, and 5 mm from, the infusion needle and dropped into the kerosene-bromobenzene column. Specimens from similar positions in the contralateral hemisphere were also analysed. Tissue water content of the samples was calculated from the SG values using the standard equation after sham, saline, arachidonic acid and bradykinin infusions (Marmarou et al, 1978) and the corrected formula after 20% protein and glioma cyst infusates (Marmarou et al, 1982).

2.3.viii Blood brain barrier disruption and light microscopic tissue changes

One hour prior to sacrifice of the animal Evans Blue 2% was administered intravenously at 1 ml/kg body weight. After sacrifice of the animal brain tissue specimens were taken for gravimetric analysis and then the brain was placed in 10% formalin/saline. After fixation for five days the brain was coronally sectioned and examined macroscopically for extravasation of the blue dye. The brains were photographed and the area of Evans blue extravasation in the coronal plane of infusion quantitated. Selected brains were examined using light microscopy after staining with hematoxylin and eosin (H & E), luxol blue-PAS and solochrome-cyanin.

2.4 INFUSATES

The following infusates were used;

1 - Normal saline. (Sodium chloride 0.9%, Boots Hospital products, The Boots Company PLC, Nottingham). This solution contained Sodium and chloride ions 150 mmol/l with pH of 6.89. The pH of the saline/5% ether infusate was 7.05.

2- 20% protein solution (see appendix 1) This solution was buffered to pH 7.50 using a 0.5 M tris amino buffer.

3- Bradykinin 5 and 150 ug/ml (5×10^{-6}M and 1.5×10^{-4}M respectively) in normal saline. (Bradykinin, Sigma B-3259, Sigma Chemical company St Louis, Mo, USA). The pH of these solutions were 6.98 (5 ug/ml) and 7.25 (150 ug/ml).

4-Arachidonic acid 2 to 15 mg/ml (6.6×10^{-3}M to 5×10^{-2}M respectively. Arachidonic acid (Sigma A-6382, Sigma Chemical company) was dissolved in diethyl ether and further solubilized in normal saline so that the final concentraton of ether in the solutions was 5%. The pH of the arachidonic acid 10 mg/ml infusate was 6.21.

5 - Human glioma cyst fluid. Cyst fluid was obtained following CT guided stereotaxic biopsy from four patients. Two had glioblastoma (EB and GD), one an anaplastic astrocytoma (JH) and one an oligodendroglioma (TF). The electrolyte, protein, and enzyme contents of these fluid are listed in Appendix 2. The pH of these four cyst fluids varied from 7.51 to 7.62.

All infusates were either freshly prepared or stored at - 40^{o}C before usage.

2.5 STATISTICAL METHODS

Statistical analysis was performed using the dedicated commercial computer package MINITAB (Ryan et al, 1983). Correlation coefficients were calculated by linear regression analysis. Linear regression data was compared by analysis of covariance. Paired data was analysed by using the paired or unpaired Student's t-test. Data was considered significantly different if p 0.05, unless multiple comparisons were being made in which case Bonferroni's correction was used.

2.6 JUSTIFICATION OF METHODOLOGY

2.6.i The infusion model of brain oedema

Experimental studies of brain oedema induced by cold lesions, ischemic insults, tumour xenotransplantation, irradiation, systemic or focal exposure to toxins and infectious agents have examined many aspects of oedematogenesis, the biomechanics of brain oedema and mechanisms of oedema resolution (Herzog et al, 1965; see Klatzo, 1967; Westergaard, 1975; Csanda, 1980; Baethmann et al, 1980;; Hossmann et al, 1980; Klatzo et al, 1980; Reulen et al, 1977; 1980; Bothe et al, 1984; Hatashita and Hoff, 1988). However these models are in general unsatisfactory for examining the relationships between brain oedema and specific aspects of altered brain physiology since it is difficult to differentiate between the neurophysiological changes attributable to the destructive cerebral lesion generating the oedema and those attributable to the oedema per se. Compartmental herniation of cerebral tissues and the effects of raised ICP also complicate interpretation of data (Schaul et al,

1976).

To overcome many of these problems a model of focal brain oedema that was generated by slow intracerebral infusion of fluid into the forebrain white matter of the cat was developed (Marmarou et al, 1980). This model has the advantage of avoiding any primary neural destruction and allows the regulated infusion of specific solutions. Such a model of cerebral oedema can be used to study the oedematogenic, biomechanical, electrophysiological and cerebrovascular effects of putative vaso and neuromodulating agents in the infusate. Direct delivery of the fluid into the white matter also provides a more relevant evaluation of the possible roles of the infused compounds in brain oedematogenesis and dysfunction, associated with intracranial neoplasms, ischemia, encephalitis or trauma, than perfusion of the compound(s) through the ventricular system, on isolated vessels or over the cortical surface (Oettinger et al, 1976; Westergaard, 1975; Unterberg & Baethmann, 1984; Unterberg et al, 1987b). The latter experimental approaches may be appropriate for evaluating brain oedema associated with meningitis but a recent study evaluating the oedematogenic potential of bradykinin, histamine, serotonin and arachidonic acid administered to the brain surface demonstrated that findings with regard to pial vascular permeability cannot reliably be extrapolated to their action on brain parenchymal vascular permeability (Watanabe & Rosenblum, 1987). A study of the oedematogenic potential of particular compounds in normal white matter is more relevant to common clinical patterns of brain oedema. Some studies which have addressed this question have utilised an intracerebral microinjection technique to evaluate the oedematogenic potential of arachidonic

acid, LTB4, LTC4 and LTE4 as well as xanthine oxidase, cyclic adenosine monophosphate, ouabain and serotonin (Bulle, 1957; Osterholm et al, 1969; Go et al, 1980; Long et al, 1980; Chan et al, 1983; Aritake et al, 1983; Black & Hoff, 1985; Unterberg et al, 1987a). None of these workers have however simultaneously investigated changes in cerebral vasomotor tone or electrophysiology that could be attributed to either the agent or the associated oedema. Marmarou's initial studies with the infusion oedema model analysed the biomechanics of brain oedema, and in a series of other experiments his group briefly described biomechanical, neurophysiological and ultrastructural sequelae of intracerebral saline, protein and CSF infusion and confirmed the infusion model resembled the "classical" histological and ultrastructural findings of brain oedema (Lax et al, 1979; Walstra et al, 1980; Marmarou et al, 1980; Tanaka et al, 1983; Tsubokawa et al, 1983).

If intracerebral saline infusion provides a good histological, and biomechanical model of brain oedema that causes minimal changes in electrophysiological and cerebrovascular function what particular poblems may be usefully addressed using this model? If a brain neoplasm, with abnormal capillary endothelium, is simply conceptualized as a point source generator of oedema fluid that passes into an otherwise undamaged peritumoural region then the infusion models fits this concept. Utilisation of the infusion model followed by post mortem examination of coronal sections of the brain for extravasation of intravenous vital dyes would seem an ideal method with which to assess the potency of postulated secondary mediators of vasogenic brain oedema. Simultaneous studies of cerebrovascular and

electrophysiological parameters also enable a study of the relationship between brain oedema, compounds in the infusate and brain dysfunction.

2.6.ii Limitations of the infusion oedema model

Although the infusion model of brain oedema has several advantages it has no clinical parallel. The acute nature of oedema production, the rate of infusion, the hydrostatic infusion pressure and composition of the infusate may have little relevance to the dynamics of oedema production in the clinical situation. The infusion causes acute distention of the extracellular white matter and separation of axonal fibres which may damage synapses and astrocytic or oligodendroglial processes. The phenomenon of spreading cortical depression (Leao, 1944; Leao, 1986) can occur after intracerebral injection of compounds that alter the brain electrolyte microenvironment and may alter vascular and electrophysiological regulation making the effects of infusates difficult to interpret (Lauritzen, 1984; Leao, 1986; Wahl et al, 1987). Infusion of particular compounds in saline or buffered solutions may spuriously evaluate their oedematogenic or neuromodulating potential since in vivo the compound may be readily inactivated by enzyme systems, or other components of oedema fluid. For example the adverse effects of arachidonic acid on cellular respiration, choline uptake and acetyl choline accumulation are blocked by the addition of albumin to perfusates (Boksa et al, 1988; Hillered & Chan, 1988), and kinin activation would be limited by smaller MW enzymes in oedema fluid exudate (see next section).

A major disadvantage of the infusion model in rats is the

relative paucity of the subcortical white matter. Vasogenic brain oedema is essentially a white matter phenomenon and deposition of fluid into the corpus striatum, which is obligatory to minimise leakage of the infusate back along the needle tract, probably involves clearance mechanisms and vascular responses that cannot be extrapolated to either the clinical situation or effects on white matter. This is a particular criticism of previous studies utilising arachidonic acid and LT infusions (Aritake et al, 1983; Black & Hoff, 1985; Chan et al, 1983).

2.6.iii Choice of infusates

Sham and Saline Infusions

Sham and normal saline infusion were chosen to evaluate the general and neurophysiological effects of intracerebral infusion and to demonstrate any methodological shortcomings. Since the sodium contents of both human and cat peritumoral oedema fluid have been shown to lie between 130-150 mEq/ml (Bothe et al, 1984; Bodsch et al, 1987) these preliminary experiments should provide realistic baseline data against which the effects of other infusates could be compared.

Arachidonic acid (MW 304)

Arachidonic acid and both its cyclooxygenase generated prostanoid (prostaglandin (PG) and thromboxanes) and lipoxygenase generated leukotriene (LT) metabolites are produced or released in several disorders that are also associated with brain oedema formation (Bazan et al, 1980; Fishman & Chan, 1981; Gamache et al, 1986; Dempsey et al,

1987; Shimizu et al, 1987; Westcott et al, 1987; Katz et al, 1988). Following ischemic brain damage influx of extracellular calcium causes activation of phospholipase A2 and the release of arachidonic acid from membrane phospolipids such as phosphatidylinositol and phosphatdycholine (Bazan et al, 1980; Wolfe, 1982; Walker and Pickard, 1985; Shimizu et al, 1987; Katz et al, 1988). Cell membranes from human glioma cell lines, normal glia and neurones all contain high levels of these phospholipids, but the phospholipids in glial tumours contain more arachidonic acid and linoleic acid than control brain (Poduslo et al 1983; Hattori et al, 1987). Brain tumours grown in tissue culture produce PGE2, PGF2 alpha, 6 oxo PG F1 alpha and thromboxane B2 (Cooper et al, 1984; Lauro et al, 1986; Castelli et al, 1987). The production of prostanoids by tumours was variable, but was highest in the meningomas and poorly differentiated gliomas. Metastatic brain tumours produced large amounts of LTC4 (13.8 $\pm$ 8.5 pg/mg tissue) when compared to levels in nondiseased (0.4 pg/mg tissue) brain (Black et al, 1986). The level of LTC4 in gliomas was found to be 6.2 $\pm$ 2.3 pg/mg and there was a positive correlation between the amount of peritumoural oedema and the tissue LTC4 level.

Arachidonic acid, LTC4, LTD4, PGE_2 and PGF_2alpha modulate cerebral arterial and pial vessel tone and also increase capillary permeability when they are administered by either cortical or isolated vessel superfusion (see Walker & Pickard, 1985; Olesen & Crone, 1986: Unterberg et al, 1987b). These findings, together with the known large amounts of phospholipid contained in neoplastic cells, the large areas of ischemic and coagulative necrosis seen in malignant gliomas, and the release of eicosanoids from inflammatory cells (Gamache et al, 1986; Shinonaga et al,

1988) all suggest that eicosanoids have a role in peritumoural brain oedematogenesis.

Bradykinin (MW 1000)

Bradykinin, a nonapeptide formed from the beta-2 macroglobulin (MW 180,000) kininogen-prekallikrein, is a potential secondary mediator of vasogenic brain oedema since it is a potent peripheral vasodilator and modulator of capillary permeability (Baethmann et al, 1980; Regoli & Barabe, 1980). Elevated bradykinin levels have been found in brain oedema fluid generated by freeze lesions and cerebral ischemia (Maier-Hauff et al, 1984), and beta-2 macroglobulins are likely to be extravasated into human gliomas (see Seitz & Wechsler, 1987). Aprotinin, a protease that inhibits bradykinin formation, can limit oedema caused by freeze injury to and surgical excision of the brain (Czernicki, 1979; Unterberg et al, 1986). Other studies evaluating the possible role of bradykinin in brain oedematogenesis have delivered bradykinin to the brain by ventriculo-cisternal perfusion, cortical superfusion and isolated cerebral vessel perfusion.

Cortical superfusion studies have shown that bradykinin vasoconstricts cat and human pial veins in concentrations as low as 4 x 10^{-7}M (Unterberg et al, 1984) and 10^{-6}M (Hardebo et al, 1987) respectively. Pial arteriolar dilation has been recorded with bradykinin concentrations ranging from 1ug/ml (10^{-6}M) (Kontos et al, 1984) to 4 x 10^{-5} M (Unterberg et al, 1984). Pial venule permeability is increased by 10^{-6} M bradykinin but leakage is limited to Na+-fluorescein (MW 376), since concentrations up to 4 x 10^{-3}M failed to cause leakage of larger MW tracers (Unterberg et al, 1984; Wahl et al, 1988). Ventriculo-

cisternal perfusion of 10^{-6} M bradykinin causes mild subependymal oedema (Unterberg & Baethmann, 1984).

Although these studies may be appropriate for evaluating the possible role of bradykinin in brain oedema associated with meningitis for several reasons they are a suboptimal model for predicting its role in brain oedema related to intracranial tumours, cerebral infarction and parenchymal infection. Firstly brain parenchymal vessels may not have the vasomotor and permeability characteristics of the pial vasculature (Watanabe & Rosenblum, 1987) and secondly normal brain contains kininases, oligopeptidases and endopeptidases all of which enzymatically cleave bradykinin under a variety of physiological conditions (Camargo et al, 1987; McDermott et al, 1987). The activity of these enzymes, and other plasma protease and kallikrein inhibitors such as alpha-1-antitrypsin (MW 54,000) and antithrombin III (MW 58,000), is crucial when considering pathophysiological effects since normally in vivo these enzymes limit the $T_{1/2}$ of bradykinin in various tissues to between 30 seconds and 3 minutes (Regoli and Barabe, 1980). Therefore pathophysiological findings using bradykinin perfusion of the brain surface, at particular concentrations may have little relevance to the pathophysiological action of similar concentrations of bradykinin on cerebral parenchymal vessels in vivo.

Protein Solution

When designing this study it was proposed to grow gliomas in tissue culture and infuse the culture supernatant into the brain to evaluate the oedematogenic and neurophysiological modulating potential of tumour related products. A 20% protein solution (Appendix 1) was the

chosen culture medium and would therefore have acted as the control infusate for the culture infusions. However due to logistic and technical difficulties tissue culture was not established. Nonetheless the 20% protein solution would seem an appropriate infusate since oedema fluid due to brain abscess and tumours, in both humans and cats, has a protein content of 4 to 16 mg/ml which is equivalent to between 6 to 25% plasma protein (Bothe et al, 1984; Bodsch et al, 1987). Analysis of extravasated protein using immunofluorescent, biochemical and immunoperoxidase techniques has shown that most is albumin (MW 69,000), pre-albumin (MW 61,000) and low MW immunoglobulins (Cummings, 1961; Brett & Weller, 1978; Hossman et al, 1980; Szymas & Hossman, 1984; Seitz & Wechsler, 1987). This extravasated extracellular protein may modulate glial membrane potential since intracellular uptake of polyanionic protein may alter the Gibbs-Donnan equilibrium, and K^+ efflux (Bodsch et al, 1987). Since peritumoural protein extravasation is diminished by steroid therapy in experimental and clinical situations (Hossmann et al, 1983; Bodsch et al, 1987; Nakagawa et al, 1987; Ito et al, 1988), some extravasated plasma proteins may alter BBB permeability (Unterberg & Baethmann, 1984; Oettinger et al, 1976) and since extracellular plasma protein is cleared more slowly from the cortex than the white matter (Go et al, 1980) they may contribute to the pathophysiology of brain oedema and dysfunction.

Glioma Cyst fluid

Since the tissue culture of gliomas was not established, to test the hypothesis that gliomas produce factors that mediate vasogenic brain oedema and neuronal or axonal modulation, glioma cyst fluid was infused. Although the

electrophoretic and biochemical studies suggest that most of the protein in these fluids was extravasated plasma proteins, they would undoubtedly also contain tumour secretions and tumour cell debris that would be unique to a particular tumour. Levels of the polyamines putrescine and N^1-acetylspermidine are higher in cyst fluid from malignant gliomas compared to low grade astrocytoma (Yamazaki et al, 1986), and the quantities of higher MW proteins such as Ig M, transferritin, ceruloplasmin show similar variations (Seitz and Wechsler, 1987; see Appendix 2).

The glioma cyst fluid was obtained during CT guided stereotactic tumour biopsy, using a Nashold cannula and the BRW stereotaxic system (Apuzzo et al, 1983). Cyst fluid was tested from four patients with supratentorial gliomas. Two patients with glioblastoma (GD-GBM and EB-GBM) had major peritumoural oedema and associated brain dysfunction, one with an anaplastic astrocytoma (JH-AA) had moderate oedema and clinical dysfunction and one, with an oligodendroglioma causing intractable focal epilepsy, (TF-Oligo) had minimal peritumoural oedema and no clinical deficit (Appendix 2). It was postulated that experimental BBB disruption and neuronal modulation would correspond to the extent of CT imaged peritumoural oedema and associated clinical dysfunction.

2.6.iv Assessment of brain oedema

Indirect calculation of water content in oedematous brains from specific gravimetric data has been widely used since Nelson and colleagues (1971) described their simple method of quantitating water content from the SG_{tissue} (SG_t) and SG_{solids} (SG_s) of small tissue samples (5-15 mg)

utilising a layered bromobenzene-kerosene column. Tissue water content can be calculated from the equation

$$\text{gm } H_2O/\text{gm tissue} = 1 - (SG_t - 1)/(1-1/SG_s)\ SG_t$$

Using a water intoxication model the SG_s of white matter was shown to be a constant (Nelson et al, 1971), however if the oedema fluid contains protein and other solutes the SG_s is raised and tissue water may be underestimated. This problem led to correction factors being introduced when the oedema fluid contained protein (Marmarou et al, 1982). However the content of oedema fluid rarely parallels serum protein levels and empirical corrections may have to be made (Bell et al, 1987b). Others however maintain that SG_t gives a good measure of brain tissue water content regardless of oedema fluid constituents (Bothe et al, 1984). The major advantages of microgravimetric methods over wet/dry weighing are its simplicity, rapidity and the facility to analyse small tissue samples (Marmarou et al, 1978). However there are other limitations with the method due to factors, independent of the tissue water content, that will alter SG_t. These variables include the sample size, timing of isogravimetric point, the blood volume of the tissue sample as well as the the SG of the oedema fluid (Ferzst et al, 1980). These problems are acknowledged by proponents of the technique and studies have been made about the effect of sample size and timing of isogravimetric point (Ferzst et al, 1980), and of the influence of changes in tissue blood volume (Picozzi et al, 1985). Microgravimetry has been widely used in both experimental and human material and has produced water content values similar to those obtained using wet/dry weighing techniques (Marmarou et al, 1982; Bell et al, 1987; 1987b).

2.6.v Assessment of ICP dynamics and brain biomechanics

The classical changes in brain biomechanics that occur with brain oedema (ICP, craniospinal compliance, PVI and R_t) have been alluded to in section 1.4.i. The mathematical models for studying these parameters have been developed validated and applied in cats using a variety of experimental protocols (Marmarou et al, 1975; Marmarou et al, 1980; Takizawa et al, 1985; 1986a;1986b; Gray and Rosner, 1987; Hatashita & Hoff, 1988).

2.6.vi Assessment of BBB integrity

The importance of disruption of the BBB in the genesis of the oedema was first demonstrated by Prados and colleagues (1945) who confirmed that the vital dye trypan blue was present in cerebral oedema caused by exposure of the brain to air. Trypan blue and Evans blue (both MW 576) bind to serum albumin and are markers for BBB disruption to molecules of circa 69,000. Other indicators of variable MW and hydrodynamic radius can also be used to assess BBB integrity and include Horse radish peroxidase (MW 40,000), Na-Fluorescein (MW 376), DITC-Dextran (MW 20,000 - 62,000). These compounds are generally detected by sophisticated techniques such as electron microscopy (HRP) and phase contrast microscopy (Na-Flourescien) whereas Evans Blue extravasation into the brain can be quantitated by simple planimetry or more accurately using sphectrophotometry (Durward et al, 1983). Since Evans Blue binds to albumin, which is the predominant protein in peritumoural brain oedema fluid, and it has been extensively used in studies of BBB disruption (Csanda, 1980; Hossmann et al, 1980; Durward et al, 1983; Chan et al, 1983; Black & Hoff, 1985) it would seem a simple and appropriate choice.

2.6.vii CBF quantitation

The H_2 clearance technique is a simple and inexpensive method of measuring CBF that has been widely used since its desription (Auckland, 1965; Pazstor et al, 1973). This method is based on the Fick principle and the mathematical model developed by Kety describing equilibration of freely diffusable, metabolically inert tracers between tissue and vascular compartments (Kety, 1951). The mathmatical derivation and reduction from the Fick equation

$$\frac{dQ_t}{dt} = F_t(C_a - C_v) \quad (1) \quad \text{to} \quad C_t = C_0(e^{-kt}) \quad (2)$$

where Q_t is the amount of tracer taken up by the tissues, F_t the tissue blood flow, C_a and C_v the concentrations in the arterial and venous blood, C_t and C_0 the concentrations of tracer in the tissue at time t and 0, and k the blood flow per unit of tissue has been extensively reviewed (Young, 1980; Farrar (1987). This derivation utilises the unitary partition coefficient of hydrogen, and the zero value of C_a during desaturation.

Integration of equation (2) provides

$$\ln C_t = \ln C_0 - kt$$

which corresponds to a regression equation $y = b - mx$. Therefore by plotting the logarithm of the H_2 desaturation curve with time, the slope of desaturation gives the tissue blood flow. Desaturation curves are obtained by recording the current generated by the oxidation of tissue hydrogen on the surface of the platinum electrodes (Auckland et al, 1965)

This method relies on assumptions concerning the rate of H_2 equilibration between tissue and vascular compartments, the arterial H_2 level being zero during desaturation and the electrical potentials being generated solely by H_2 interaction with the platinum electrode (Young, 1980). CBF values obtained using hydrogen clearance techniques are similar to those obtained using microspheres (Heiss & Traup, 1981) and some studies using ^{14}C antipyrine autoradiographic studies (Fieschi et al, 1969). There are several accepted limitations to the technique which include the problem of tissue damage caused by insertion of electrodes, uncertainty as to the volume of tissue represented by a flow value, the bi or polyexponential nature of some clearance curves (occurring when cortical and white matter clearance curves are superimposed) and spurious oxidative potentials generated by tissue O_2, pH and ascorbic acid concentrations (Young, 1980; Farrer, 1987). Despite these problems the technique has been extensively used to record rat and cat CBF and CBF CO_2 reactivity (Marmarou et al, 1980; Tanaka et al, 1983; Bell et al, 1985; Ianotti et al, 1984; Gray & Rosner, 1987).

2.6.viii Evoked potential recording

Generation of evoked potentials by stimulation of a particular sensory system and recording an averaged electrical response at various points along the ascending pathway is now a standard neurophysiological investigative technique. The ascending somatosensory pathway includes the dorsal column nuclei, the medial lemniscus, the ventroposterior thalamic nuclei, the thalamocortical projections, the primary somatosensory cortex and cortical association fibres. In both cats and rats these pathways have been extensively studied and the cortical SEP

waveform and generators of the various components described using an array of stimulating parameters and cortical electrode placements (Towe et al, 1964; Poliakowa, 1972; Hall & Lindholm, 1974; Wiederholt and Iragui-Madoz, 1977; Iragui-Madoz and Wiederholt, 1977; Sutton et al, 1980; 1982; Allison et al, 1982; Dong et al, 1982; Chapin et al, 1984; Dykes and Lamour, 1988; Fehlings et al, 1988).

The cortical MEP waveform following transcranial (skull overlying M_1 to pharynx) or direct motor cortical stimulation in the cat consists of an initial direct (D) wave due to either pyramidal or basal dendrite excitation followed by indirect (I) waves due to either recurrent stimulation of the same neuron or interneurone excitation (Patton and Amassian, 1954; Levy et al, 1984; Amassian et al, 1987). The neuronal generators of the MEP waveform are currently the subject of some debate particularly with regard to the contribution of nonpyramidal descending pathways (see review by Amassian et al, 1987; York, 1987). The descending MEP recorded from the midthoracic spinal cord following transcranial stimulation of the motor cortex consists of a polyphasic waveform thought to represent axonal volleys generated by the D and I waves (Levy et al, 1984). The morphology and latency of the MEP varies with stimulus intensity, frequency and duration, the stimulating electrode size and location and recording location (Levy et al, 1984; Geddes, 1987). If these parameters are defined the descending MEP would seem a satisfactory method of assessing the integrity of conduction through oedematous brain.

If brain oedema or a particular infusate in the oedema fluid modulates axonal function then changes should occur

in specific components of either the SEP or MEP waveform if the fluid is deposited into the relevant fibre tracts. Both these evoked potentials are readily acquired, easy to interpret and have known anatomical substrates which makes them ideal parameters for functional monitoring (Dong et al, 1982; Levy et al, 1984; Amassian et al, 1987; Fehlings et al, 1988).

2.6.ix Histological studies

The histological features of brain oedema have been reviewed in section 1.3. To validate that the infusion model causes these histological features a standard stain (H & E), a myelin stain (Solochrome-cyanin) and stain showing proteinaceous material (PAS) were selected. These simple studies provide an analysis of tissue reaction and patterns of spread of the infusate(s). They may also provide some insight into mechanisms of BBB disruption following particular infusates.

SECTION 3: RESULTS

3.1 RODENT MODEL OF INFUSION OEDEMA

3.1.i General comments

Preparation of the rat for the infusion oedema studies usually took two hours. Induction of anaesthesia following intraperitoneal urethrane usually occurred within five minutes. Generally the rats remained metabolically and physiologically stable throughout the duration of an experiment. If the animal was not anaesthetised by ten minutes it was assumed that delivery of the anesthetic had not been completely intraperitoneal. In a number of such animals watery diarrhoea occurred, probably due to enteric injection. In such circumstances the experiment was discontinued and any data discarded.

Experiments using sham infusion, 0.1 ml saline infusion and 0.1 ml 20% protein infusion were performed in over 80 rats. Spatial limitations dictated that several series of experiments were performed to compile all data (focal brain tissue SG, total hemispheric water content, intracranial pressure, brain tissue hydraulic resistance, cerebral tissue compliance, cortical SEPs, regional CBF and CBF CO_2 reactivity) for one infusate. The intraparenchymal infusion was always into the left frontal region and the series of experiments performed included-

L frontal infusion - R intraventricular pressure monitoring
L frontal infusion - Bilateral CBF recording
L frontal infusion - Bilateral SEP recording

Data concerning infusion pressure, brain water content, cortical and subcortical specific gravity was compiled from the various series of experiments.

3.1.ii BRAIN WATER CONTENT AND SPECIFIC GRAVITY

The specific gravity of 2-4 mm^3 segments of cortical and subcortical tissues following (1) sham infusion - placement of a 25G needle stereotactically into the white matter for one hour with no infusion, (2) infusion of 0.1 ml saline and (3) infusion of 0.1 ml 20% protein solution over one hour, were recorded. The **subcortical** tissue specific gravity (Appendix 6; Table A-1), adjacent to the infusion site, was significantly reduced, when compared to the noninfused "control" hemisphere, following both saline (mean 1.0325; $p < .001$) and 20% protein (mean 1.0332; $p < 0.001$) infusions, but was not significantly reduced by sham infusion (mean 1.0384; $p = 0.69$.). There was no significant change in the SG of **cortical** tissue (Table A-2) adjacent to any of the infusion sites (mean 1.0423) when compared to the contralateral hemisphere (1.0417).

Total brain hemispheric water content was determined in 26 rats after either saline (mean 77.5%) or 20% protein (78.3%) infusion. Although there were minor differences in water content between infused and contralateral hemispheres none of these differences were statistically significant (Table A.3).

3.1.iii INTRAVENTRICULAR PRESSURE

Intraventricular CSF pressure was recorded in 14 rats. There was a small rise from baseline values during intracerebral infusion in both saline and 20% protein groups (Tables A-4, A-5). After completion of the saline infusion this increase was just statistically significant ($p = .04$) however part of this increased is related to the higher P_aCO_2 at the completion of the infusion. When correction is made for the differences in P_aCO_2 the ICP change is not significant (see Appendix 3).

3.1.iv BRAIN TISSUE HYDRAULIC RESISTANCE (R_t) AND BRAIN TISSUE COMPLIANCE (C_t)

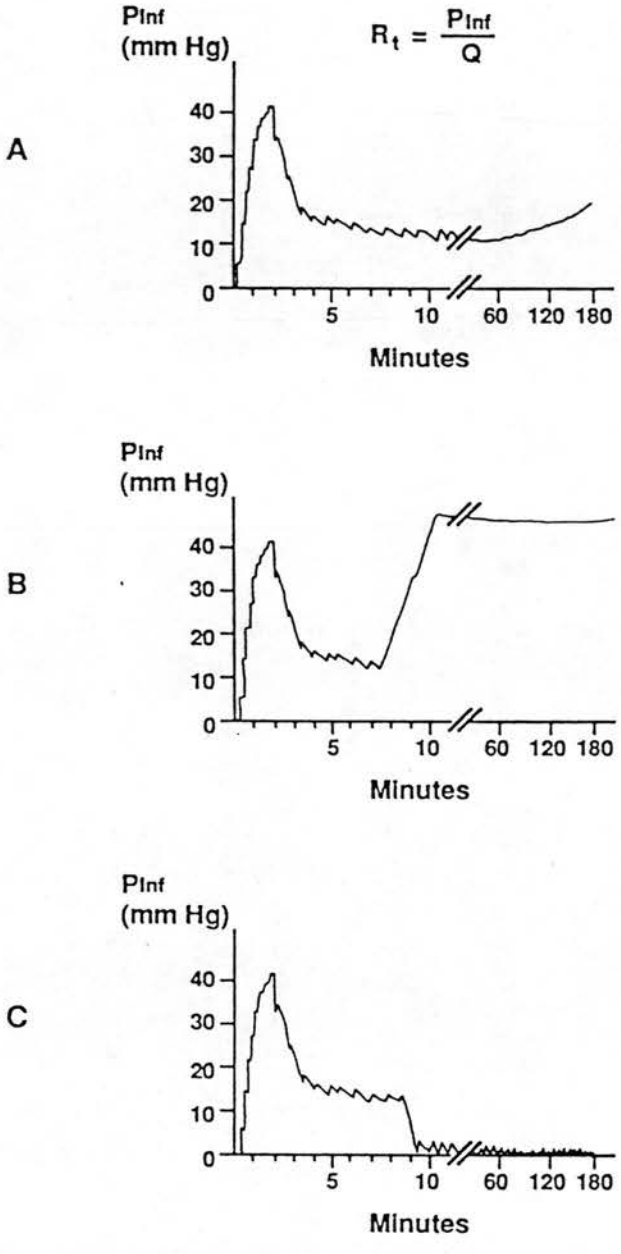

Figure 4: Patterns of infusion pressure (P_{inf}) recorded during intracerebral infusion. A normal experimental record with early peak rise in P_{inf} followed by a rapid fall to levels just above ICP. Figures B and C illustrate patterns of P_{inf} that occur if the infusion line is blocked (B) or leaks (C). Such patterns were occasionally recorded in the rat but not in the cat experiments.

Using both the saline and protein infusates characteristic infusion line pressures (P_{inf}) were obtained (Fig 4). There was a peak infusion pressure of approximately 40

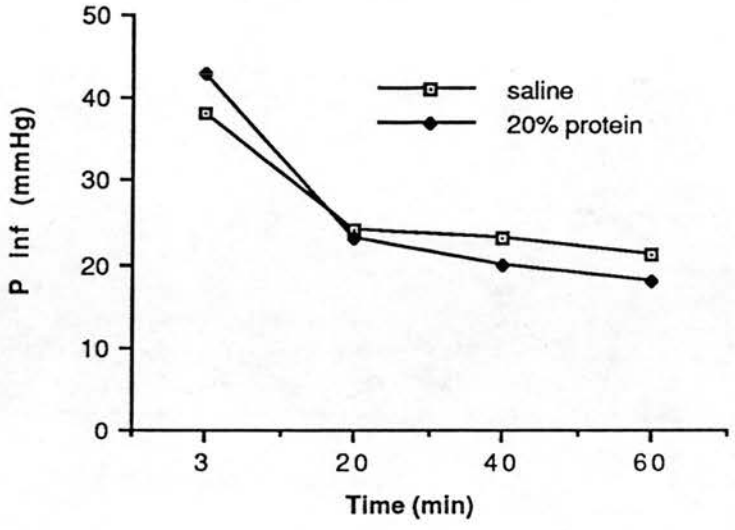

Figure 5: Changes in mean infusion pressure (P inf) during 0.1 ml/hr infusion with saline and 20% protein into the rat nucleus caudatoputamen.

mmHg between 1 - 3 minutes after commencement of the infusion. In the susequent 1 -2 minutes there was a 15 - 20 mmHg fall in pressure until a fairly constant was obtained (Fig 5). Measurement of P_{inf} was particularly useful for detecting occult blockage of the infusion line or leakage of the infusate around the infusion needle, presumably into the subarachnoid or subdural spaces (Fig 4).

Calculation of R_t and C_t revealed characteristic and similar patterns of change in both the saline and 10% protein infusion groups. R_t fell significantly from peak values (mean 24.3 x 10^3 mmHg/ml/min) the first 20 minutes, and then by less significant amounts throughout the course of infusion to mean values of 11.5 x 10^3 mmHg/ml/min at 60 minutes (Tables A.6 and A-7). With both infusates C_t increased during the infusion from an initial mean value of 0.21 x 10^{-3} ml/mmHg to 4.85 (saline) and 5.55 x 10^{-3} ml/mmHg (20% protein) at 60 minutes (Tables A-6, A-7).

3.1.v CORTICAL SOMATOSENSORY EVOKED POTENTIALS

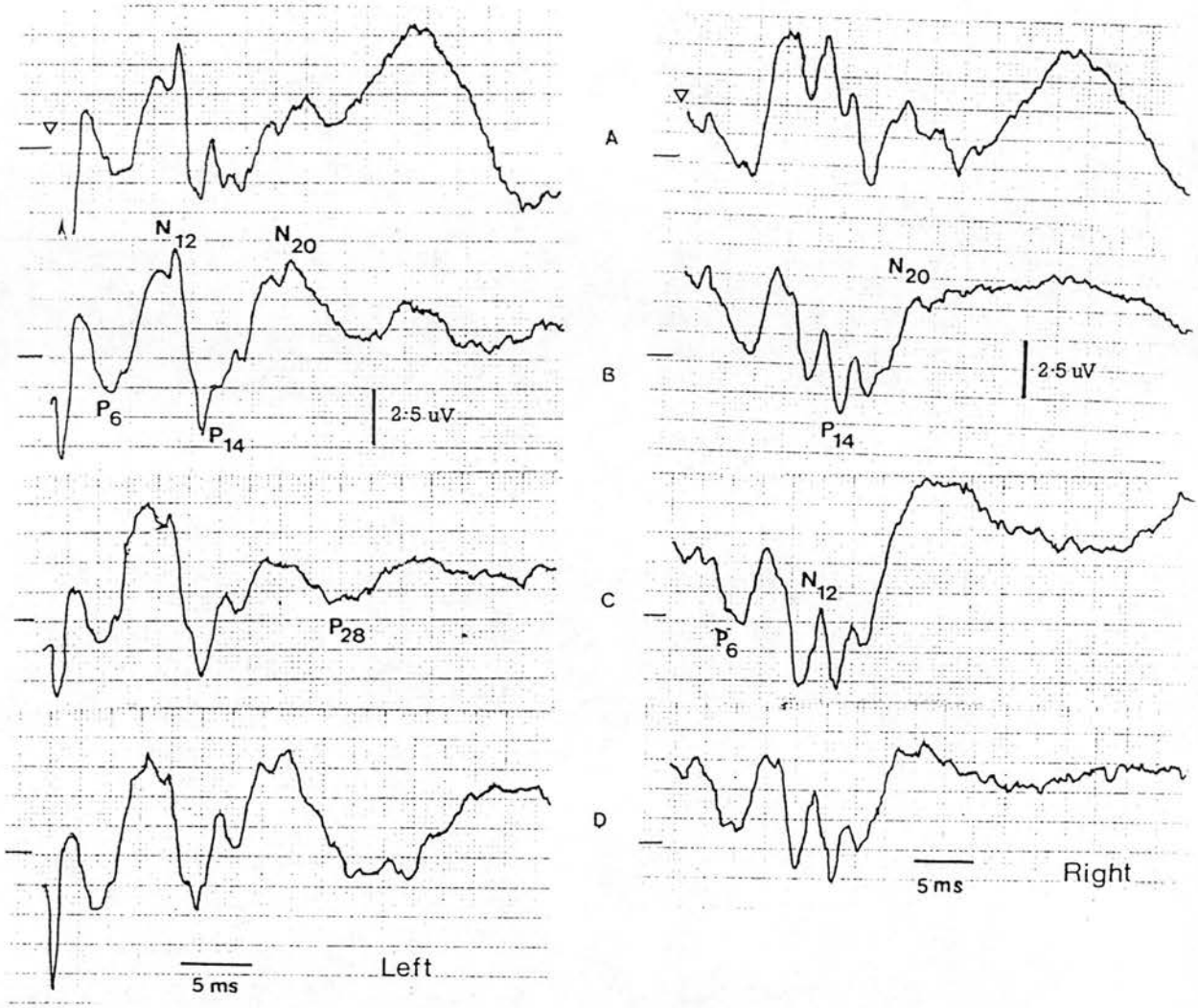

Figure 6: Right and left rat cortical SEP waveforms following contralateral forepaw stimulation during left frontal intracerebral infusion of 0.1 ml 20% protein/hr. A = baseline; B = 20 min; C = 40 min; D = 60 min.

Characteristic cortical SEPs following forepaw stimulation were obtained (Fig 6). The major components in the initial 35 ms were P_6 N_{12} P_{14} N_{20} and P_{28}. The amplitude of the maximal N-P component varied between animals from 3 to 13 uv, but in general amplitude of the SEP remained stable for both infused and control hemispheres during the study. For comparative purposes the latencies of the SEPs from the infused hemisphere were compared to those of the contralateral hemisphere. There was no significant

asymmetry in SEP short or long latency components in the 0.1 ml saline infusion group (Table A.8). In the 20% protein infusion group the P_{28} component from both the infused and contralateral hemisphere was increased by 2-3 ms over the one hour infusion period, otherwise the SEP waveform remained stable (Table A.9).

3.1.vi CEREBRAL BLOOD FLOW

CBF data was pooled so that at least 10 flows were obtained for each electrode locus in both ssaline and 20% protei infusion experiments. Twenty five minute intervals between flows were required in order to obtain stable electrode baselines. Two clearances were performed in each experiment to check electrode stability before recording baseline data. In all experiments CBF values below 20 ml/100g brain/min were considered to be flows from either white matter or damaged cortex, and were discarded.

During saline infusion there was a tendency for the CBF adjacent to the left frontal infusion needle to decrease from a mean baseline value of 37 ml/100g/min to 29 ml/100g/min and remain depressed during the infusion (Fig 7 and Table A-10). A similar but transient (20 minute) reduction was also seen in the left posterior parietal region. Because of the spread of the data and the magnitude of the SD the reduction in CBF adjacent to the infusion site was not statistically significant ($p = 0.15$). The large SD occurred because individual CBF values ranged from 22 - 81 ml/ 100 g brain/ minute for baseline flows, and remained at these levels, at all locations, throughout the experiment. The right hemispheric CBF remained stable (mean circa 37 ml/100g/min) throughout the course of infusion.

During 20% protein infusion the CBF decreased at all electrode locations over the initial 20 minutes but by 70

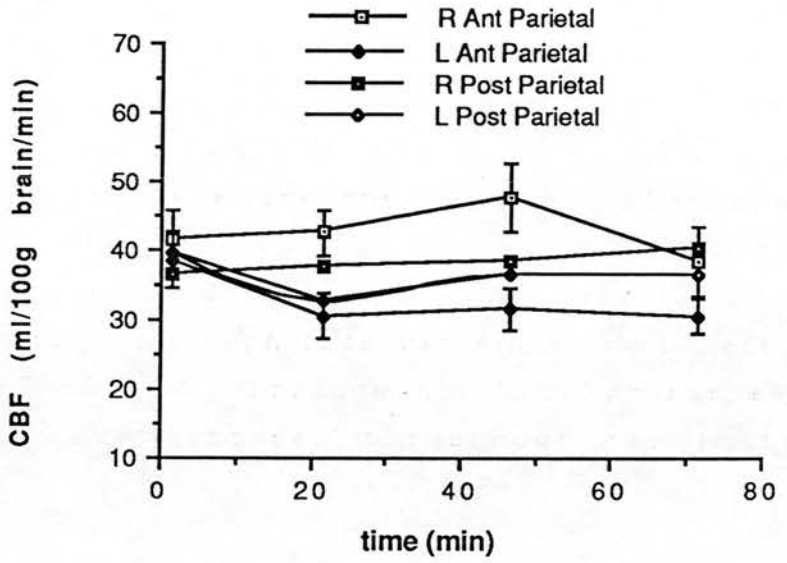

Figure 7: Regional CBF changes during 0.1 ml/hr saline infusion into the left caudatoputamen nucleus. Data points are mean, and where shown, ± SEM.

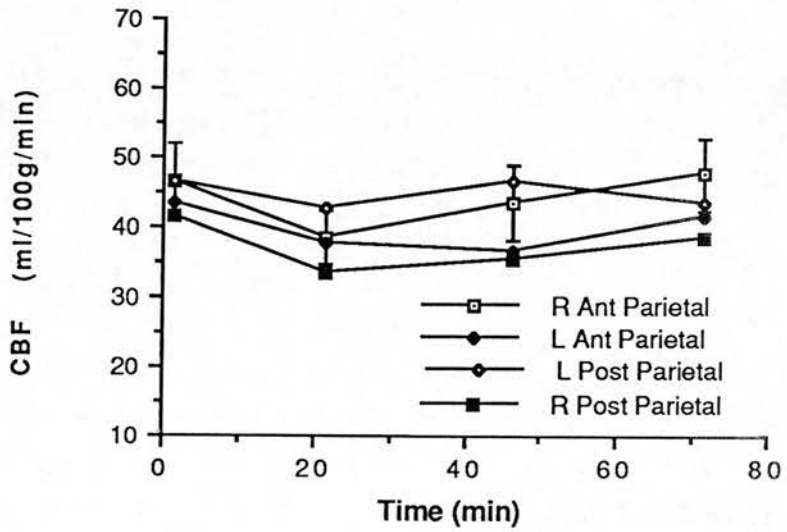

Figure 8: Regional CBF changes during 0.1 ml/hr 20% protein infusion into the left caudatoputamen nucleus. Data points are mean, and where shown, ± SEM.

minutes was similar to baseline values (Fig 8 and Table A.11). Due to the size of the SD none of these changes were statistically significant ($p = 0.26$ for the difference between baseline and 20 minute CBF values at the L anterior parietal electrode). The range of individual values for baseline CBF was large (25 - 81 ml/ 100 g brain/ min), although this was smaller at later time points (21 -67 ml/100 g brain/min). Similar ranges were recorded at all electrodes throughout the course of experiments.

Following the left frontal intracerebral infusion the cerebrovascular reactivity to P_aCO_2 was tested over the range 25 to 59 mmHg. CBF data was pooled from a large series of experiments (n = 16 saline infusion, n = 11 protein infusion) to enable acquisition of sufficient flow values across the spectrum of CO_2 values.

A series of experiments performed to obtain normal cerebrovascular reactivity data for rats using this anaesthetic protocol has previously been published and recorded an increases of 1 ml/ 100 g brain/ min for each one torr increase in P_aCO_2 in the P_aCO_2 range 23 to 60 mmHg (Bell et al, 1985). The regression equation that described this relationship was;

$$CBF = 1.0\ (P_aCO_2) + 2$$

$$n = 50 \qquad r = 0.70 \qquad p < 0.001$$

with CBF expressed as ml/100g brain/min and P_aCO_2 as mmHg.

Following saline infusion cerebrovascualr reactivity to changes in P_aCO_2 was preserved at all electrode locations with an increase in CBF of 1 - 1.5 ml/ 100 g brain / min per torr increase in CO_2 (Table A.12). Following the 20% protein infusion focal CBF CO_2 reactivity adjacent to the infusion site was reduced by 65% compared to the noninfused hemisphere (Table A.12). The correlation coefficient for the CBF and P_aCO_2 data at this location

was also substantially reduced when compared to the other locations but analysis of covariance revealed the differences between the two anterior parietal locations to be not statistically significant. Reactivity was preserved at normal levels at the other locations following 20% protein infusion (Table A.13).

3.1.viii BLOOD BRAIN BARRIER DISRUPTION AND HISTOLOGICAL STUDIES

Light microscopic studies of H & E stained sections of the rat forebrain were studied after left frontal infusion of 2% Nile blue. These studies showed that the infusate was deposited at the junction of the hemispheric white matter and caudate nucleus, and spread along the white matter planes medially into the corpus callosum, and laterally into the corona radiata. There was also mild ipsilateral ventricular effacement (Fig 9). Light microscopic studies following saline infusion revealed pallor, vacuolation and expansion of the subcortical white matter from the corpus callosum medially to the anterior amygdaloid area laterally. The space between fibre tract bundles was clearly enlarged but astrocytes and oligodendroglia appeared normal. The caudate nucleus and deep cortical laminae were normal.

Examination of coronal sections of the rat brains that were given 1 ml/kg of 2% Evans blue one hour after infusion and one hour prior to sacrifice revealed no intraparenchymal staining following the sham, saline or 20% protein infusions. There was also minimal staining detected beneath both the burr hole and at the site of the infusion needle tract.

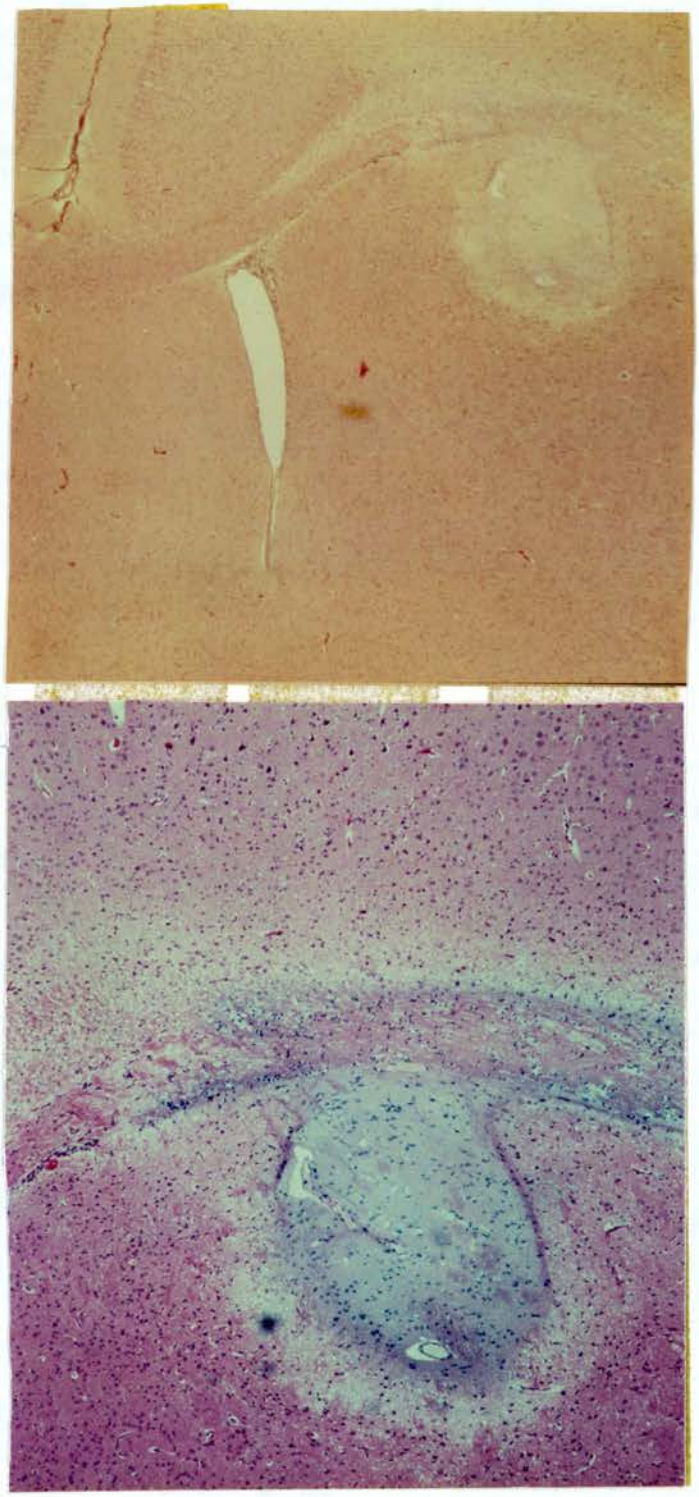

Figure 9: Low (x40) and high (x100) power photomicrographs of coronal sections of the rat brain at the plane of infusion site. The infusate (2% Nile Blue in saline) is deposited into the external part of the caudatoputamen nucleus deep to the subcortical white matter (cf Fig 2). There has been spread of the infusate into the callosal fibres and deeper cortical laminae, but spread within the caudatoputamen nucleus is limited. The white matter extracellular space appears trabeculated. Both sections H & E.

3.2 FELINE MODEL OF INFUSION OEDEMA

3.2.i General comments

A total of 40 experiments was performed, these included

4 Sham infusion	7 Arachidonic acid infusion
4 Saline infusion	8 Glioma cyst infusion
9 20% protein infusion	8 Bradykinin infusion

Administration of the intraperitoneal barbiturate was uncomplicated and general anaesthesia was usually present within 10-15 minutes. Thereafter the animal tended to remain metabolically and physiologically extremely stable over a total anesthesia time of 10-11 hours. After the cat was positioned in the stereotaxic frame, the order of cranial preparation of the experiment was (1) drilling of all burrholes, (2) placement of 6 platinum iridium electrodes, (3) placement of infusion needle, (4) placement of intraventricular needle and (6) placement of Ag/AgCl extracranial disc electrodes. This sequence enabled a longer period of stabilization for the platinum /iridium electrodes, and least probability of dislodging the ventricular needle. Preparation usually took four hours, followed by the three hour infusion period and a further three hours to acquire the CBF CO_2 and MEP data.

3.2.ii BRAIN WATER CONTENT AND SPECIFIC GRAVITY

In all series of experiments mean water content of cortical tissue from the noninfused (control) left hemisphere ranged between 78.5 % (SG 1.0465) and 81.0 % (SG 1.0399). Following the various infusates the cortical water content of the infused right hemisphere was either similar to or slightly greater (1 - 2 %) than the noninfused hemisphere. The maximal increase in cortical

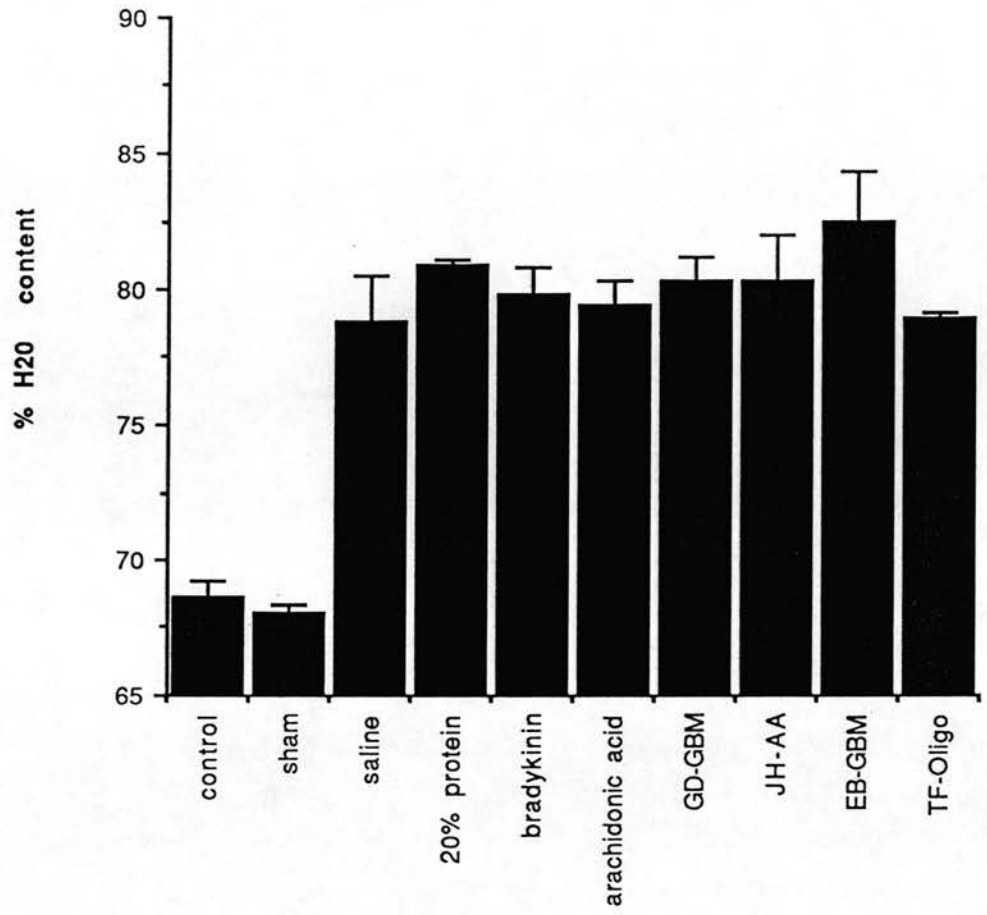

Figure 10: White matter water content following 0.6 ml infusion of various solutions into the right forebrain white matter. Control values are for the left anterior forebrain white matter. All data mean + SD.

water content (2.2 %) occurred following arachidonic acid infusion. Although this represented a statistically significant increase ($p = 0.008$) the elevated cortical water content (80.7 %) was lower than control values from other experiments (Tables A.13 to A.22).

The mean white matter water content for the noninfused (control) left anterior centrum ovale ranged from 67.2 % (SG 1.0436) to 69.9 % (SG 1.0407). In the sham infused cats no significant difference ($p = 0.45$) in white matter water content was detected (Table A.13). Increases in white matter water content following the various infusions

ranged from 7.9 to 12.5 g H_2O/100 g tissue and were all highly significant (Fig 10 and Tables A.14 to A.22). The increase in white matter water content was not related to the administered dose of either arachidonic acid (2 - 15 mg/ml) or bradykinin (5 - 150 ug/ml). Infusion of cyst fluids from glioblastoma, anaplastic astrocytoma or oligodendroglioma all produced similar increases in white matter water content (Tables A.19 to A.22).

3.2.iii INTRAVENTRICULAR PRESSURE

ICP monitoring through the ventricular needle was usually obtained without difficulty. Ventricular placement of the needle was confirmed by a rapid 5 - 10 mmHg increase in ICP with manual compression of the cat abdomen. Baseline mean ICP recorded in the various series of experiments ranged from 4.8 to 9.8 mmHg, with a pulse pressure of 1 -2 mmHg, at P_aCO_2 levels of 33 mmHg and mean arterial BP of 120 mmHg.

Various patterns of ICP change were recorded both during and after the infusions (Fig 11). In the 3 sham infusion cats mean ICP, at normocapnia, increased from baseline mean of 4.8 mmHg to 7.8 mmHg at 180 minutes (Table A.23). In two of these animals ICP remained stable at around 5 mmHg whilst in the third animal ICP increased from baseline levels of 5 mmHg to 15 mmHg at 180 minutes.

ICP was recorded in four cats having intracerebral saline infusion. In all animals mean blood pressure (120 mmHg) and P_aCO_2 (34 mmHg) were similar throughout the course of experiment. Three cats (including one saline/5% ether infusion) had infusion at 0.2 ml/hr and one had an infusion at 0.3 ml/hr. The mean baseline ICP was 5.5 mmHg which increased at three hours to 16 mmHg with a 0.2

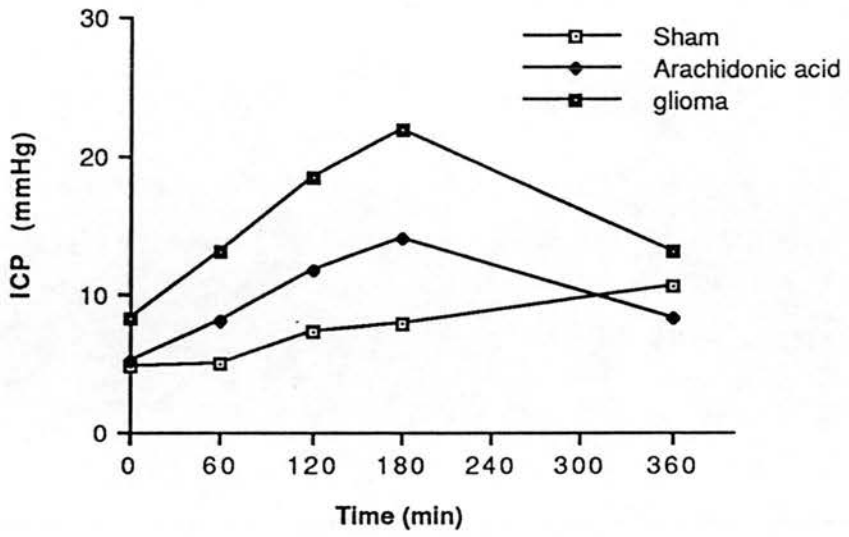

Figure 11: Changes in mean ICP in the cat during and after a 180 minute period of either sham infusion or intracerebral infusion with arachidonic acid or glioma cyst fluid. The mean rise in ICP with saline and 20% protein infusates was very similar to that recorded with arachidonic acid infusion. The mean rise in ICP recorded with bradykinin infusates was between that recorded with arachidonic acid and glioma cyst infusate. With the exception of the sham infusion mean ICP rises were statistically significant (see Tables A-24 to A-31).

ml/hr infusion and 36 mmHg with a 0.3 ml/hr infusion (Table A.24).

There were moderate elevations in ICP during bradykinin, 20% protein and arachidonic acid infusion at 0.2 ml/hour (Fig 11). ICP increases, from baseline means of around 5mmHg, ranged from 8.9 to 14 mmHg at 180 minutes and all were statistically significant (Tables A.25 to A.27). Three hours after cessation of the infusions ICP had decreased from 180 minute values in all series of experiments.

After infusion with the various glioma cyst fluid infusates ICP at 180 minutes had risen from mean baseline values of between 3 and 9.8 mmHg by between 9.2 and 15.3

mmHg. Three hours after completion of the infusion mean ICP had fallen back towards baseline values (Tables A.28 to A.31). When the glioma cyst fluid experiments were analysed collectively the rise from baseline to 180 minute ICP values was highly significant ($p < .001$).

When the 180 minute sham infusion mean ICP was compared to the 180 minute mean ICP after the various infusions there was no statistically significant difference between any group. P values ranged from 0.19 (sham versus 20% protein) to 0.013 (sham versus glioma cyst infusion). Significance required a p value of < 0.0083.

3.2.iv INTRACRANIAL PRESSURE VOLUME INDEX

PVI was calculated following a 0.1 ml saline intraventricular bolus in all series of experiments before, each hour during and after intracerebral infusion. Baseline mean PVI ranged from 0.343 to 0.538 ml for all series of experiments. PVI did not alter significantly in any group throughout the 6 hour period of experiment (Tables A.32 and A.33).

3.2.v CSF OUTFLOW RESISTANCE (R_o)

R_o was calculated following 0.1 ml saline intraventricular bolus before, each hour during and after the intracerebral infusion. In all except one series of two experiments, where mean baseline R_o was 170 mmHg/ml/min, mean baseline R_o ranged from 70 to 99 mmHg/ml/min.

Statistically insignificant rises from baseline to 180 minute R_o values were encountered with sham (mean increase 79 mmHg/ml/min), 20% protein (64), and saline (85) infusates (Table A-34). Rises from baseline to 180 minute

R_o values that were statistically significant at the 0.05 to 0.01 level (Table A-34) occurred after bradykinin (mean increase of 119 mmHg/ml/min and arachidonic acid (336) infusions. The most significant increase in R_o occurred after the glioma cyst infusates ($p = .002$; when analysed collectively), although the increases with specific cyst fluids did range from 82 (EB-GBM) to 319 (GD-GBM) mmHg/ml/min (Table A-35).

Three hours after completion of infusion R_o was returning towards baseline values in the sham, arachidonic acid, bradykinin and OLI-TF infusates, but remained elevated in the 20% protein and all malignant glioma infusates.

3.2.vi CRANIOSPINAL COMPLIANCE (C_i)

Lumped C_i was calculated using PVI data before, during and after infusion. Baseline C_i in different series of experiments ranged from 0.022 to 0.047 ml/mmHg. During all series of experiments C_i fell during the period of infusion (Fig 12). This decrease in C_i was lowest (.018 ml/mmHg), and not statistically significant, in the sham infusion cats (Table A.36). Mean C_i decreased by 70% during the period of saline infusion ($p = 0.013$). In the other infusion groups the fall in C_i was of similar magnitude and level of statistical significance (Table A-36 and A-37).

At the completion of the infusions C_i was lowest in the glioma cyst infusion experiments. Although these animals also had the lowest mean baseline levels of C_i the reduction in C_i, when all glioma cyst infusion cats were analysed collectively, was highly significant ($p = 0.003$). Three hours after completion of the infusion C_i values were generally similar to 180 minute values.

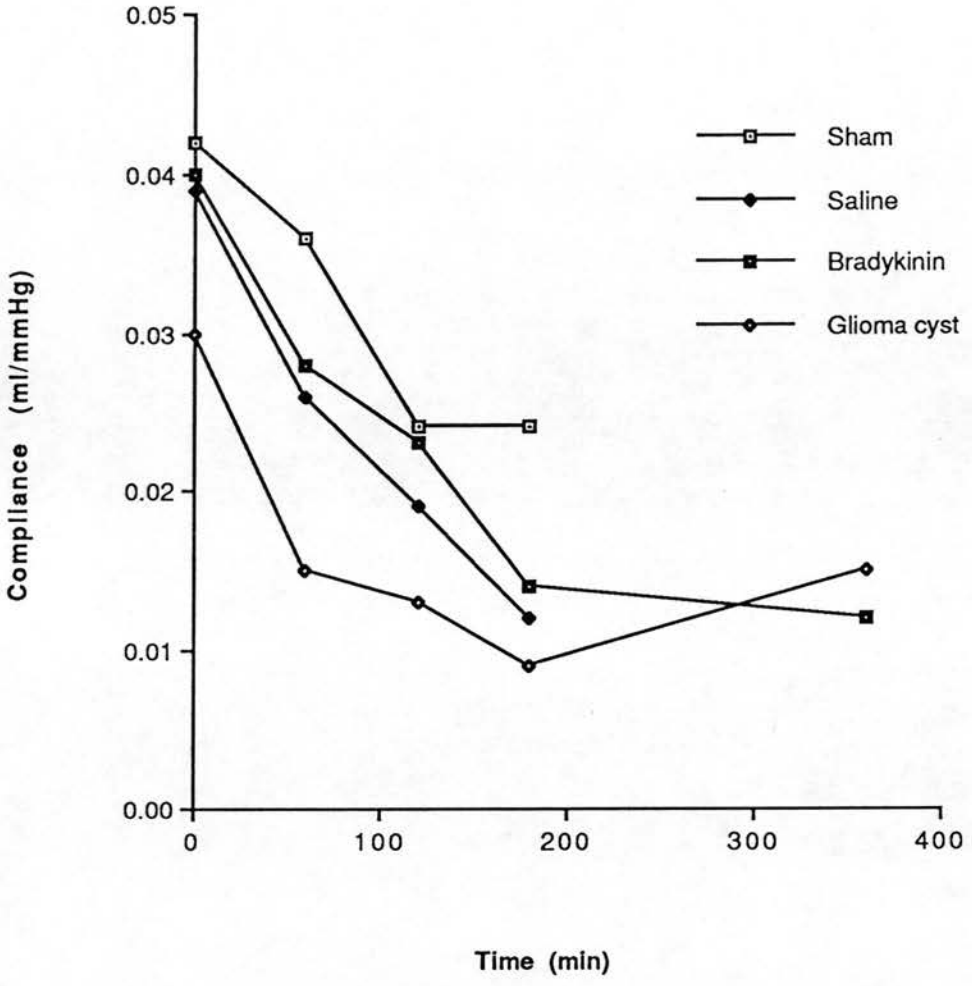

Figure 12: Patterns of change in lumped craniospinal compliance from baseline values during 180 minute period of intracerebral infusion. Compliance fell significantly during the infusion period with all solutions. After cessation of the infusion compliance either stabilised around 180 minute values or slowly increased. The fall in compliance with sham infusion is not statistically significant,

3.2.vii BRAIN TISSUE HYDRAULIC RESISTANCE

Brain tissue hydraulic resistance (R_t) was recorded during infusion in 8 cats. The pattern of infusion pressure (P_{inf}) change was similar regardless of the infusate, in that P_{inf} rose in the initial three minutes to around 35 mmHg, then over the subsequent 2- 5 minutes fell to around 15 mmHg. Thereafter P_{inf} slightly increased until the infusion was complete (cf Fig 4 and Table A.38). In most

cases after the initial 10 minutes of infusion the P_{inf} was several mmHg above the ICP. Calculation of the R_t ($R_t = P_{inf} / Q$, where Q, the flow rate was .0033 ml/min) revealed that there was a highly significant decrease ($p < 0.001$) in R_t from mean peak (2-3 minute) value of 9.8 x 10^3 mmHg/ml/mins to 4.3 x 10^3 mmHg/ml/min 10 minutes after the start of infusion (Table A.38). Although R_t susequently increased over the remaining 170 minutes of infusion, these changes were not significant.

3.2.viii CORTICAL SOMATOSENSORY EVOKED POTENTIALS

Cortical SEPs following contralateral forepaw stimulation were recorded in all series of experiments. Epochs were set at 50 and 100 ms to enable documentation of both the short and long latency components. Waveforms recorded were polyphasic and contained major components with latencies at N_6 P_{10} N_{17} P_{28} and N_{47}. This pattern of cortical SEP is illustrated in Fig 13. The amplitude of the P_{10} - N_{17} component was variable between cats (range 3 - 35 uV) but remained stable to within several uV for any individual hemisphere during an experiment. For comparative purposes the latencies of the infused right hemisphere SEPs were compared with those of the noninfused (control) hemisphere

The components of the cortical SEP with latencies shorter than the P_{28} were generally highly reproducible throughout all series of experiments although in some animals the N_6-P_{10} component was a W shaped complex with latencies of N6-P7-N8-P10 (see 4 hour right hemispheric waveform Fig 15). Where there was a either shortening or delay in waveform latency such changes were recorded bilaterally (Tables A-40, 41 and A-44). The P_{28} and especially the N_{47} latencies were subject to some variation but there was no particular trend in any series of experiments. In particular the

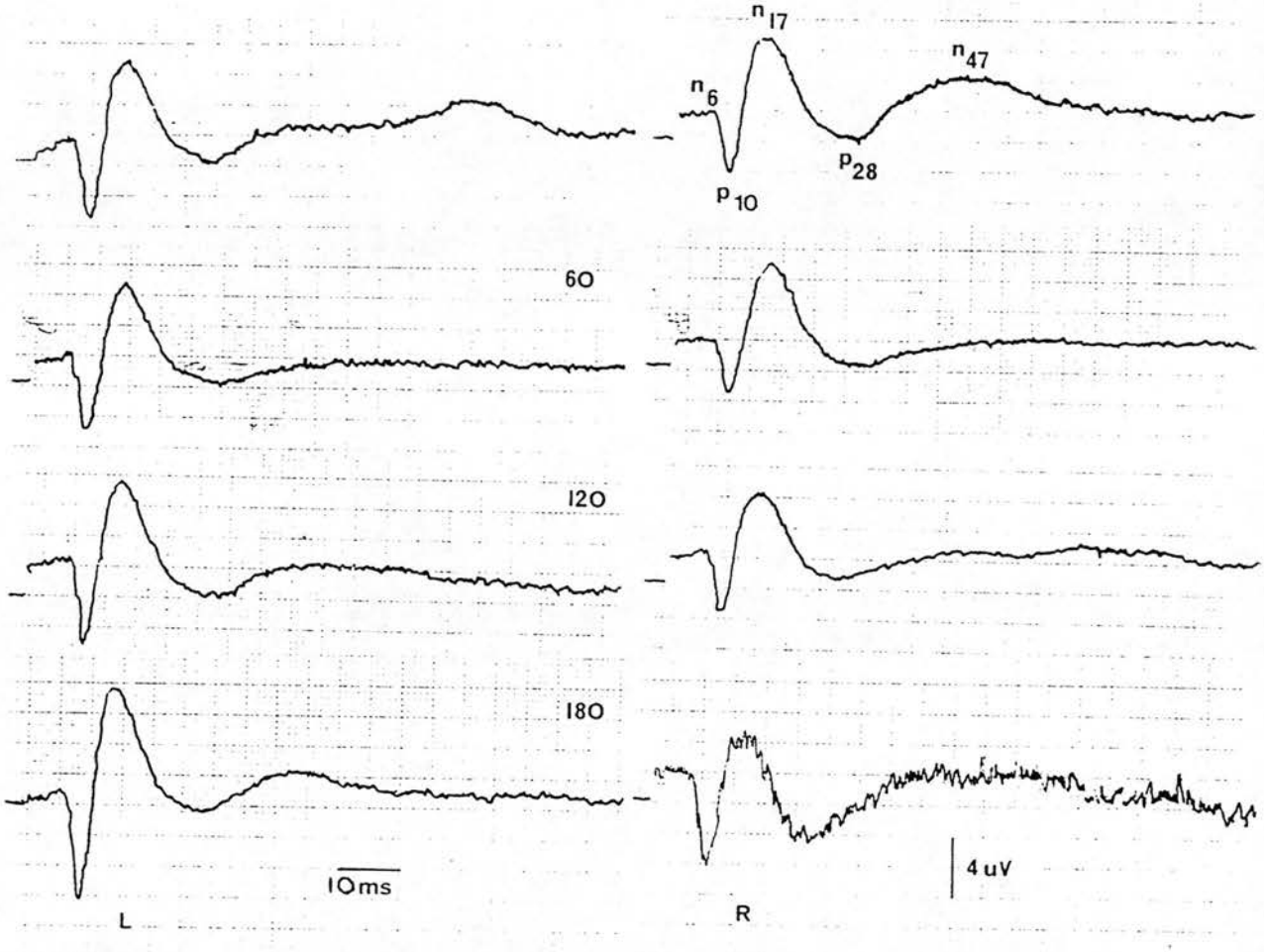

Figure 13: Cortical SEP waveforms recorded from the left (L) and right (R) hemispheres following contralateral median nerve stimulation in the cat, during a 180 minute period of saline infusion into the right forebrain white matter. The waveform is composed of N_6, P_{10}, N_{17}, P_{28} and N_{47} components that are reproducible throughout the infusion period.

range of values recorded for these two components was similar for the two hemispheres (Tables A-39 to A-47).

Cortical SEPs from the infused hemisphere changed in three cats. These were the GD-GBM cat number 1 (Fig 14), the solitary cat infused with 150 ug/ml bradykinin (Fig 15)

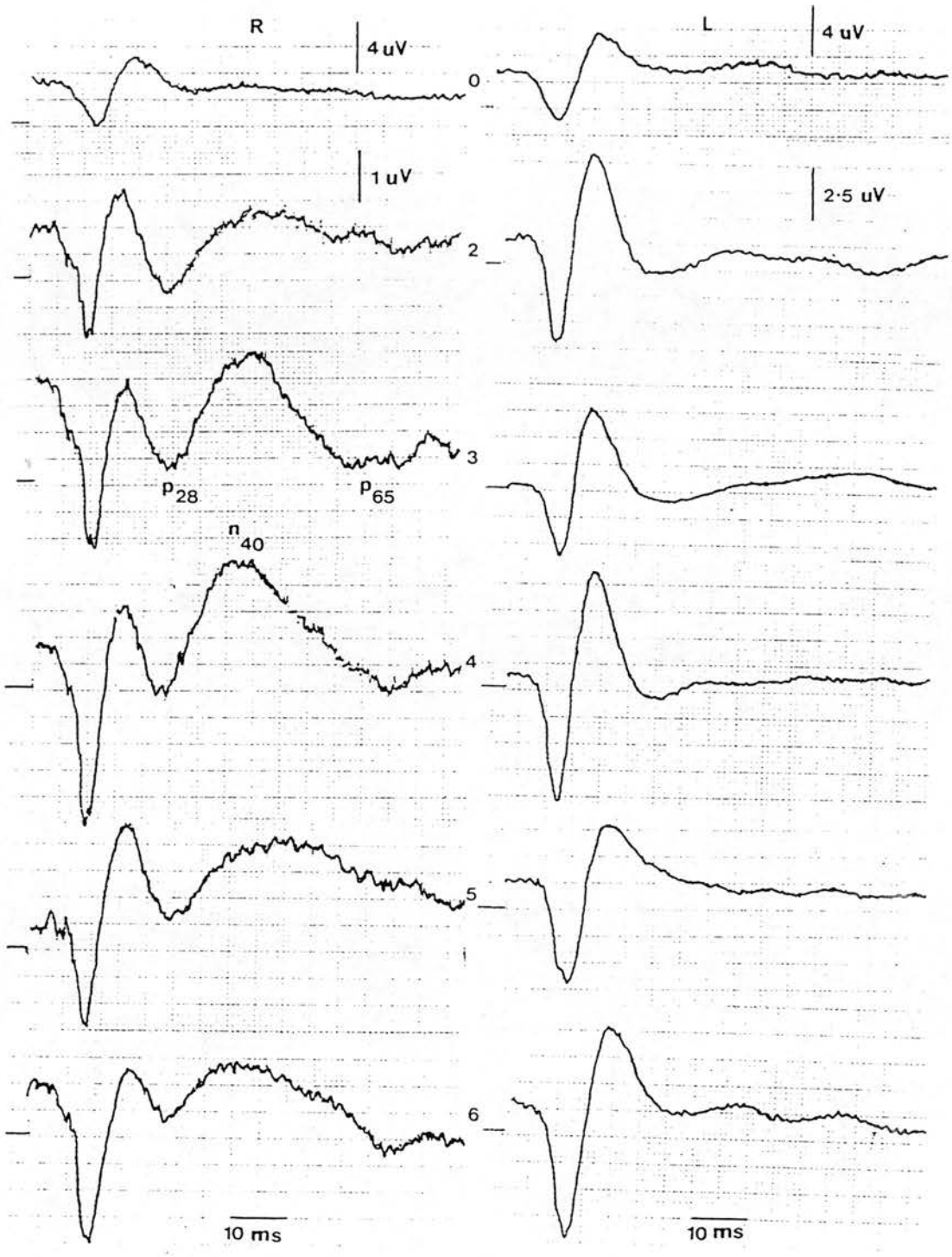

Figure 14 : Cat cortical SEP waveforms recorded from the right (R) and left (L) hemispheres following contralateral median nerve stimulation, during and after three hour period of infusion of GD-GBM glioma cyst fluid into the right forebrain white matter. The baseline waveforms are symmetrical (0). After two hours a P_{28}-N_{40}-P_{65} component becomes prominent in the right cortical SEP and persists, although decreasing in amplitude after three hours, until the end of the experiment. The left cortical SEP remains stable. 0 - 6 refer to hours after start of the infusion.

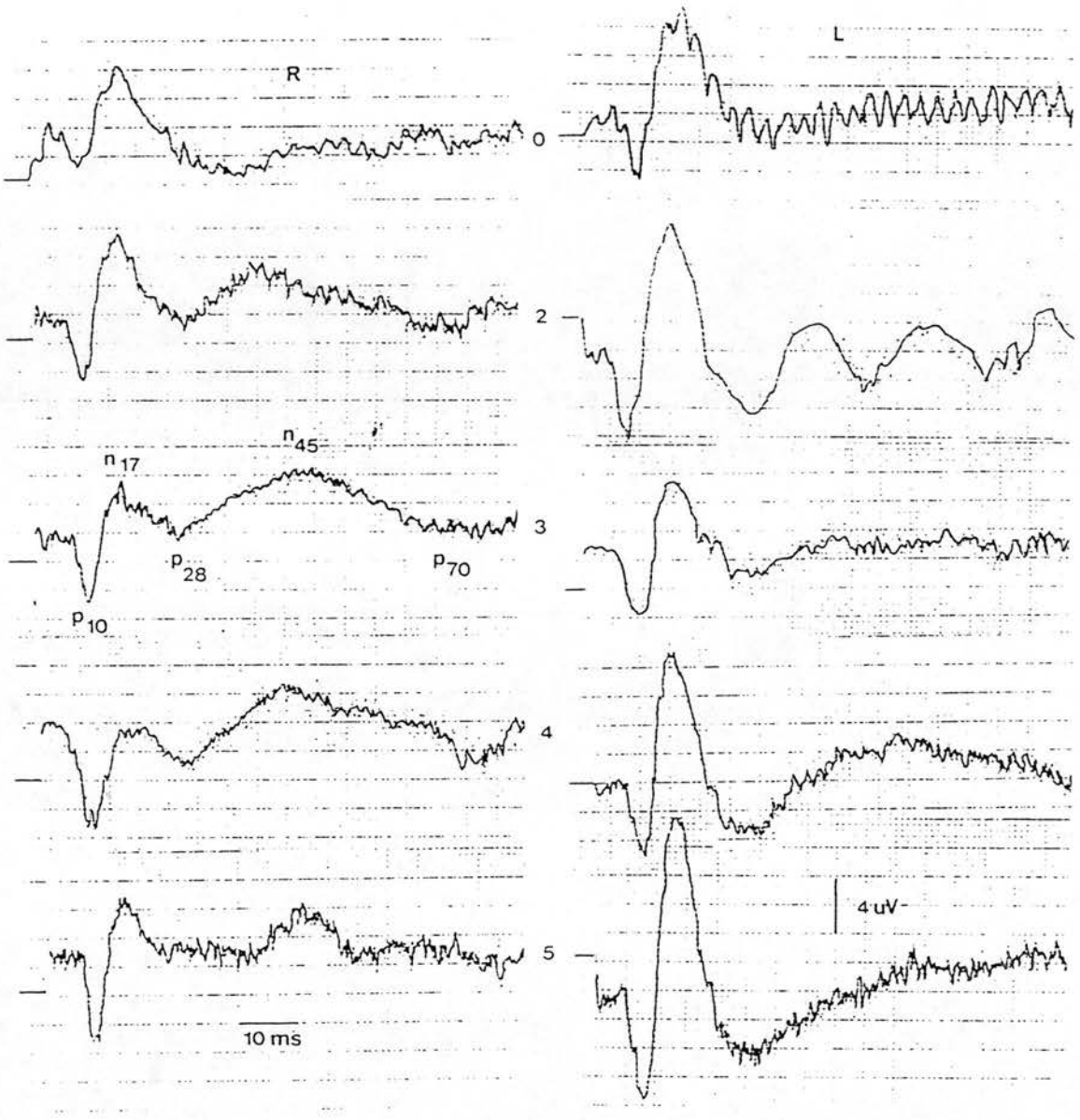

Figure 15 : Cat cortical SEP waveforms recorded from the right (R) and left (L) hemispheres following contralateral median nerve stimulation, during and after three hour period of infusion of bradykinin 150ug/ml into the right forebrain white matter. The baseline waveforms are symmetrical although a little "noisy" (0). After two hours a P_{28}-N_{45}-P_{70} component becomes prominent in the right cortical SEP and persists, although decreasing in amplitude after four hours, until the end of the experiment. Between three and four hours there is also flattening of the N_{17}-P_{28} amplitude. 0 - 5 refer to hours after start of the infusion.

and the TF-oligo cat. The major changes seen in these

experiments were flattening of the N_{17}-P_{28} component, the development of a large amplitude, broad latency negative wave with peak latency around 40 -50 ms and a prominent P wave with latency between 57-67 ms (Fig 14 and 15). In none of these cats was there impairment of cerebral perfusion pressure although there was a significant focal (right frontal) reduction in rCBF in the GD-GBM cat (see 3.2.x). The change in SEP with the GD-GBM infusion occurred only in the first of the two cats studied with this glioblastoma cyst fluid even though both cats had a similar focal reduction in rCBF.

3.2.ix MOTOR EVOKED POTENTIALS

Motor evoked potentials (MEPs) were recorded subdurally at between T_6 and T_{12} following transcranial stimulation, at the conclusion of the cerebrovascular reactivity experiments. Polyphasic waveforms consisting of one or two large initial negative (N_1, N_2) waves and subsequent smaller amplitude, longer latency N waves were recorded in each cat (Fig 16). All the waveform components were short latency with the longest component being less than 7 ms.

In no experiment was there any significant asymmetry of response when comparing the latencies of the N_1 waves generated by right and left hemicranial stimulation or by direct cortical stimulation throught the platinum iridium electrodes (Tables A.48 to A-53). The amplitudes for the N_1-P_1 component are also included in these tables. The magnitude of this component wave was directly related to stimulus intensity when a submaximal stimulus was used to evoke the response. This phenomenon is well illustrated in a series of experiments performed using graded direct cortical stimulation through a frontal platinum iridium electrode (Appendix 4)

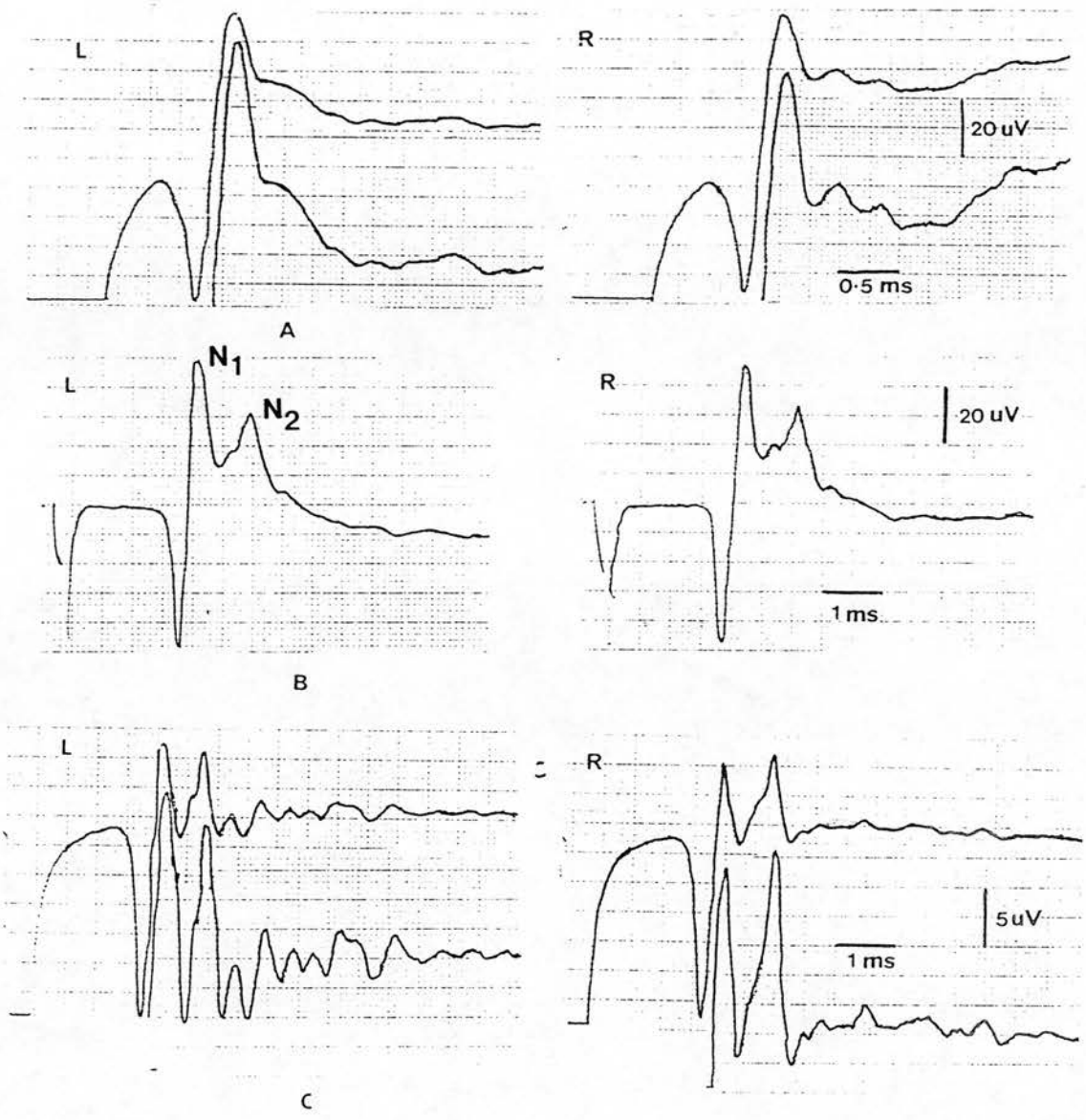

Figure 16: Patterns of thoracic spinal MEPs recorded following hemicranial stimulation in the cat. The waveform was usually characterised by one (A) or two (B,C) large amplitude negative components, with a variable number oflonger latency smaller amplitude negative waves (A right and C left). The large amplitude N components were symmetrical in all animals despite the right sided subcortical oedema and presence of arachidonic acid, bradykinin, 20% protein and glioma cyst fluid in the oedema fluid. The number of smaller longer latency negative waves was variable but was not confined to the waveform following right hemicranial stimulation (cf A and C). L = MEP waveform recorded following left hemicranial stimulation, R that following right sided stimulation. Traces A, B cats infused with JH-AA glioma cyst fluid, Traces C infused with bradykinin 5 ug/ml.

The number of waveform components following N_1 was variable and ranged from none to eight. The number of these subcomponents varied between experiments using the same infusate, however these differences were not confined to the MEP generated by stimulation of the right (infused) motor cortex or hemisphere (see Fig 16 and Table A.53).

3.2.x CEREBRAL BLOOD FLOW

Characteristic exponential washout patterns of H_2 clearance curves were obtained in all experiments. For purposes of the study the flows in the right frontal region (ie adjacent to the infusion locus) were compared to those in the left frontal region. Electrodes recording baseline CBF of less than 20 ml/100 gm brain/min were considered to represent pure white matter blood flow.

Baseline frontal and parietal mean rCBF varied from 26 to 52 ml/100 gm brain /min in the various series of experiments, with most values lying between 40 and 50 ml/100 g brain/min (Tables A.54 to A.62). The baseline R and L frontal CBF values recorded in the sham cats (26 and 28 ml/100 g/min respectively) were significantly lower than in any other series. However similar flow values were recorded consistently throughout the experiment (Table A.54).

Mean CBF adjacent to the right frontal infusion site did not change consistently or significantly from baseline values throughout the saline, 20% protein, bradykinin, arachidonic acid, JH-AA and TF-Oligo infusions. Mean CBF also remained constant at the other three electrode locations. The standard deviations for some of these flow values was high (22 and 23 ml/100 g brain/min) due to the spread of flow values eg the highest CBF value was 110

ml/100 gm brain/ min.

Following infusion of the GD-GBM cyst fluid there was a significant reduction in mean CBF adjacent to the right frontal infusion site from 49 to 19 ml/100 g/min (Table A.59). There was also a significant reduction in mean CBF (from 41 to 30 ml/100 g/min) adjacent to the infusion site with EB-GBM infusion. However a similar flow reduction was also seen in the contralateral frontal region (Table A.61).

CBF was recorded from electrodes in the white matter during the arachidonic acid and 20% protein infusion experiments. In neither of these experiments was there a significant change in CBF_w from baseline mean values of 17-21 ml/100 g/min, in either the infused or contralateral hemisphere (Table A.63 and A.64).

At the completion of intracerebral infusion CBF CO_2 reactivity was studied over the range of P_aCO_2 values 25 to 56 mmHg. In 3 sham infusion experiments cerebrovascular reactivity was present bifrontally in all five functioning electrodes. rCBF increased by between 0.99 and 1.39 ml/100 g brain/min for each one torr increase in P_aCO_2. The equations denoting the relationship between frontal CBF and P_aCO_2, derived from linear regression analysis are

R Frontal $CBF_g = 1.39\ P_aCO_2 - 20$
$n = 11 \qquad r = .83 \qquad p < 0.01$

L Frontal $CBF_g = 0,99\ P_aCO_2 - 7.1$
$n = 17 \qquad r = .88 \qquad p < 0.001$

Following saline infusion CBF CO_2 reactivity was preserved in both frontal regions. rCBF increasing by 0.86 (right)

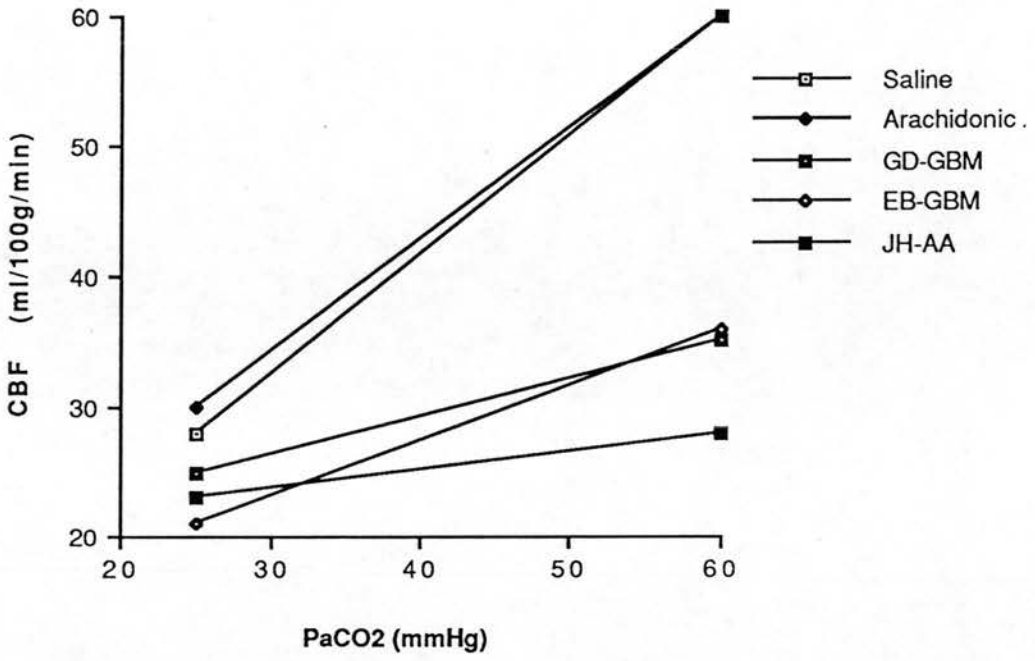

Figure 17: Patterns of CBF CO_2 reactivity seen after the various infusates. After saline, arachidonic acid and sham (not shown) infusion CBF increased approximately 3% for each mmHg rise in P_aCO_2. However after the malignant glioma cyst, bradykinin and 20% protein (both not shown) infusates CBF CO_2 reactivity is profoundly impaired.

and 0.88 (left) ml/100 g/min per torr increase in P_aCO_2. CBF reactivity was also preserved at all electrode sites following arachidonic acid infusion with CBF increasing by between 0.77 and 1.36 ml/100 g/min per torr increase in P_aCO_2 for the cortical electrodes (Fig 17) and 0.31 and 0.63 ml/100 g/min for the white matter electrodes (Tables A.65 and A.66).

With protein or peptide infusates CBF CO_2 reactivity was variably impaired. Following 20% protein infusion CBF reactivity was impaired with the correlation coefficients being low ($r = 0.30$ to 0.35) with no significant

correlation between CBF and CO_2 at any electrode location (Table A.67). Following bradykinin infusion CBF CO_2 reactivity was also similarly impaired at all electrode locations. The correlation coefficients ranged from 0.007 to 0.33, with none of these values being statistically significant (Table A.68).

After infusion of the tumour cyst fluids JH-AA and GD-GBM CBF CO_2 reactivity adjacent to the infusion site was impaired with neither correlation coefficient being statistically significant (Fig 17 and Table A.69). CBF CO_2 reactivity was present after infusion of EB-GBM cyst fluid but the level of reactivity (0.42 ml/100 g/min per one torr increase in P_aCO_2) was 60% lower than controls. Paradoxically following the TF-Oligo cyst fluid infusate reactivity was enhanced with CBF increasing by 2.2 ml/100g/min per torr increase in P_aCO_2. Following the tumour cyst fluid infusates reactivity was, with the exception of EB-GBM cyst fluid (where a decrease in CBF CO_2 reactivity was similar to the infused side) preserved in the contralateral frontal and parietal regions (Table A.69).

3.2.xi BLOOD BRAIN BARRIER DISRUPTION

Coronal sections of the cat brains revealed no intraparenchymal staining with Evans Blue following the sham infusion, saline and saline/5% ether infusions (Fig 18a). Following the 20% protein infusion there was extensive but light staining of the centrum ovale adjacent to the infusion site that extended posteriorly into the capsular fibres (Fig 18b). Following bradykinin 5000 ng/ml infusion staining was either absent or light and limited to the region directly adjacent to the infusion site. With 150 ug/ml bradykinin infusion there was light staining

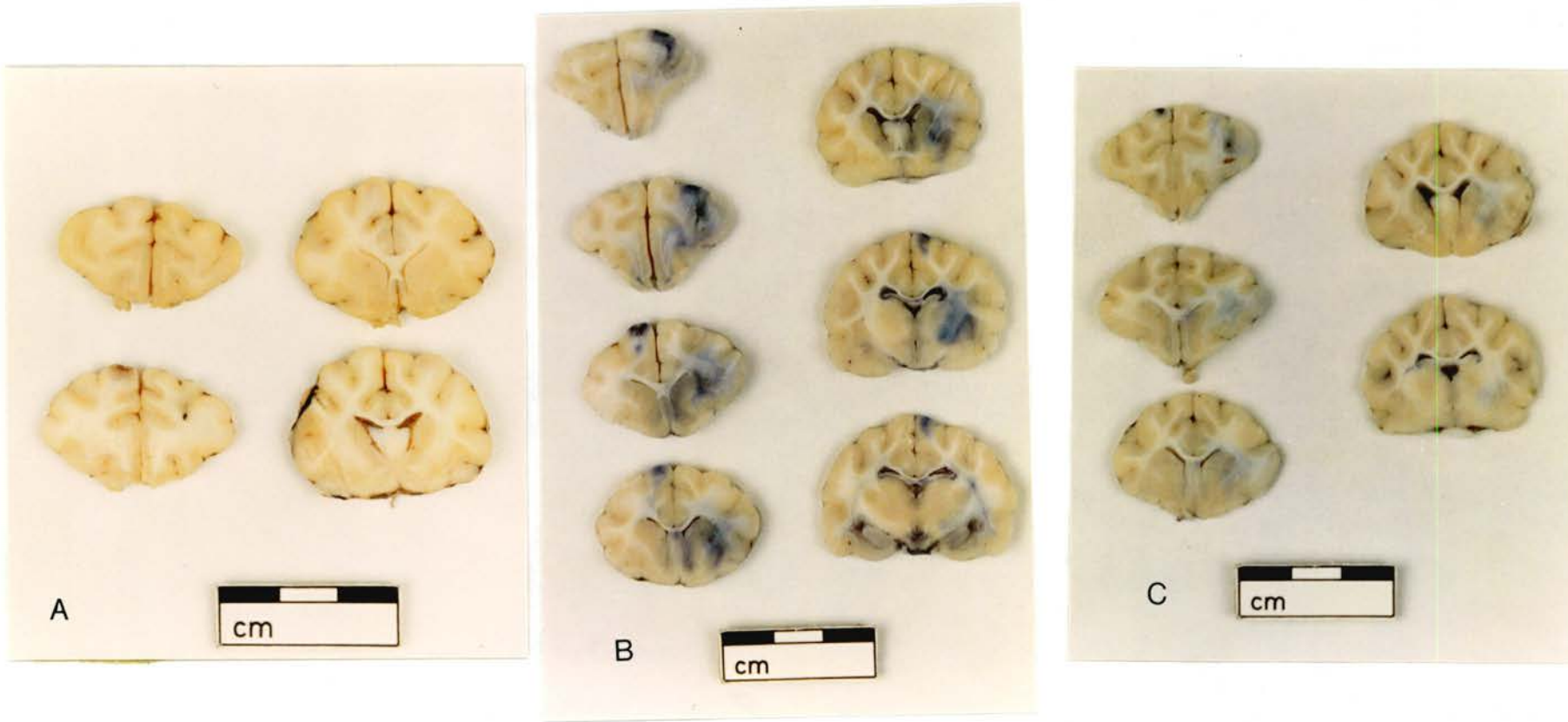

Figure 18: Coronal sections of the cat brain following infusion of various solutions into the right anterior forebrain white matter. After saline infusion there is minor local tissue expansion but no extravasation of intravenous Evans Blue dye (A). Following 20% protein infusion there is extensive extravasation of Evans Blue and local expansion of the white matter. There is also focal Evans Blue staining of the cortex in relation to the burrholes for both the intraventricular and infusion needles (B). Bradykinin infusion (15 ug/ml) caused local tissue expansion with flattening of adjacent gyri and extravasation of Evans Blue (C). The intensity and area of Evans Blue extravastion after arachidonic caid infusion was similar to that shown with bradykinin.

over a region of 20 mm^2 that extended posteriorly from the infusion site into the capsular and longitudinal association fibres (Fig 18c).

Intraparenchymal staining following arachidonic acid infusion was variable in area (range 15 - 50 mm^2) but generally light in intensity. Paradoxically this was maximal (50 mm^2 staining in the section 2 mm posterior to infusion site) with the lowest dose of arachidonic acid tested (2 mg/ml). With 10 mg /ml arachidonic acid infusion Evans blue extravasation was limited to a 15 - 30 mm^2 region adjacent to the infusion needle with minimal antero-posterior spread. In one cat there was also a small (estimated 0.3 ml) hematoma adjacent to the ventricular needle tract in the hemisphere contralateral to infusion. There was minimal BBB disruption adjacent to this hematoma cavity.

The most extensive extravasation of Evans Blue, and focal brain swelling, was found in all seven cats following the glioma cyst infusates. With GD-GBM cyst fluid the area of intense blue staining 2 mm posterior to the plane of infusion was 40 mm^2 (cat 1) and 64 mm^2 (cat 2). In both cats the disruption extended posteriorly in the association fibres to the thalamic region (Fig 19a). Following infusion of EB-GBM cyst fluid, similar patterns and degrees of Evans blue extravasation were noted although the hemispheric swelling was worse. Following infusion of JH-AA cyst fluid there was intense staining of the entire centrum ovale, arcuate fibres and outer cortical laminae in both cats. The blue staining extended both frontally and posteriorly to the retrothalamic region (Fig 19b). Infusion of TF-Oligo fluid aslo caused extensive Evans blue extravasation of variable intensity (Fig 19c).

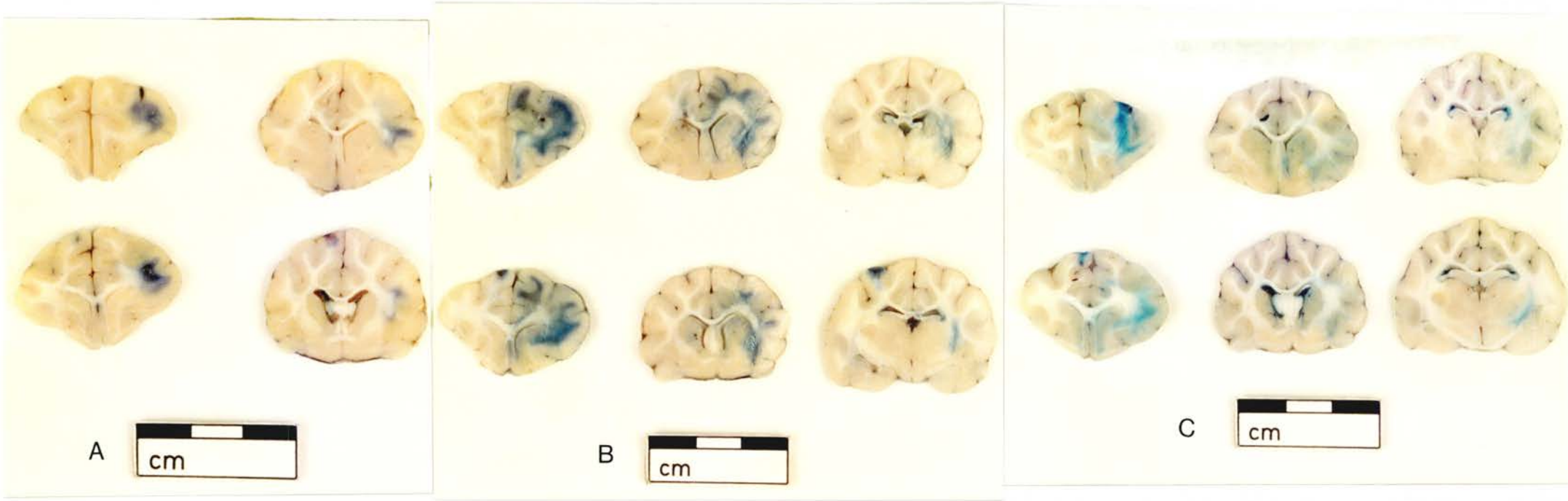

Figure 19: Coronal sections of the cat brain showing extravasation of intravenous Evans Blue dye following infusion of various glioma cyst fluids into the anterior forebrain white matter. With all infusates there is marked expansion of the white matter and flattening of the overlying gyri and obliteration of adjacent sulci. Extravastion after GD-GBM cyst fluid was limited but relatively intense (A). There is diffuse Blue staining of the white matter with hemispheric swelling after infusion of JH-AA cyst fluid (B). Extravasation is also extensive after infusion of TF-Oligo cyst fluid (C). With both the latter infusates the fibres of the corpus callosum show minimal local Evans Blue extravasation although the capsular fibres show extensive blue discolouration.

Blue staining of variable intensity was also noted in the cortex beneath some of the burrholes. In most cats two of the 8 drilled areas exhibited some cortical staining. In most animals this was superficial but in others very light, and local, staining of the deeper cortical lamina also occurred.

3.2.xii BRAIN HISTOLOGY

Some histological features were common to all infusates. In the regions adjacent to the infusion site there was obvious pallor of the white matter using both H&E and solochrome-cyanin stains. This pallor radiated rostrally into the gyral white matter, anteriorly and posteriorly along the long association fibres of the centrum ovale and caudally into the periventricular and capsular regions. In these areas there was expansion of the extracellular space of the white matter, which appeared vacuolated, and dissolution of the eosiniophilic ground substance (Fig 20a-c). Between the deep cortical laminae and oedematous brain there was a clear zone of approximately 300 u that clearly demarcated the cortical from the subcortical tissues (Fig 20b and c). In some sections there was a transitional zone between oedematous and normal white matter (Fig 21a). The subependymal white matter in the region of the right frontal ventricular horn was also oedematous but the ependymal epithelium was preserved. Axons and myelinated fibres appeared separated particularly in the oedematous corona radiata (Fig 21c). In all studies the cortical laminae appeared normal. In most animals there was some polymorphic infiltration of the subarachnoid and Virchow-Robin spaces.

Following saline infusion there were no additional features to those described above. After arachidonic acid

Legends to Figure 20 overleaf.

Figure 20a: Normal cortex and white matter stained with solochrome-cyanin. The gyral white matter is a uniform bluish green whilst the cortex (bottom right and top left) stains maroon (x 50)

Figure 20b: Cortex and oedematous white matter following infusion of saline into the forebrain white matter. The cortex (top right and bottom left) appears normal but the white matter appears vacuolated and stains less intensely than normal. In addition there is a clear zone demarcating the deepest cortical laminae from the underlying white matter. Beneath this clear zone the subcortical arcuate fibres appear to stain more intensely than the underlying gyral white matter (Solochrome-cyanin, x 50).

Figure 20c: Oedematous gyral white matter following saline infusion into the forebrain white matter. The white matter is vacuolated with partial dissolution of the normal eosinophilic ground substance. The deep cortical laminae are clearly demarcated from the gyral white matter by a vacuolated and relatively acellular zone (H & E x 100).

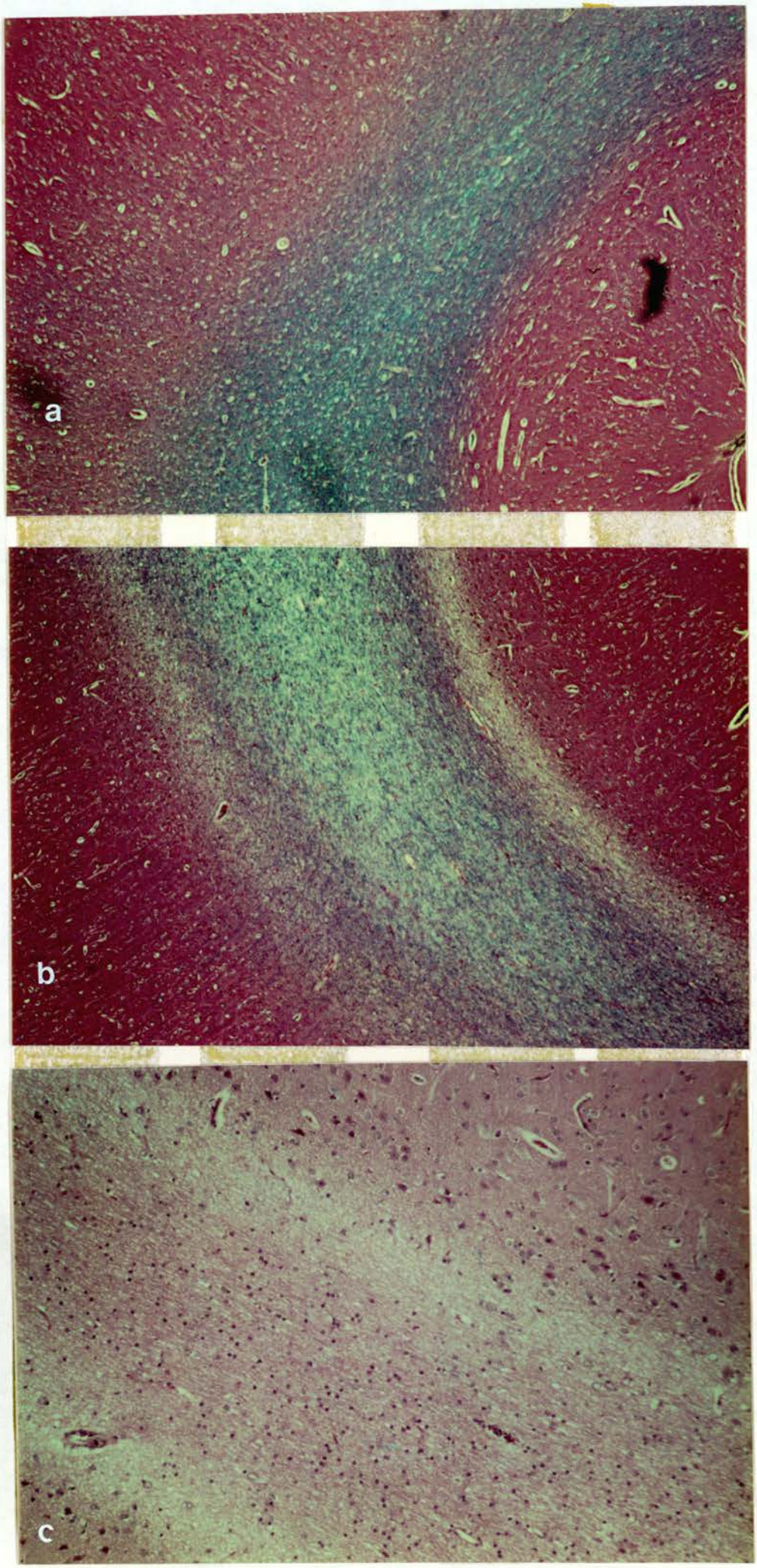
a
b
c

Legends to figure 21 overleaf.

Figure 21 a: Spreading oedema "front" in the white matter following 20% protein solution into the forebrain white matter of the cat. The normal white matter (Left) is composed of glial nuclei and relatively homogenous staining ground substance. The oedematous white matter (right) is vacuolated with dissolution of the ground sustance. There is also some perivenous polymorphic infiltration (top right). H & E x 200

Figure 21 b: Collection of polymorphic leucocytes in a venule in oedematous brain following bradykinin (150ug/ml) infusion into the forebrain white matter. The white matter (in which three neurones can clearly be seen) is oedematous with expansion of the extracellular space. The central venule contains many polymorphs but few have migrated into the surrounding tissue (H & E, x 200).

Figure 21 c: Separation of the fibres of the corona radiata and intense venular polymorhonuclear leucocytic stasis following infusion of arachidonic acid (10 mg/ml) into the forebrain white matter of the cat. Vacuolation and expansion of the oedematous white matter is clearly seen together with separation of the myelinated fibres of the corona radiata. There are large numbers of polmorphs in the venules and some can be seen in the perivenular white matter (H & E, x 200).

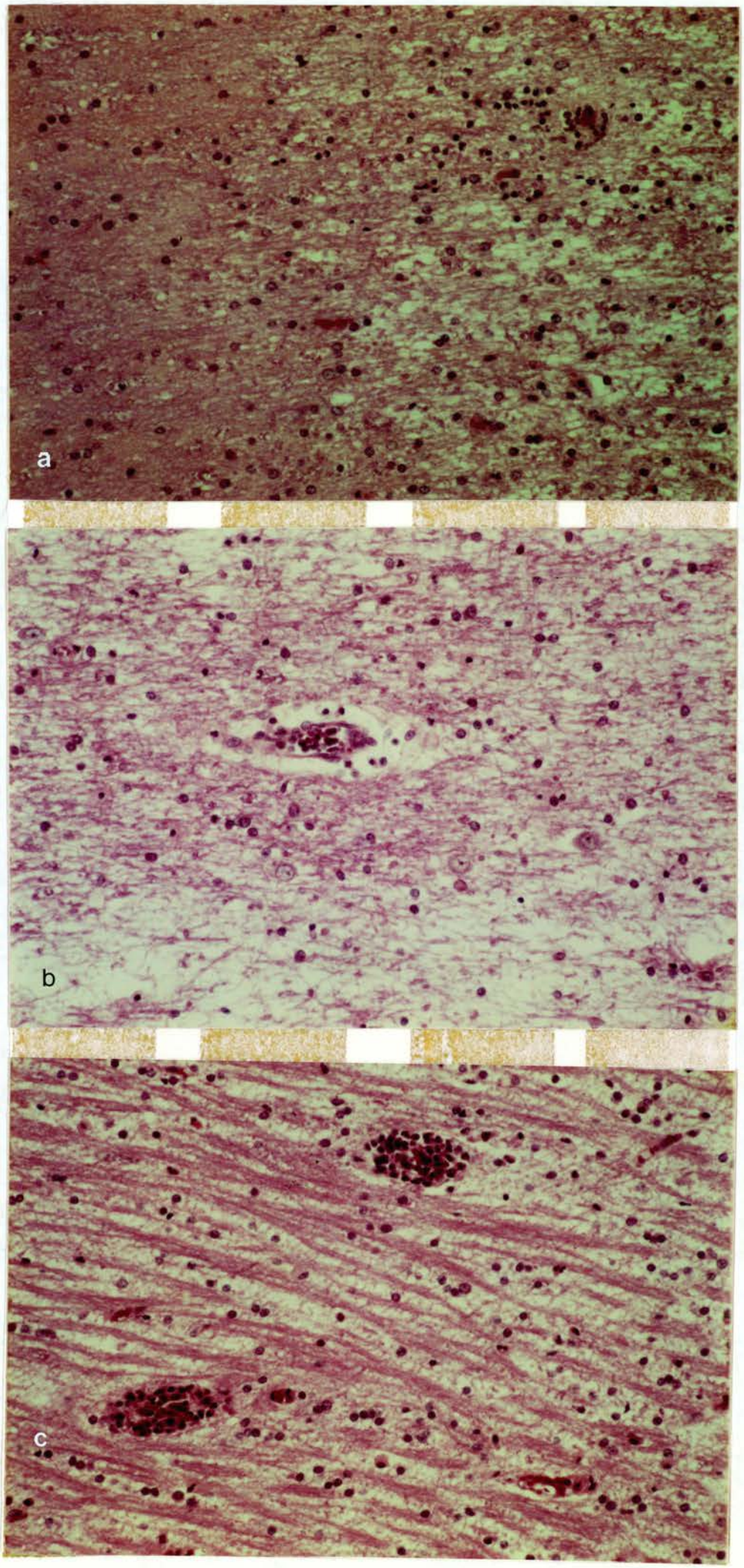
a
b
c

features to those described above. After arachidonic acid and bradykinin infusions there was patchy perivenous leucocytic infitrates, and engorgement of some white matter venules with polymorphic collections (Fig 21b and b). Polymorphic infiltration of the white matter was more florid after the 20% protein and glioma cyst infusates (Fig 21a). After some of the glioma cyst infusates there were amorphous hyalinized areas around the infusion site that were strongly PAS positive. In other regions the PAS material could be seen spreading through the white matter.

4 DISCUSSION

4.1 The quantitative, histological and biomechanical validity of a feline infusion model of brain oedema.

A model of brain oedema must increase tissue water content and tissue volume. Infusion of saline into the deep forebrain white matter at a rate of 3.3 uL/min for three hours increases local white matter water content by a mean of 11.6 ml/100 g tissue but does not alter adjacent cortical water content. These findings are similar to those described in clinical cases of brain oedema, experimental models of vasogenic brain oedema and a previous study using intraparenchymal infusion (see Table 2; Yamada et al, 1979; Marmarou et al, 1980; Reulen et al, 1980; Hossmann et al, 1980; MacDonald et al, 1986; Bell et al, 1987).

Macroscopic examination of coronal sections of the brain revealed local tissue swelling and light microscopical studies confirmed that the oedema fluid was distributed within the expanded and trabeculated white matter extracellular space. Widening of the extracellular space, separation of myelinated fibres and loosening of the ground substance made the tissue appear pale with both H & E and myelin stains and mimicked demyelination (Greenfield, 1939; Feigin & Popoff, 1963). These features together with preservation of cortical architecture are characteristic of the histological findings in human peritumoural oedema (Caspar, 1933; Jaburek, 1936; Greenfield, 1939; Perret and Kernohan, 1943; Scheinker, 1947; Hossmann et al, 1980). Glial swelling (Alzheimers amoeboid glia), changes in glial nuclei, and irregularity of the axis cylinders were not features presumably because of the time course of the experiment and the crystalloid nature of the infusate. The failure of Evans Blue extravasation into the oedematous brain confirms previous

ultrastructural studies that have shown the BBB, as well as the endothelium and glial processes in the region of the saline infusion remain normal (Lax et al, 1979; Marmarou et al, 1980),

The saline infusion studies (at 3.3 ul/min) showed only a moderate (10 mmHg over three hours) increase in ICP. This increase was not statistically significant ($p = 0.06$) and was also not significantly different from the mean ICP recorded at the end of the sham infusion animals. The increase in ICP in this study is almost identical to that described using a 0.5 ml infusion over five hours (Marmarou et al, 1980). However a major increase in ICP occurred with an infusion rate of 6.6 uL/min. The baseline values for ICP recorded in this model are similar to the 3-10 mmHg range previously described as normal in the cat (Marmarou et al, 1980; Iannotti et al, 1984; Takizawa et al, 1986a; Gray and Rosner, 1987). Intracranial hypertension is probably limited by the fall in brain tissue hydraulic resistance (from mean 9.8 to 4.3 x 10^3 mmHg/ml/min) that enables the additional infusate to be more readily dissipated into the white matter extracellular space. Similar decreases in R_t have previously been reported with the infusion oedema model (from maximum mean 6.4 to a minimum mean 0.8 x 10^3 mmHg/ml/min) using different infusion rates (Walstra et al, 1980; Marmarou et al, 1980) and in oedematous brain adjacent to ischemic lesions (Hatashita and Hoff, 1988).

The studies of PVI, C_i, and R_o during saline infusion showed that the only significant change was in reduction of C_i. This suggests the pressure-volume buffering capacity of the craniospinal axis is just beginning to be compromised by this volume of infusate. This expected decrease in compliance during saline infusion reflects the impairment of viscoelastic properties of the brain as it becomes more water laden and less distensible.

The mean baseline values recorded for PVI, C_i and R_o are similar to those described in cats studied under a variety of physiological circumstances using various anesthetic regimes. Mean normal PVI ranges from 0.43 to 0.90 ml (Marmarou et al,1975; Gray and Rosner, 1987; Takizawa et al, 1986a; 1986b), mean normal CSF outflow resistance values recorded at the lateral ventricle range from 55 to 110 mmHg/ml/min (Marmarou et al, 1975; Sullivan et al, 1979; Takizawa et al, 1985; 1986b) with mean intracranial compliance values of .026 ml/mmHg (Marmarou et al, 1975). The decrease in C_i during the sham experiments ($p = 0.11$) probably reflects a large normal variance for this parameter since the range of compliance values recorded during the sham experiments was within the range of baseline compliance values recorded for different series of cats in this study (Tables 3.36 and 3.37). Similar variations in baseline compliance values have been recorded in individual cats during other experiments in our laboratory (I R Piper and I R Whittle, unpublished observations). These findings may be partly explained by the difficulties in recording compliance at low ICP where small errors in absolute ICP values cause large errors in compliance.

The infusion pressure data shows that P_{inf} was, with the exception of a brief period following onset of the infusion, only a few mmHg higher than IVP. Studies of oedematous brain tissue pressure in subcortical tissue underlying cortical freeze lesions and adjacent to ischemic brain have also shown that tissue pressure rarely rises more than 10 mmHg higher than intraventricular pressure (Reulen et al, 1977; Iannotti et al, 1984; Hatashita and Hoff, 1988). The existence of this tissue pressure gradient together with the decrease in R_t is thought to facilitate bulk flow of the oedema fluid and its clearance by transependymal resorption (Reulen et al, 1977; 1980; Klatzo et al, 1980).

The experiments with saline infusion confirm that the infusion model provides an area of focal brain oedema that histologically, biomechanically, quantitatively, and spatially mimicks human brain oedema. This model of focal oedema does not cause BBB dysfunction, significant changes in the viscoelastic properties of the brain, intracranial hypertension, compartmental shifts or reduction of the CPP. These studies provide a baseline against which other infusates may be compared.

4.2 The effects of focal brain oedema caused by saline infusion on CBF, cortical SEP and MEP waveforms.

There were no significant changes in either the cortical SEP or MEP waveforms despite focal increases of brain water content by 10-12 % in the white matter of the primary thalamo-cortical somatosensory, primary cortico-spinal motor and fronto-parietal association fibres. The N_6 P_{10} N_{17} P_{27} cortical SEP waveform and standard deviations of the latencies of the particular waveform components, are similar to that previously described in cats. The N_6 (labelled P_6 by others) and the N_{10} (P_{11}) components represent thalamic and primary somatosensory cortical activity, whilst the later components represent association cortical activity (Towe et al, 1964; Poliakova, 1972; Sutton et al, 1980; 1982; Allison et al, 1982; see Dong et al, 1982).

If the focal oedema was to alter the SEP waveform the P_{10} and later components should theoretically be affected since the oedema does not extend caudal to the thalamus. That no changes in either waveform or amplitude were induced by the saline infusion is similar to previous experimental studies of the SEP in both cold induced (Sutton et al, 1980) and infusion brain oedema (Tanaka et al, 1983). These findings also complement clinical studies that recorded normal or near normal cortical SEPs

despite severe human peritumoural oedema (Penn, 1980; Ebner et al, 1982; Whittle et al, 1987).

The waveform and latencies of the feline spinal MEPs recorded following hemicranial stimulation are similar to those previously described using various anesthetic techniques and parameters of stimulation and recording (Levy et al, 1984; Haghigi and Oro, 1989)). In these studies the latency of the initial major negative component, which corresponds to the D wave, in the low to mid thoracic region ranged from 2.2 to 6 ms. The subsequent waveform components, which are related to the I waves, are multiple with interpeak latencies of 0.8 to 1.0 ms. No previous studies have examined the stability of these waveforms in oedematous brains although hypoxia, structural damage to the spinal cord and brain do alter the waveform (Levy et al, 1984; Haghigi and Oro, 1989).

The mean levels of rCBF, flow value standard deviations and CBF CO_2 reactivity recorded in this study are comparable with values previously described in the cat using similar anesthetic protocols and the H_2 clearance technique (Marmarou et al, 1980; Tanaka et al, 1983; Iannotti et al, 1984; Gray and Rosner, 1987; Hatashita and Hoff, 1988). Neither sham nor saline infusion caused any significant change in rCBF or CBF CO_2 reactivity. This finding complements previous work in both cats and dogs using the infusion model where both cortical and white matter CBF remained stable over a five hour infusion period (Marmarou et al, 1980; Tsubokawa et al, 1983; Tanaka et al, 1983). These findings may be partly explained by the maintenance of normal CPP since there is no significant intracranial hypertension and the infusion pressures, which are reflective of brain interstitial pressure (Iannotti et al, 1984), are with the exception of a brief period following onset, similar to the intraventricular pressure. The absence of either global or

focal decreases in CPP complements the stability of the SEP and MEP waveforms since these are sensitive to ishemia (Branston et al, 1974; Levy et al, 1984; Haghigi and Oro, 1989).

The saline model of infusion oedema does not alter rCBF, impair cerebrovascular reactivity to changes in P_aCO_2, or alter SEP or MEP waveforms. These results show that focal brain oedema with its attendant histological and biomechanical changes, when not complicated by a primary neural destructive lesion, does not alter these parameters of brain physiology.

4.3 BBB opening following arachidonic acid, bradykinin, 20% protein and glioma cyst fluid infusates

Intracerebral extravasation of intravenously administered 2% Evans blue was maximal following infusion of glioma cyst fluid, intermediate after arachidonic acid and 20% protein and lowest after bradykinin infusion. These findings support a role for arachidonic acid, bradykinin and components of the protein and glioma cyst solutions as secondary mediators of vasogenic brain oedema. How do these findings relate to previous studies and what contribution do they make to the mechanisms and etiology of vasogenic brain edema?

Focal opening of the BBB to Evans blue occurred with 3 ug of free interstitial bradykinin whilst 90 ug caused a more extensive and intense extravasation of the vital dye. These findings suggest that at 5ug/ml, which corresponds to a concentration that would be obtained following activation of all kininogen in plasma (Unterberg & Baethmann, 1984), the infused bradykinin was either rapidly enzymatically degraded, or that this concentration was around the level required to increase brain capillary permeability. The latter explanation is supported by

ventriculo-cisternal perfusion studies in which similar levels of bradykinin in mock CSF (3-5ug/ml) failed to open the subependymal BBB to Evans Blue (Unterberg & Baethmann, 1984). In brain oedema caused by a freeze lesion concentrations of bradykinin of 600 ng/g fresh tissue have been recovered (Maier-Hauff et al, 1984). This would correspond to levels of 750 ng/ml (7×10^{-7}M) assuming the tissue contained 80% water. There are also intrinsic kininogen-kinin systems within the brain that can be activated by plasma kallikrein (MW 95,000) however at present the potential of this system is not known (Kamitani et al, 1985; Ellis et al, 1987) . In view of these figures the concentrations of bradykinin infusion used in this study range from maximal physiological to pharmacological.

High local bradykinin levels may however occur in some neuropathological environments since kinin activity may be potentiated by a decrease in the normal oligopeptidase or endopeptidase levels, increased activation of local tissue kinins as well as activation of plasma kininogen-kinins from extravasated beta-2 macroglobulins. Conversely several other enzymes derived from extravasated plasma proteins would limit kallikrein and kinin activity (see Section 2.5). The net effect of the kinin generating and degrading enzyme systems would therefore be influenced by the physiological microenvironment which in a malignant glioma, would show considerable regional variation (Russell & Rubinstein, 1989). The functional effects of this bradykinin would in turn depend upon the presence of Beta 1 and beta 2 bradykinin receptors in the tissue (Regoli, 1986).

Several studies in rodents and cats have examined the potential of arachidonic acid, PGs and LTs to increase BBB permeability. Intraparenchymal injection of from 10 to 160 ug arachidonic acid into the frontal lobe and caudate

nucleus of rats (Chan et al, 1983; Aritake et al, 1983; Black & Hoff, 1985) and cats (Unterberg et al, 1987a) caused focal BBB opening to Evans blue and I^{125} Bovine Serum Albumin. These effects were dose dependent and not blocked by the cyclooxygenase inhibitor indomethacin but could be blocked by pretreatment with the lipoxygenase and cyclooxygenase inhibitor BW 755 C, suggesting that LTs, but not PGs, have an important role. Other cerebral microinjection studies in the rat using between 20ng to 2ug of either LTB4, LTC4 and LTE4 confirmed that LTs caused BBB opening with LTB4 being the most potent BBB opener (Black & Hoff, 1985). Conversely using the infusion oedema model in cats, 15 umol of LTC_4, LTD_4 and LTE_4, did not cause BBB opening to sodium-fluorescein (Unterberg et al, 1987a). These differences may reflect species effect or differences in the susceptibility of the deep cortical (rat studies) and white matter (cat studies) capillaries to LTs. The effects of arachidonic acid on capillary permeability and vasomotor tone are known to be species specific and within one species brain parenchymal vessels may react differently to pial arterioles or venules (see Walker & Pickard, 1985; Wei et al, 1986; Watanabe & Rosenblum, 1987).

Cortical superfusion with various concentrations of sodium arachidonate and 200 ug/ml arachidonic acid caused opening of the feline pial capillaries to horse radish peroxidase (HRP), sodium flourescein and flourescein isothiocyanate (MW 62,000) an effect that was not blocked by either indomethacin or BW 755 C nor reproduced using LTC_4, LTD_4, LTE_4, PGE_2 or PGH_2 (Kontos et al, 1980; Wei et al, 1986; Unterberg et al, 1987b). The studies with indomethacin and BW 755 C support the hypothesis that feline pial vascular permeability, like white matter capillary permeability, is modulated by arachidonic acid and not PGs or LTs. Interestingly frog brain endothelial capillary permeability is modulated in a similar fashion

(Olesen & Crone, 1986).

The focal extravasation of intravenous administered Evans Blue at the infusion site in this study confirms that arachidonic acid has the capacity to increase permeability of the normal BBB. The minimal concentration of arachidonic acid infused was 100 times that used in feline cortical perfusion experiments (Unterberg et al, 1987b), and either 10 times greater (Aritake et al, 1983) or similar (Chan et al, 1983; Black & Hoff, 1985) to those used in rodent intraparenchymal injection studies. The relationship of these concentrations to those attained in vivo is difficult to assess because of the problems with accurate quantitation of arachidonic acid and its metabolites. Eicosanoids have variable, but usually short half lives, and artifactual post mortem production is another problem (Walker & Pickard, 1985). However the concentrations used in this study would seem greatly in excess of those encountered pathologically. In normal CSF arachidonic acid concentrations range between 10-200 ng/ml, and are 5 -10 fold higher after brain injury (Westcott et al, 1987). Maximal concentrations of arachidonic acid, PGs and or LTs measured in human brain tumours range from 13 ug/ g (Black & Hoff, 1987) to 1 ug/g (Castelli et al, 1987). Slightly higher levels (50 ug/g protein) have been recorded following ischemia in the gerbil (Dempsey et al, 1987).

The mechanisms of BBB opening by bradykinin and arachidonic acid have not been elucidated by these experiments. The limited BBB opening caused by bradykinin may reflect its interstitial location since some of its permeability altering properties are mediated through endothelial relaxation (Rosenblum, 1988). Some BBB opening may be secondary to polymorphic infiltration since both agents have chemotaxic properties and perivascular leucocytic infiltrates were present (Gamache et al, 1986).

Other possible mechanisms involve synergistic effects between bradykinin and prostaglandins (Walker & Pickard, 1985; Rao et al, 1988; Regoli, 1986). The beta 2, but not beta 1, bradykinin receptor depends on the activation of arachidonic acid (Regoli, 1986) and bradykinin stimulates arachidonic acid release and metabolism as well as indirectly generating superoxide radicals (Kontos et al, 1984). Free oxygen radicals are also released in association with arachidonic acid metabolism, principly by PG synthetase rather than lipoxygenase, and can cause lipid peroxidation (Chan et al, 1984; Olesen & Crone, 1986; Wei et al, 1986). Peroxidation may mediate the direct endothelial damage caused by arachidonic acid since adverse effects on the endothelium can be prevented by superoxide dismutase, catalase and mannitol, which are all scavengers of free oxygen, and by cyclooxygenase inhibitors which also block oxygen consumption (Del Maestro et al, 1980; Kontos et al, 1980; Aritake et al, 1983; Wei et al, 1986).

The precise mechanisms of BBB opening following infusion of 20% protein solution and glioma cyst fluid have also not been elucidated by this study. The glutamate concentration in the 20% protein infusate (2 uM) was 50 times less than that of normal plasma (Baethmann et al, 1989) and is unlikely to be a major factor. Glutamate levels in the cyst fluids were not quantitated but were probably either similar to or higher than plasma levels in view of the the biochemical similarity to plasma and the local ischemia seen in the malignant gliomas.

Although ventriculo-cisternal perfusion of mock CSF containing plasma protein can cause subependymal opening of the BBB (Oettinger et al, 1976; Unterberg & Baethmann, 1984) a major problem in this study arises because the proteins (bovine and human) infused are not allogeneic. This may partly explain the infiltrates of

polymorphonuclear cells in the region of the infusion since the time course of the leucocytic response is similar to that described following intraventricular injection of carrageenan, an inflammatory provoking mucopolysaccaride, in mice (Gamache et al, 1986). Neuropathologically the focal cerebritis also resembles early bacterial abscess formation (Britt et al, 1981). However major bacterial contamination of the 20% protein and glioma cyst infusates is unlikely since all were meticulously handled and stored prior to infusion. Furthermore to experimentally generate such cerebritis large numbers (more than 10^6 of virulent bacteria) must be in the innoculum (Britt et al, 1981). The inflammatory infiltrates probably are an epiphenomenon of the experimental model that has little clinical in vivo relevance since polymorphic neutrophils, components of which are responsible for "granulocytic brain oedema" (Fishman et al, 1977), are uncommon in gliomas (Hanwehr et al, 1984; Shinonaga et al, 1988) and were not observed in histological examination of the tumour samples. Lymphocytes and macrophage infiltrates are found in up to 60% of gliomas and the intensity of these infiltrates has been correlated directly with the extent of peritumoural oedema (Hanwehr et al, 1984; Shinonaga et al, 1988).

Since the absolute protein contents of the four glioma cyst infusates were similar BBB opening mediated solely by an immunological or inflammatory mechanism against the foreign protein is not consistent with differences in intensity and extent of extravasation of Evans blue. Immunological mechanisms similar to those seen in acute experimental encephalomyelitis cannot be involved since this requires prior sensitization and it is unlikely that either bovine or human serum contains anti-cat brain antibodies (Unterberg & Baethmann, 1984). Acute degranulation of mast cells could occur after exposure to foreign protein or specific antigen, but these cells are

uncommon in the white matter of the cat (Ibrahim, 1974; Edvinsson et al, 1976). If the various glioma cyst infusates contained a specific BBB modulating compound (Bruce et al, 1987; Criscuolo et al, 1988) its activity in the experimental system does not directly relate to its in vivo potency. The amount of oedema caused by each of the four glioma cyst fluids in vivo was different but these differences were not reproduced experimentally either by the spatial distribution of Evans blue extravastion or water contents of the oedematous brain. In particular BBB opening was extensive following administration of cyst fluid from an oligodendroglioma whereas in vivo, as shown by CT scan, minimal oedema was associated with this lesion. This inconsistency between in vivo and in vitro brain oedema may be related to the preoperative dexamethasone therapy that was administered to the patients (see Appendix 2). Given that steroids are known to influence production of a permeability modulating protein as well as protein extravasation into the tumour interstitium this preoperative therapy may have significantly changed the BBB modulating potential of the fluids (Hossmann et al, 1983; Bruce et al, 1987; Nakagawa et al, 1987; Criscuolo et al, 1988).

When the infusion model is used to evaluate particular agents as potential secondary mediators of vasogenic brain oedema the capacity of that particular compound to disrupt normal BBB is assessed. However in almost all clinical and experimental studies of peritumoural brain oedema the peritumoural BBB is preserved and the site of vascular leakage is the tumour itself (see Section 1. 3.iii). The crucial factor in vivo however is the potential for the putative agent to increase further the neoplastic capillary permeability. Damaged or neoplastic capillaries may be more susceptible to the modulating effects of arachidonic acid, bradykinin, tumour secretions or plasma protein components than the normal BBB.

Differential capillary sensitivity to various agents is demonstrated in the hamster cheek pouch preparation where concentrations of arachidonic acid as low as 10^{-10} M (Del Maestro et al, 1980) increase permeability, whilst a concentration of 10^{-5} M was required to increase pial vascular permeability (Unterberg et al, 1987b). The hydraulic reflection coefficient of normal cerebral capillaries is 10^{3} greater than that of intestinal capillaries (Fenstermacher & Patlak, 1976) so differential sensitivity of normal brain parenchymal and neoplastic capillaries to particular agents would not be surprising . Since bradykinin, arachidonic acid, 20% protein solution and glioma cyst fluid can open the normal BBB it is likely, that they will focally potentiate oedema formation if the active components of these infusates are generated in sufficient quantities in the tumour interstitium.

Planimetric quantitation of dye extravasation alone proved to be an unsatisfactory measure of BBB disruption since the intensity, but not necessarily area, of dye staining was variable with the selected infusates. Future studies should optimally incorporate quantitation of vital dye extravasation using spectrophotometric techniques (Durward et al, 1983) so that relative potencies of different agents and the effects of different concentrations of the same agent can be assessed. The contribution of various agents to BBB opening could also be more vigorously tested using a battery of agents that detect differential BBB opening eg HRP, Na-fluorescein, Evans Blue. Such studies would enable BBB dysfunction to be quantitated, and perhaps provide additional information about mechanisms of BBB opening.

4.4 Brain oedema and biomechanics following arachidonic acid, bradykinin, 20% protein and glioma cyst fluid infusion

The focal increases in white matter water content following infusion of bradykinin, arachidonic acid, 20% protein solution and glioma cyst fluid were not significantly different (range 10.4 to 12.5 %) and were similar to values obtained after saline infusion (11.6%). This similarity is probably the result of limited clearance of the infused fluid volume, the small contribution from extravasated fluid with some infusates during the time course of the experiment as well as the limited spatial distribution of the white matter samples that were analysed for water content.

Brain oedema caused by arachidonic acid is maximal at between 6 (Aritake et al, 1983) and 24 hours (Chan et al, 1983) after intracerebral injection. The dynamics of bradykinin or other intracerebral protein induced oedema is not known, however ischemic, cold induced and toxin induced oedema are all maximal at 8-72 hours. The maximal increase in brain water in experimental and clinical brain oedema is usually less than 12 ml/100 g tissue and it would seem that bulk flow of the oedema fluid is enhanced by decreased brain tissue hydraulic resistance once such levels are reached. Therefore although the volume of oedematous white matter, which was not quantitated in this study, may vary the absolute increase in tissue water content at the oedema epicentre may be constant due to tissue water saturation (Ito et al, 1986). This hypothesis is supported by examination of coronal sections of the brains which showed that volumetric swelling was variable although tissue water contents close to the infusion sites were similar (see Fig 18, 19). Analysis of further white matter samples more distant from the infusion locus would have enabled an estimate of relative brain swelling

(Elliot & Jaspar, 1947)

The elevations in ICP following bradykinin. arachidonic acid, 20% protein solution and glioma cyst fluid were not statistically different from that recorded following infusion of a similar volume of saline. Since PVI, R_o and compliance are derived from ICP values the patterns of change in these parameters were also generally similar to those observed with saline infusates. The significant fall in C_i and rises in ICP were not associated with any significant or consistent change in PVI. Normally the PVI decreases with increased ICP due to intracranial mass lesions (Marmarou et al, 1975; Takizawa et al, 1986a), therefore measurement of the C_i may be a more sensitive indicator of early loss of craniospinal pressure-volume reserve. However the fall in C_i in these experiments is relatively small compared to that encountered following intracranial hypertension caused by intracranial balloon inflation or CSF infusion in cats (I R Piper & I R Whittle, unpublished data). The increased protein content of the glioma cyst fluids may account for part of the highly significant rise in R_o with these infusates since, after completion of the infusion R_o, remained elevated. This may be caused by some of the infused protein entering the CSF (Reulen et al, 1980). Further monitoring might have shown further rises in R_o.

4.5 CBF and cerebrovascular reactivity to CO_2

Overall the CBF and CBF CO_2 reactivity values were similar to those previously reported using the H_2 clearance technique and barbiturate anesthesia (Marmarou et al, 1980; Tanaka et al, 1983; Ianotti et al, 1984; Grey & Rosner, 1986). An isolated decrease in CBF adjacent to the infusion locus was recorded in only one series of experiments (GD-GBM). A bilateral decrease in frontal CBF was recorded in one series of experiments (EB-GBM

infusate) and a global transient increase in CBF was seen in the solitary cat infused with oligodendroglioma cyst fluid (TF-Oligo). Otherwise there was no consistent or significant change from baseline rCBF at any electrode location, during the course of the various infusions. In the GD-GBM experiments it is possible that part of the reduction in rCBF was due to tissue swelling so that flows later in the experiment were weighed towards white matter rather than cortical values.

The apparent stability of CBF during the infusions may reflect the shortcomings of the initial slope method of determining CBF. If the clearance curves were biexponential, with the fast component reflecting cortical flow and the slow component white matter flow, a change in one of these flows may be masked by determining only five points over a two minute interval. To examine this possibility, during the last four experiments, clearance curves were recorded on a dedicated computer programme designed to sample 120 points over a two minute interval (Piper I R, unpublished work) and the curves analysed to determine how many were biexponential, and by how much CBF values derived from the initial slope (IS) method over one minute differed from those recorded by analysis of the IS over 2 minutes. The results (see Appendix 5) showed that 20% of curves were biexponential, and the 2 minute IS derived CBF gave a flow value that was a median of 3 ml/100g/brain /min less than the computer derived 2 minute IS flow. Stability of the rCBF during the various infusions would therefore appear real.

After arachidonic acid infusion there was a focal, but not significant, reduction in CBF CO_2 reactivity in the white matter adjacent to the infusion site not associated with any reduction in cortical CBF CO_2 reactivity. Following the 20% protein, bradykinin and all malignant glioma (but not the oligodendroglioma) cyst fluid infusates there was

focal loss of CBF CO_2 reactivity adjacent to the infusion site. How do these findings compare to previous work and what is their significance?

PET and ^{133}Xenon studies have shown that blood flow in human peritumoural brain is either normal or low (Palvolgyi, 1969; Mosmans, 1974; Lammertsma et al, 1985) and there may be reductions in distant ipsilateral and contralateral hemispheric cortical CBF and CMR_{glu} (De La Paz et al, 1983; Beaney et al, 1985). Normal white matter CBF has also been reported in experimental studies of peritumoural oedema (Hossmann et al, 1980). In the PET studies there was no evidence of peritumoural brain hypoxia since if CBF was low there was a compensatory increase in oxygen extraction ratio (Brooks et al, 1986). A similar mechanism may account for the preservation of phosphocreatine, ATP and ADP levels despite a 20-33% reduction in blood flow in oedematous brain following a freeze lesion (Frei et al, 1973).

The effects of bradykinin and eicosanoids on cerebral arteriolar and pial vasomotor tone have been extensively studied (Regoli and Barabe, 1980; see Table 1, Walker & Pickard, 1985; Regoli, 1986). These studies reveal responses that differed between species, doses of drug tested, vascular bed studied and experimental protocol employed. In the cat arachidonic acid and most PGs except PGI_2 are cerebral vasodilators, whilst in man they are vasoconstricters. Bradykinin generally dilates arterioles and constricts venules. Extrapolation of experimental data concerning the vasomotor modulating actions of these compounds to both clinical situations and other experimental models is difficult. In peritumoural brain oedema, the differential effects of eicosanoids, that are released by active tumour secretion (Cooper et al, 1985; Lauro et al, 1986; Black et al, 1986) and ischemic tumour undergoing coagulative necrosis, on neoplastic vessels is

unknown. It would seem from the PET studies (Lammertsma et al, 1985; Beaney et al, 1985; Brooks et al, 1986) that tumour and peritumoural blood flow is certainly not increased in spite of extensive interactions between eicosanoids and other vasomodulating peptides, particularly bradykinin (Wahl et al, 1988; Unterberg et al, 1984).

The most significant experimental finding with respect to CBF is the loss of focal CBF CO_2 reactivity in the regions of brain made oedematous by the bradykinin, 20% protein and the malignant glioma cyst infusates. Brain oedema per se would not seem to be a cause of this loss of CO_2 reactivity since it was not seen after saline or arachidonic acid infusions. Although it would appear that kinins, activated plasma proteins or products of malignant glioma secretion or necrosis mediate this impairment of cerebrovascular CO_2 reactivity, the preservation of CBF CO_2 reactivity after infusion with oligodendroglioma cyst fluid compounds simple intepretation of this observation. Biochemical and electrophoretic analysis of the various cyst fluids shows only minor differences between the malignant glioma and oligodendroglioma (Appendix 2), this suggests that unless the oligodendroglioma secreted a factor that enhanced CBF CO_2 reactivity (see Section 4.6) extravasated proteins alone have little role. Previous studies using topical application of bradykinin (10 ug/ml) to pial vessels showed no impairment of CO_2 reactivity (Kontos et al, 1984), suggesting that vasoparalysis is not mediated by B_2 receptors which have been found on both cerebral endothelial and vascular smooth muscle cells (Unterberg & Baethmann, 1984).

The mechanism(s) causing this impairment of CBF CO_2 reactivity following intracerebral infusion could be mediated biochemically in two ways. Firstly bradykinin or other peptide components of the infusates may effectively

paralyse the vascular smooth muscle. Alternatively they may cause increased arteriolar resistance, so that at normocapnia the more distal blood vessels are dilated to maintain CBF, and the arteriole is incapable of further dilatation in response to hypercapnia although the reactivity mechanisms are intact. The vasoconstriction and decrease in focal cerebral blood volume seen after steroid therapy in some patients with brain tumours suggest that in some cases the latter mechanism may be important (Leenders et al, 1985). Alternatively a phenomenon similar to spreading cortical depression could also mediate the impairment of CBF CO_2 reactivity, since both CBF CO_2 reactivity and pial vascular responses to bradykinin are impaired after intracortical KCl microinjection, which causes transient spreading depression (Lauritzen, 1984; Leao, 1986; Wahl et al, 1987).

The mechanisms of global vasoparalysis after the 20% protein and bradykinin infusions are unclear. Spreading depression or vasoregulatory dysfunction of serotonergic or adrenergic fibre projections from the raphe nuclei and locus coeruleus could be involved. Serotonin levels in the rodent brain increase after intracerebroventricular injection of bradykinin (Rao et al, 1988) and it is possible that these infusates may have a similar effect in cats. However similar global patterns of CBF CO_2 dysautoregulation were not seen after any of the glioma cyst infusates and the precise roles of these ascending fibres in CBF regulation is itself controversial (see MacKenzie and Scatton, 1987).

Reduction of peritumoural brain CBF CO_2 reactivity has been noted in brain tumour patients (Palvolgyi, 1969; Mosmans, 1974), and in peritumoural brain in cats following experimental tumour implantation (Hossmann et al, 1980). CBF CO_2 reactivity is also reduced in brain

made oedematous (with a plasma rich fluid) by freeze lesions (Frei et al, 1973). This loss or impairment of CBF reserve could possibly be clinically significant since an "inverse" steal phenomenon could occur in response to hypercapnia or increased local brain metabolism leading to relative ischemia in the oedematous brain (Palvolgyi, 1969).

4.6 Electrophysiological findings

Cortical SEP waveform component latencies recorded from the infused and "control" hemispheres were reproducible throughout the experiment with the standard deviations for each component being similar to those previously described (Poliakova, 1972; Iragui-Madoz & Wiederholt, 1977; Sutton et al, 1980;1982; Dong et al, 1982). Few significant electrophysiological changes were recorded despite the focal brain oedema and in some cats, leucocytic infiltration of white matter. The lack of change in the cortical SEP, particularly the components with latencies of 10 ms or longer, may reflect the relative insensitivity of this pathway to modulation in the absence of frank cerebral ischemia or hypoxia (Branston et al, 1974 ; Sutton et al, 1980; Dong et al, 1982; Levy et al, 1984; Kataoka et al, 1987). Preservation of the cortical SEP waveform has also been reported following cortical freeze lesions that produce profound oedema (Sutton et al, 1980) and in many patient with brain tumours (Penn, 1980; Ebner et al, 1983). It is unlikely that the barbiturate anesthesia had a cerebral "protective" effect since, for this, barbiturate levels that cause EEG burst suppression are required. In cats such EEG changes occur 15 minutes after intravenous doses of pentobarbital of 27 mg/kg, such levels also cause marked systemic hypotension (Sutton et al, 1982).

In the three experiments where attenuation of the P_{10}-N_{17}

component occurred with development of a prominent P_{28}-N_{45}-P_{65} component it is tempting to postulate that these changes represent deafferentation of the somatosensory cortex. Similar changes in the cortical SEP have been described following ablation of all cortex except the parietal association areas (Poliakova, 1972). In another study however ablation of the primary and secondary somatosensory cortex produced only attenuation of the N_{17}-P_{28} component (Dong et al, 1982). Although these SEP changes were not reproduced in a second experiment with the GD-GBM cyst fluid, despite similar levels of focal reduction in frontal CBF, the similarity of SEP waveform changes seen with bradykinin 150 ug/ml and TF-Oligo infusate, suggests they are in some way related to the infusate and are not artifactual. In patients with peritumoural oedema however the changes in cortical SEPs usually involve loss, rather than enhancement, of longer latency components (Ebner et al, 1983; Whittle et al, 1987)

The lack of distortion of the cortical SEP and cortically derived spinal MEP waveforms by arachidonic acid infusions into the primary somatosensory and corticospinal motor fibre tracts was disappointing in view of previous electrophysiological and biochemical findings. Incubation of frog sciatic nerve with arachidonic acid (10 mg/ml) diminished the height of the action potential and caused myelin damage (Kasckow et al, 1986). Arachidonic acid and PGs in concentrations as low as 10^{-7}M can modulate membrane potentials and neuronal function by altering neurotransmitter uptake, synthesis and binding sites as well as inhibiting brain mitochondrial function (Dorman et al, 1986; Yu et al, 1986; Boksa et al, 1988; Schwarz et al, 1988; Hillered & Chan, 1988). Exposure of rat cortical slices to arachidonic acid perfusates (3×10^{-3}M) causes cytotoxic neuronal and glial swelling, uncoupling of oxidative phosphorylation and inhibition of Na+/K+ ATPase

(Chan & Fishman, 1978; Chan et al, 1983). Althought the lowest concentration of arachidonic acid (6.6 x 10^{-3}M) infused into the brain was much greater than the reported concentrations of 10^{-4} and 10^{-5}M in various types of brain oedema (Wahl et al, 1988), much of its pathophysiological effect will depend on its rate of uptake or metabolism. Normal astrocytes metabolize arachidonic acid to both prostanoids and LTs but metabolic rates are profoundly influenced by the tissue microenvironment (Walker & Pickard, 1985; Hartnung & Toyka, 1987)

The enzymatic degradation of infused bradykinin by brain oligopeptidases and endopeptidases may account for the paucity of electrophysiological modulation with this nonapeptide. These findings would suggest that bradykinin probably does not influence axonal conduction or glial function in the clinical setting even though there have have been several in vitro studies showing that bradykinin, at concentrations of 10^{-7} to 10^{-9}M, can alter cell membrane K^{+} conductance, synaptosomal uptake of choline, intracellular Ca^{++} levels as well as the levels of the important intracellular messengers cyclic guanosine monophosphate (cGMP) and inositol phosphate (Reiser & Hamprecht, 1982; 1985; Hamprecht, 1984; Reiser et al, 1984; Francel and Dawson, 1986; Pirola et al, 1986; Osugi et al, 1986).

The paucity of electrophysiological changes following infusion of the glioma cyst fluids may, as with the BBB findings, be related to whether the patients had preoperative steroid therapy. The TF-Oligo cyst fluid induced some experimental SEP changes. Mr TF, who had no preoperative steroid therapy, was having 5 - 7 complex partial siezures a day at the time of surgery and it is speculative to consider that the cyst fluid contained some "excitotoxin" (Baethmann et al, 1989). This possibility is supported by the transient global increase in CBF seen

during infusion of this cyst fluid (Table A-62). Bradykinin at 150 ug/ml may have a similar excitotoxic function, and hence the similar SEP changes, since microinjection studies into the rat brain have shown disruption of the EEG (Kariya et al, 1981). However why GD-GBM cyst fluid should produce similar SEP changes is difficult to explain since this patient had no seizures and her clinical deficit has considerably improved during the one week course of preoperative dexamethasone.

The symmetry of the MEP waveform in all experiments raises the questions of either bilateral generation of the descending spinal EP or activation of subcortical or extrapyramidal descending pathways. This is a controversial area since descending spinal feline EPs were abolished following bilateral pyramidal section (Levy et al, 1984) but recent work suggests that extrapyramidal pathways may be involved in transmission of the rat MEP (Fehlings et al, 1988). The contribution of nonpyramidal pathways, such as corticobulbar, bulboreticuler, cortico-cortical, corticopontine and corticoreticuler fibres to the descending spinal EP following transcranial stimulation is unclear (Patton & Amassian, 1954; York, 1987). If some of these nonpyramidal pathways were also activated the spinal EP should be polyphasic with discrete peaks corresponding to the different conduction velocities of the different tracts. Most waveforms in this study had three negative components, however the complexity and amplitude of the waveform were directly related to the stimulating current (see Appendix 4). Whether the stimulating currents used in these experiments would cause both local cortical and deep nuclear activation is speculative (see Geddes, 1987; cf Amassian et al, 1987). However the waveforms shown in Appendix 4 suggest activation of a nuclear pool (? vestibular nucleus) with fast conducting axons. Physiological factors that alter MEP generation and conduction have not been as extensively

studied as those that alter the cortical SEP (Branston et al, 1974) but recent studies suggest that hypovolemia and hypotension are critical (Haghigi and Oro, 1989).

4.7 Comments on the rodent model of infusion oedema

Although the rodent model of infusion oedema is cheap, readily available and has been shown to be technically feasible its main disadvantage when studying vasogenic brain oedema is the paucity of white matter. The subcortical white matter is at most 1 mm thick (Paxinos & Watson, 1982) and rapidly thins laterally. The thinness of the white matter also makes accurate SG quantitation difficult since white matter samples invariably include portions of deep cortical laminae or the corpus striatum. Nonetheless the fall in SG of oedematous brain is similar to that recorded in other rodent models of oedema although the SG values recorded for cortex were lower than previous values (Aritaki et al, 1983; Nakagawa et al, 1987).

The paucity of hemispheric white matter also required that infusates had to be delivered into the corpus striatum to overcome the problem of leakage back along the needle track (cf Black & Hoff, 1985). Changes in R_t and brain tissue compliance therefore primarily reflect the response of the corpus striatum rather than that of white matter. This may account for the the mean initial rat R_t (22×10^3 mmHg/ml/min) being double that of the cat (cf Tables A-6, A-7 & A-38). The pattern of change in these parameters from initial values is however similar to the feline infusion model and in oedema surrounding an ischemic focus in the cat (Hatashita & Hoff, 1988). Deposition of the infusate into the more vascular caudate nucleus may lead to a more rapid clearance of the infused fluid as well as to a more rapid buffering, degradation or metabolism of neuro or vasomodulating components within the infusate. These factors may explain the small differences in total

hemispheric water content and the stability of ICP, rCBF and cortical SEPs during both saline and 20% protein infusion.

The increase in ICP over the infusion period would seem biologically insignificant. However, following acute intracerebral injection of 50 ul of autologous blood (ie equivalent to 5% of the rat hemishere volume), rat ICP increases by a mean of only 4 mmHg (Kingman et al, 1988). Small rises in rat ICP may be associated with major reduction in craniospinal pressure-volume reserve however the small size of the rat ventricle and CSF volume make it very difficult to assess accurately the changes in the viscoelastic properties of the brain caused by the intracerebral infusions.

The CBF and CBF CO_2 reactivity data from the rodent infusion model are comparable with some other studies (Lauritzen, 1984; Bell et al, 1985). The relatively low CBF, compared to those obtained using autoradiographic techniques (Nakagawa et al, 1987), is probably related to the effects of the anaesthetic and methodological differences. The reduction of CBF CO_2 reactivity at the electrode adjacent to the 20% protein infusate could be explained in terms similar to those mentioned for the cat (see Section 4.4). However, the more focal impairment of CBF CO_2 reactivity would favour some biochemical effect on vasomotor tone. This effect could be mediated by inhibition of the normal glial carbonic anhydrase-CO_2 mediated response, inhibition of prostacyclin production or local paralysis of vasomotor innervation (Walker & Pickard, 1985; McKenzie & Scatton, 1987). If clearance or buffering of the protein infusate was limited its alkalinity would impair local CBF CO_2 reactivity.

This study describes cortical SEP waveforms of longer latency than previous studies which were primarily

concerned with short latency (< 6 ms) components and the primary thalamo-cortical (the P_6) response (Wiederholt and Iragui-Madoz, 1977; Allison et al, 1982). The cortical SEP waveforms recorded in the initial 30 ms following forelimb stimulation are similar to those described following hindlimb stimulation (Fehlings et al, 1988). The failure of saline or protein infusates to alter waveform components, particularly those with a latency >6 ms, may be related to the preservation of CBF or to the limited diffusion of the infusate since the forelimb primary somatosensory cortex covers a large area (Hall & Lindholm, 1974).

The rodent infusion model does provide a ready and cheap model of brain oedema. However, the small size of the rodent brain and relative paucity of subcortical white matter impose limitations on its use. Autoradiographic methods are probably required to optimally exploit this model (see p 123).

4.8 Final summary and future research

The major findings of this work are

1) Using normal saline infusate the feline model of infusion oedema produces focal brain oedema that quantitatively, histologically and biomechanically resembles vasogenic brain oedema found in patients and experimental models. The feature of this oedema is that it is confined to the extracellular space of the white matter, where it causes expansion and vacuolation of the ground sustance and separation of myelinated fibres. The cortical laminae are not involved. In the oedematous region, brain tissue hydraulic resistance falls and cerebral tissue compliance rises but PVI and CSF outflow resistance remain constant. There is a small rise in ICP associated with a fall in lumped craniospinal compliance. Infusion pressure data suggests that brain tissue

interstitial pressure in the oedematous area closely parellels ICP. Ipsilateral hemispheric CBF, CBF CO_2 reactivity, cortical SEPs, cortically derived MEPs and BBB function all remain normal.

2) The studies of BBB integrity, as assessed by extravasation of intravenous 2% Evans Blue, revealed that bradykinin (3 and 90 ug), arachidonic acid (1.2 - 9.0 mg), 20% protein solution and fluid aspirated from cystic human gliomas could all disrupt BBB function in normal white matter. In view of the biophysical properties of normal white matter capillaries it is considered that either these compounds or their metabolites, and specific components of the 20% protein and glioma cyst fluids are likely to be secondary mediators of vasogenic brain oedema. The mechanisms of BBB modulation by each of these compounds have not been identified, although it is possible that leucocytes and inflammatory mechanisms may contribute to the BBB opening by all these infusates.

3) Studies of rCBF during the three hour infusion period with arachidonic acid, bradykinin and 20% protein solution revealed stable flow values both adjacent to and distant from the infusion site. This finding suggests that at normal CPP and normocapnia neither brain oedema per se nor the presence of these compounds in brain oedema fluid causes cerebral hyperemia or ischemia. The effects of the glioma cyst fluid infusates on rCBF during the period of infusion were variable and may reflect the biological heterogeneity of the tumours, methodological problems or the effects of preoperative steroid therapy given to the patients from whom the cyst fluids were obtained.

CBF CO_2 reactivity was impaired either locally or globally by bradykinin, 20% protein and the malignant glioma cyst fluid infusates but not by intraparenchymal arachidonic acid, the oligodendroglioma cyst fluid or saline. The

mechanisms of this action were not elucidated but it does support previous clinical and experimental studies showing paralysis of CBF CO_2 regulation in oedematous brain and patients with brain tumours.

4) Despite profound white matter oedema (mean 10 - 12 ml/100 g tissue increase in brain water content), and with the oedema fluid containing compounds (arachidonic acid 1.2 - 9.0 mg, bradykinin 3 ug) known to be capable of endothelial, vasomotor, axonal and neuronal modulation or cytotoxicity, the waveforms of cortical SEPs and cortically generated spinal MEPs remained constant. Similar findings were noted after infusion of 20% protein solution and in 5 of 7 cats infused with human glioma cyst fluid. There was attenuation of the P_{10}-N_{17} SEP component with development of a large P_{28}-N_{45}-P_{65} component after infusion of bradykinin 90 ug, TF-Oligo and GD-GBM cyst fluid. In none of these experiments was there a change in MEPs, and the findings in GD-GBM were not reproducible in a second experiment. These findings suggest that if compounds in the oedema fluid mediate electrophysiological or oligodendroglial dysfunction, either more sensitive methods of assessment of local neurophysiology are required to detect such dysfunction or that in the case of the glioma cyst fluid infusates glial or neuromodulative activity was modified by preoperative steroid therapy given to 3 of the 4 patients.

5) A rodent model of infusion brain oedema was also utilised but suffered from several shortcomings. These were principally related to the small size of the rodent brain and attendant paucity of white matter. Infusion into the superficial aspect of the nucleus caudatoputamen was required to avoid leakage around the infusion needle. This grey matter infusion site probably modifies clearance, uptake and metabolism of the infusate and compounds quantification of the subcortical SG.

Nonetheless changes in brain biomechanics were similar to those encountered with the feline model and ICP, CBF and cortical SEPs all remained stable despite focal brain oedema caused by either saline or 20% protein infusates. Interestingly the 20% protein infusate caused a reduction in local CBF CO_2 reactivity, a finding also noted in the feline model.

What relevance does this thesis have with respect to advancing knowledge on the etiology and pathophysiology of human vasogenic brain oedema and in particular peritumoural brain oedema? Firstly it provides an experimental substrate for the common clinical observation that in many patients brain function is preserved despite profound brain oedema. Focal brain oedema per se does not cause focal brain dysfunction, ischemia or significant rises in brain tissue pressure. However if the brain oedema fluid contains certain peptides or proteins this model has confirmed previous experimental and clinical observations that there is focal loss of CBF reserve. In patients this loss of flow reserve may predispose patients to flow-metabolism uncoupling should they experience hypotension, hypoxia, raised ICP, hypercapnia or epilepsy. If such a mechanism does underlie peritumoural brain dysfunction steroids may cause clinical improvement by reducing noxious protein or "exocitotoxin" extravasation into the tumour interstitium, or by blocking synthesis or release of vasomodulating compounds by the tumour

Secondly it suggests that bradykinin, arachidonic acid, plasma proteins and glioma products may secondarily contribute to brain oedematogenesis (ie they are secondary mediators of vasogenic brain oedema). However in view of the levels of bradykinin and arachidonic acid infused it is unlikely that in patients either of these compounds modulate axonal function in the oedematous brain. If the initial hypothesis is correct then what compounds do

mediate peritumoural brain dysfunction and how can neural dysfunction be optimally evaluated?

One approach to the identification of such mediators would be the use of microdialysis in peritumoural brain (Baethmann et al, 1989: Persson et al, 1989). A spectrum of compounds in this region could be identified and quantified, and compared to those found in normal white matter. Such studies could be performed experimentally or in humans studied during operations (Persson et al, 1989). Peptides such as glycine, gamma-ABA, aspartate and glutamate would be of particular interest in view of their roles in neuromodulation. One of the criticisms of the infusion model is that most neuromodulators alter function via synaptic transmission and not at the axonal level (Cooper et al, 1986). Exposure of cortical neurones to concentrations of bradykinin and arachidonic acid such as used in these experiments may have caused neuronal modulation or cytotoxicity (Chan & Fishman, 1978; Wahl et al, 1988). However, such an experimental design does not complement the formation and distribution of peritumoural brain oedema fluid in patients.

The problem of relating neuronal modulation, cerebral dysrhythmia or alteration in evoked potentials to brain dysfunction is profoundly difficult. Current investigative techniques in neuropharmacology include the use of neural tissue slice preparations and single cell explants to study ion channels and other aspects of membrane neurophysiology (Chan & Fishman, 1978; Cooper et al, 1986). The use of single cell recording techniques in the oedematous region was considered but brain tissue swelling would make data difficult to interpret (Lemon, 1984; A G Brown, personal communication, 1986). The problem also arises of extrapolating events at the single neurone or even molecular level in vitro to in vivo events and overall neurological function. Autoradiographic studies

using the infusion model could be used to quantitatively study CBF, CMR_{glu}, BBB function and protein synthesis in precisely defined brain regions using deoxyglucose, iodopyridine, gamma-isobutyric acid and radiolabelled leucine respectively (Nakagawa et al, 1987; P A T Kelly, personal communication 1988). The infusion model in the rat would be particularly suitable for such multi-modality analysis since the high resolution of quantitative autoradiographic methods would enable precise analysis of the effects of the infusate not only locally but also on functionally related white and gray matter regions. Although such studies would be expensive they have the advantage of providing data about the modes of action of infusates, their effects on flow-metabolism coupling and the effects of hypercapnia.

This work has shown that under certain conditions CBF CO_2 reactivity is lost in focally oedematous brain. The functional significance of this finding merits further study in view of the previous correlative clinical and experimental observations. Recording of CBF, cortical SEPs, MEPs and EEG, at various P_aCO_2 levels, following particular infusions into the cat forebrain would enable this question to be addressed. Such studies would demonstrate, if the loss of CBF CO_2 reactivity was reproduced, whether an inverse steal phenomenon caused focal ischemia severe enough to cause EEG dysrhythmia or changes in the evoked potentials. Subfractionation of plasma proteins, infusion of glioma conditioned media (with and without added steroid) and varying concentrations of bradykinin could also elucidate the source of the dysautoregulation. The author hopes to continue investigation into the enigma of peritumoural brain dysfunction using the infusion model and refinements offered by intracerebral microdialysis and autoradiographic techniques.

REFERENCES

Adachi M, Feigin I (1966). Cerebral edema and the water content of normal white matter. J Neurol Neurosurg Psychiat 29; 446-450

Alajouanine T, Hornet T (1939). L'oedeme cerebral generalisée (étude anatomique). Ann d'anat Path 16; 133-163

Aleu F, Sawells S, Ransohoff J (1966). The pathology of cerebral edema associated with glioma in man. Report based on 10 biopsies. Am J Path 48, 1043-61

Alexander L, Looney J M (1938). Physicochemical properties of brain especially in senile dementia and cerebral edema. Arch Neurol Pyschiat (Chic) 40; 877-902

Allison A C (1987). Biochemistry and biology of eicosanoids, oxidants and other mediators of vascular permeability. In Cohadon F, Baethmann A, Go K, Miller J D (Ed's), Traumatic Brain Edema, Liviana press, Padua, p 65-73

Allison T, Wood C C, McCarthy D et al. (1982). Short latency somatosemsory evoked potentials in man, monkey, cat and rat: comparative latency analysis. In Courjon J, Mauguiere F, Revol M (Ed's) Clinical applications of evoked potentials in neurology, Raven press, New York, pp 304-311

Amassian V E, Stewart M, Quirk G J, Rosenthal J L (1987). Physiological basis of motor effects of a transient stimulus to the cerebral cortex. Neurosurgery 20; 74-93

Andral G (1838). Vorlesungen uber die Krankheiten der Nervenheerde. Christain E Kollmann, Leipzig, p 260.

Apuzzo M L, Sabshin J K (1983). Computed tomographic guidance stereotaxis in the management of intracranial mass lesions. Neurosurgery 12; 277-285

Arenander A T, Vellis J de (1980). Glial-released proteins in clonal cultures and their modification by hydrocortisone. Brain Res 200; 401-409

Arenander A T, Vellis J de (1981). Glial-released proteins:II Two dimensional electrophoretic identification of proteins regulated by hydrocortisone. Brain Res 224; 105-116

Aritake K, Nakai S, Asano A, Takakura K, Brock M (1983). Peroxidation of arachidonic acid and brain oedema. J CBF Metab 3(Suppl 1); S297-98

Aukland K (1965). Hydrogen polargraphy in measurement of local blood flow; Theory and empirical basis. Acta Neurol Scand 41(Suppl 14); 42-45

Baethmann A, Oettinger W, Rothenfusser O, Kempski O, Unterberg A, Geiger R (1980). Brain edema factors: Current state with particuler reference to plasma constituents and glutamate. Adv Neurology 28; 171-195.

Baethmann A, Maier-Hauff K, Schurer L, Lange M, Guggenbichler C, Vogt W, Jacob K, Kempski O (1989). Release of glutamate and of free fatty acids in vasogenic brain oedema. J Neurosurg 70; 578-591.

Bailey P, Schaltenbrandt G (1927). Die Mukose Degeneration der Oligodendroglia. Dtsch Z Nervenheilk 97; 231-237.

Bazan N G, Rodriguez de Turco E B (1980). Membrane lipids in the pathogenesis of brain edema: Phospolipids and arachidonic acid , the earliest membrane component changes at the onset of ischemia. Adv Neurology 28; 197-206.

Beaney R P, Brooks D J, Leenders K L, Thomas D G T, Jones T, Halnan K E (1985). Blood flow and oxygen utilisation in the contralateral cerebral cortex of patients with untreated intracranial tumours as observed by positron emission tomography. J Neurol Neurosurg Psychiat 48; 310-319.

Bell B A (1983). A history of the study of brain edema. Neurosurgery 13: 724-728

Bell B A, Foubister G C, Neto F, Miller J D (1985). The effect of experimental common carotid arteriotomy on cerebral blood flow in the rat. Neurosurgery 16; 322-326

Bell B A, Smith M A, Kean D M, McGhee C N J, MacDonald H L, Miller J D, Barnett G H, Tocher J L, Douglas R H B, Best J (1987). Brain water measured by magnetic resonance imaging. Correlation with direct estimation and changes after mannitol and dexamethasone. Lancet i; 66-69.

Bell B A, Smith M A, Tocher J L, Miller J D (1987b). Correction factors for gravimetric measurement of peritumoural oedema in man. Brit J Neurosurg 1; 441-446

Bennett J H (1843). Pathology and histological research on inflammation of the nervous system. Edin Med Surg J 60; 376-399

Black K L, Hoff J T (1985). Leukotrienes increase blood brain barrier permeability following intraparenchymal injection in rats. Ann Neurol 18; 349-351

Black K L, Hoff J T, McGillicuddy J E, Gebarski S S (1986). Increased leukotriene C4 and vasogenic edema surrounding brain tumours in humans. Ann Neurol 19: 592-595.

Bodsch W, Rommel T, Ophoff B G, Menzel J. (1987). Factors responsible for the retention of fluid in human tumor edema and the effect of dexamethasone. J Neurosurg 67: 250-257.

Boksa P, Mykita S, Collier B (1988). Arachidonic acid inhibits choline uptake and depletes acetylcholine content in rat cerebral cortical synaptosomes. J Neurochem 50; 1309-18

Bonkalo A (1939). Significance of the nature and position of tumours of the brain in the development of cerebral edema. Dtsch Z Nervenh 149; 243-53

Bothe H WW, Bodsch W, Hossmann K A. (1984). Relationship between specific gravity, water content and serum protein extravastion in various types of vasogenic brain edema. Acta Neuropath (Berl) 64; 37-42.

Bradac G B, Ferszt R, Bender A, Schorner W (1986). Peritumoural edema in meningiomas;A radiological and histological study. Neuroradiology 28;304-312

Branston N M, Symon L, Crockard H A, Pasztor E (1974). Relationship between cortical evoked potential and local blood flow following acute middle cerebral artery occlusion in the baboon. Exp Neurol 45; 195-208

Brett M, Weller R O (1978). Intracellular serum proteins in cerebral gliomas and metastatic tumours; an immunoperoxidase study. Neuropath Appl Neurobiol 4; 263-272

Britt R H, Enzmann D R, Yeager A S (1981). Neurpathological and computerized tomographic findings in experimental brain abscess. J Neurosurg 55; 590-603.

Brooks D J, Beaney R P, Lammertsma AA et al (1984). Quantitative measurement of blood brain barrier permeability using ^{82}Rb and positron emission tomography. J CBF Metab 4; 535-545.

Brooks D J, Beaney R P, Thomas D G T (1986). The role of positron emission tomography in the study of cerebral tumours. Semin Oncol 13; 88-93

Bruce J N, Criscuolo G R, Merrill M J, Moquin R R, Blacklock J B, Oldfield E H (1987). Vascular permeability induced by protein product of malignant brain tumours; inhibition by dexametasone. J Neurosurg 67; 880-884

Bucknill J L, Tuke D H (1874). A Manual of psychological medicine. London, J Churchill, 3rd Edition pp 587.

Bulle H P (1957). Effects of reserpine and chlorproamzine in prevention of cerebral oedema and reversible cell damage. Proc Soc Exp Med Biol 94; 553-6

Burger P C, Dubois P J, Schold S C, Smith K R, Odom G L, Crafts D C, Giangaspero F (1983). Computerized tomographic and pathological studies of the untreated, quiesent and recurrent glioblastoma. J Neurosurg 58; 159-169

Canstatts Jahrbericht uber die Fortschritte der Gesammten Medizin im Jahre 1858 (1859). Dritte Band, Wurzburg, 12-14

Camargo A C, Oliviera E B, Toffoletto O, Metters K M, Rossier J (1987). Brain endo-oligopeptidae A, a putative enkephalin converting enzyme. J Neurochem 48; 1258-63

Casanova M F (1984). Vasogenic brain edema with intraparenchymal expanding masses. A theory on its pathophysiology. Med Hypothes 13; 439-50

Castelli M G, Butti G, Chiabrando C, Cozzi E, Fanelli R, Gaetani P, Silvani V, Paoletti P (1987). Arachidonic acid metabolic profiles in human meningiomas and gliomas. J Neuro-oncol 5; 369-375

Caspar J (1933). Uber die Veranderungen des Hirngewebes, insbesondere der neuroglia, in der Umgebung der Hirngeschwulste. Ztschr f d ges Neurol u Psychiat 145; 208-248.

Cervos-Navarro J, Ferszt R (1980). Introduction to brain oedema: Historical note. Adv Neurology 28; xix-xxvii.

Chan P H, Fishman R A.(1978). Brain edema: Induction in cortical slices by polyunsaturated fatty acids. Science 201; 358-360.

Chan P H, Fishman R A, Caronna J, Schmidly J W, Lee J (1983) Induction of brain edema following intracerebral injection of arachidonic acid. Ann Neurol 13; 625-632.

Chan P h, Schmidley J W, Fishman R A, Longar S M (1984). Brain injury, edema, and vascular permeability changes induced by oxygen-derived free radicals. Neurology 34; 315-320

Chapin J K, Lin C-S (1984). Mapping the body representation in the SI cortex of anesthetized and awake rats. J Comp Neurol 229; 199-213

Coomber B L, Stewart P A, Mayakawa K, Farrell LL, Del Maestro R F (1987). Quantitative morphology of human glioblastoma microvessels; structural basis of blood brain barrier defect. J Neuro-oncol 5; 299-307

Cooper J R, Bloom F R, Roth R H (1986). The biochemical basis of neuropharmacology. 5th Edition, Oxford Uni Press, pp 400

Cooper C, Jones H G, Weller R O, Walker V. (1984). Production of prostaglandins and thromboxane by isolated cells from intracranial tumors. J Neurol. Neurosurg. Psychiat 47, 579-584

Criscuolo G R, Merrill M T, Oldfield E H (1988). Further

characterisation of malignant glioma derived vascular permeability factor. J Neurosurg 69; 254-262

Csanda E (1980). Radiation brain edema. Adv Neurol 28; 325-46

Cummings J N (1961). Soluble cerebral proteins in normal and oedematous brain. J Clin Path 14; 289-295

Czernicki Z (1979). Treatment of experimental brain edema following sudden decompression, surgical wound and cold lesion with vasopressor drugs and proteinase inhibitor trasylol. Acta Neurochir (Wien) 50, 311-326

Daumas-Duport C, Monsaigneon V, Blond S, Minari C, Muselini A, Chodkiewicz J (1987). Serial stereotaxic biopsies and CT scans in gliomas. J Neuro-Oncol 4, 317-28

De La Paz R L, Patronas N J, Brooks R A (1983). Positron emission tomography study of suppression of grey matter glucose in human cerebral gliomas. AJNR 4; 826-9

Del Maestro R F, Thaw H N, Bjork J, Planker M (1980). Free radicals as mediators of tissue injury. Acta Physiol Scand 492; 43-57

Dempsey R J, Roy M W, Meyer K, Tai HH, Olsen J W (1985). Polyamine and prostaglandin markers in focal cerebral ischemia. Neurosurgery 17; 635-40

Dempsey R J, Combs D J, Maley M E (1987). Moderate hypothermia reduces postishemic edema development and leukotriene production. Neurosurgery 21; 177-181.

Dong W K, Harkins S W, Ashleman B T. (1982). Origin of cat somatosensory farfield and early nearfield evoked potentials. Electroenceph Clin Neurophysiol 53; 143-165

Dorman R V, Schwartz M A, Terrian D M (1986). Prostaglandin involvement in the evoked release of D-aspartate from cerebeller mossy fiber terminals. Brain Res Bull 17; 243-8

Durward Q, Del Maestro R F, Amacher L, Farrer J K (1983). The influence of systemic arterial pressure and ICP on the development of cerebral vasogenic edema. J Neurosurg 59; 803-809

Dykes R, Lamour Y (1988). Neurons without demonstrative receptive fields outnumber neurons having receptive fields in samples from somatosensory cortex of anesthetized rats and cats. Brain Res 440; 133-143

Ebner A, Einsiedel-Lechtape H, Luking C H (1982). Somatosensory tibial nerve evoked potentials with parasagital tumours; a contribution to the problem of generators. Electroencephal clin Neurophysiol 54; 508-515

Edvinsson L, Cervos-Navarro J, Larsson L I, Owman C H, Ronnberg A (1977). Regional distribution of mast cells containing histamine, dopamine, or 5-hydroxytryptamine in the mammalian brain. Neurology 27; 878-883

Elliot K A C, Jaspar H (1949). Measurement of experimentally induced brain swelling and shrinkage. Am J Physiol 157; 122-129.

Ellis E F, Heizer M L, Hambrecht G S, Holt S A, Stewart J M, Vavrek R J (1987). Inhibition of bradykinin and kallikrein induced cerebral arteriolar dilation by a specific bradykinin antagonist. Stroke 18; 792-5

Farrell C L, Stewart P A, Del Maestro R F (1987). A new glioma model in the rat. The C6 spheroid implantation technique. Permeability and vascular characteristics. J Neuro-oncol 4; 409-21

Farrer J K (1987). Hydrogen clearance technique. In Wood J H (Ed) Cerebral Blood Flow, McGraw-Hill, New York, 275-287

Fehlings D, Tator C, Linden R, Piper I R (1988). Motor and somatosensory evoked potentials recorded from the rat. Electroenceph clin Neurophysiol 69; 65-78

Feigin I, Popoff N (1963). Neurpathological observations on cerebral oedema. Arch Neurol 6; 151-160

Fenstermacher J D, Patlak C S (1976). The movements of solutes and water in the brains of mammals. In Pappius H, Feindel W (Ed's) Dynamics of brain oedema, Springer, Berlin, pp 87-94

Ferszt R, Hahm H, Cervos-Navarro J (1980). Measurement of the specific gravity of the brain as a tool in brain edema research. Adv Neurology 28; 15-26

Fieschi C, Bozzao L, Agnoli A, Nardini M (1969). The hydrogen method of measuring local blood flow in subcortical structures of the brain: Including a comparative study with 14C antipyrine. Exp Brain Res 7; 111-9

Fishman R A (1976). Brain edema, N Engl J Med 293; 705-711

Fishman R A, Chan P H (1980). Metabolic basis of brain edema. Adv Neurology 28; 207-216.

Fishman R A, Sligar K, Hake R B (1977). Effects of leucocytes on brain metabolism in granulocytic brain oedema. Ann Neurol 2; 89-94

Fishman R A, Chan P H (1981).. Hypothesis: membrane phospolipid degradation and polyunsaturated fatty acids play a role in the pathogenesis of brain edema. Ann Neurol 10; 75

Francel P C, Dawson G (1986). Bradykinin induces a rapid release of inositol triphosphate from a neuroblastoma hybrid cell line NCB-20 that is not antagonized by enkephalin. Biochem Biophs Res Commun 135; 507-514

Frei H J, Wallenfeld T, Poll W (1973). Regional cerebral blood flow and regional metabolism in cold induced edema. Acta Neurochir (Wien) 29; 15-28

Galicich J H, French L A, Melby J C (1961). Use of dexamethasone in the treatment of cerebral edema associated with brain tumours. Lancet 81; 46-53

Gamache D A, Povlishock J T, Ellis E F (1986). Carrageenan induced brain inflammation. J Neurosurg 65; 679-685

Gastaut J L, Michel B, Sabet Hassen S, Corda M, Gastaut H (1979). Electroencephalography in brain oedema (127 cases of brain tumour investigated by computerized tomography). Electroencphal clin Neurophysiol 46; 231-255

Geddes L A (1987). Optimal stimulus duration for extracranial cortical stimulation. Neurosurgery 20; 94-99

Gerschenfeld H M, Wald F, Zadunaisky J A, DeRoberts E D P (1959). Function of the astroglia in the water ion metabolism of the central nervous system. An electron microscopic study. Neurology 9; 412-18

Go K G, Edzes H T (1975). Water in brain oedema. Observations by pulsed nuclear magnetic resonance technique. Arch Neurol 32; 462-465

Go K G, Gazendam J, Meulen D A, Tielken A W (1980) . Changes in brain extyracellular space as reflected by the composition of brain edema fluid. Adv Neurol 28; 9-14

Gowers W R (1893). A Manuel of Diseases of the Nervous System. Second Edition, Vol 2, J & A Churchill, London, pp 1051.

Gray W J, Rosner M J (1987). Pressure volume index as a function of cerebral perfusion pressure; Part I and II. J Neurosurg 67; 369-380

Greenfield J G (1939). The histology of cerebral oedema associated with intracranial tumours. Brain 62; 129-152

Groothuis D R, Fischer J M, Lapin G, Bigner DD, Vick N (1982). Permeability of different brain tumour models to horse radsih peroxidase. J Neuropath Exp Neurol 41; 164-185

Guldin W O, Markowitsch H J (1984). Cortical and thalamic afferent connections of the insular and adjacent cortex of the cat. J Comp Neurol 229; 393-418

Haghighi S, Oro J J (1989). Effects of hypovolemic hypotensive shock on the somatosensory and motor evoked potential . Neurosurgery 24; 246-252

Hall R D, Lindholm E P (1974). Organization of motor and somatosensory neocortex in the albino rat. Brain Res 66; 23-38

Hamprecht B (1984). Cell culture as models for studying neural functions. Prog Neuropsychopharmacol Biol Psychiat 8; 481-6

Hanwehr R I von, Hofman F M, Taylor C R, Apuzzo M L (1984). Mononuclear lymphoid populations infiltrating the microenvironment of primary CNS tumours. J Neurosurg 60; 1138-47.

Hardebo J E, Kahrstom J, Owman C, Salford L G (1987). Vasomotor effects of neurotransmitters and neuromdulators on isolated human pial vessels. J CBF Metab 7; 612-618

Hartnung H P, Toyka K V (1987). Leukotriene production by cultured astroglial cells. Brain Res 435; 367-70

Hatam A, Bergstrom M, Yu Z Y, Granholm L, Berggren B M (1983). Effects of dexamethasone treatment on volume nad contrast enhancement of intracranial neoplasms. J Computer Assist Tomogr 7; 295-300.

Hatashita S, Hoff J T (1988). Biomechanics of brain edema in acute cerebral ischemia in the cat. Stroke 19; 91-97

Hattori T, Andoh T, Sakai N, Yamada H, Kameyama Y, Ohki K, Nozawa Y (1987). Membrane phospholipid composition and membrane fluidity of brain tumours: a spin label study. Neurol Res 9; 38-43

Hawkins R A, Phelps M E, Huang S C (1986). A kinetic evaluation of blood brain barrier permeability in human brain tumours with [^{68}Ga]EDTA and positron computerized tomography. J Cereb Blood Flow Metab 4; 507-515

Heiss W, Traup C H (1981). Comparison between H2 clearance and microsphere techniques for regional cerebral blood flow measurement. Stroke 12; 121-7

Herzog I, Levy W A, Schweinberg L C (1965). Biochemical and morphological studies of cerebral edema associated with intracerebral tumours in rabbits. J Neuropath Exp Neurol 24; 244-253

Hillered L, Chan P H (1988). Effects of arachidonic acid on respiratory activities in isolated brain. J Neurol Sci 19; 94-100

Hossman K A, Bloink M, Wilmes F, Wechsler W (1980).

Experimental peritumoural edema of cat brain. Adv Neurology 28: 323-40

Hossmann K A, Hurter T, Oschlies U (1983). The effect of dexamethasone on serum protein extravasation and edema development in experimental brain tumours in the cat. Acta Neuropath (Berl) 60;223-231

Houthof H J (1987). Pathobiology of blood-brain barrier and brain edema. In Cohadon F, Baethmann A, Go k, Miller J D (Ed's) Traumatic brain Edema, Liviana press, Padua, pp 1-9

Hwang W Z, Ito H, Hasegawa T, Shimoji T, Kida S, Fujii H, Yamamoto S (1986). Peritumoural oedema and lipid content. Acta Neurochir (wien) 80; 128-130

Ianotti F, Hoff J, Schielke G P (1984). Brain tissue pressure: physiological observations in anesthetized cats. J Neurosurg 60; 1219-1225

Ibrahim M Z M (1974). The mast cells of the mammalian nervous system. Part 1. Morpology, distribution and histochemistry. J Neurol Sci 21; 431-478

Ikeda Y, Nakazawa S (1984). (Analysis of peritumoural edema with special reference to the value of the contrast enhanced CT scan). No To Shinkei 36; 1055-1062.

Ikeda Y, Nakazawa S (1987). The role of biogenic amines in the production of peritumoural oedema. J Nippon Med Sch 52, 117-8

Iragui-Madoz V J, Wiederholt W C (1977). Far field somatosensory evoked potentials in the cat. Electroencephal clin Neurophysiol 43; 646-57

Ito U, Reulen H-J, Huber P (1986). Spatial and quantitative distribution of human peritumoral oedema in computerized tomography. Acta Neurochir (Wien) 81; 53-60.

Ito U, Reulen H J, Tomita H, Ikeda J, Saito J, Maehara T (1988). Formation and propagation of brain oedema fluid around human brain metastases. A CT study. Acta Neurochir (Wien) 90; 35-41

Jaburek L (1936). Hirnoedem und Hirnschwellung bei Hirngeschwulsten. Arch Psychiat 104; 518-547

Kamitani T, Little M H, Ellis E F (1985). Evidence for a possible role of the brain kallikrein-kinin system in the modulation of the cerebral circulation. Circ Res 57; 545-52

Kamman R L, Go K G, Brouwer W, Berendsen H L (1988). Nuclear magnetic resonance relaxation in experimental brain oedema; effects of water concentration, protein concentration and temperature. Magn Reson Med 6; 265-74

Kariya K, Iwaki H, Ihda M, Maruta E, Murase M (1981). Central action of bradykinin; Electroencephalogram of bradykinin and its degradation system in rat brain. Jpn J Pharmacol 31; 261-7

Kasckow J W, Abood L G, Hoss W, Herndon R M (1986). Mechanisms of phospholipase A_2 induced conduction block in bullfrog sciatic nerve. Brain Res 373; 384-91

Katoaka K, Graf R, Rosner G, Heiss W D (1987). Experimental focal ischemia in cats; changes in multimodality evoked potentials as related to local cerebral blood flow and ischemic brain edema. Stroke 18; 188-94

Katz B, Sofonio M, Lyden P D, Mitchell M D (1988). Prostaglandin concentrations in cerebrospinal fluid of rabbits under normal and ischemic conditions. Stroke 19; 349-51

Kety SS (1951). The theory and applications of the exchange of inert gases at the lung and tissues. Pharmacol Rev 3; 1-41

Kingman T A, Mendelow A D, Graham D I, Teasdale G M (1988). Experimental intracranial mass lesion. Description of model, intracranial pressuyre changes and neuropathology. J Neuropath Exp Neurol 47; 128-137.

Klatzo I (1967). Presidential address. Neuropathological aspects of brain edema. J Neuropathol Exp Neurol 26; 1-14

Klatzo I, Chui E, Fujiwara K, Spatz M (1980). Resolution of vasogenic brain edema. Adv Neurol 28: 359-373

Kontos H A, Wei E P, Povlishock J T, Dietrich W D, Magiera C J, Ellis E F (1980). Cerebral arteriolar damage by arachidonic acid and prostaglandin G2. science 209; 1242-1245

Kontos H A, Wei E P, Povlishock J T, Christman C W (1984) Oxygen radicals mediate the cerebral arteriolar dilation of arachidonate and bradykinin. Circ Res 55; 295-303

Krieg W J (1946). Connections of the cerebral cortex.I The albino rat. A. Topography of the cortical areas. B. Structure of the cortical areas. J Comp Neurol 84; 222-323

Lammertsma A, Wise R J, Cox T C, Thomas DGT, Jones T (1985). Measurement of blod flow, oxygen utilisation, oxygen extraction ratio and fractional blood volume in human brain tumours and surrounding oedematous tissue. Brit J Radiol 58; 725-734

Lanksch W, Oettinger W, Baethmann A, Kazner E. (1976). CT findings in brain oedema compared with direct chemical analysis of tissue samples. In Pappius H M, Feindel W,

(Ed's) Dynamics of Brain Edema, Springer-Verlag, Berlin, pp 283-287

Lauritzen M (1984). Long lasting reduction of cortical blood flow in the rat brain after spreading depression and impaired CO_2 response. J CBF Metab 4; 546-54

Lauro G M, Di Lorenzo N, Grossi M, Maleci A, Guidetti B (1986). Prostaglandin E2 as an immunomodulating factor. Acta Neuropath (Berl) 69; 278-82

Law Dr (1855). White softening of the brain. In Transactions of Fellows and licentiates of the Kings and Queens College of Physicians in Ireland. Dublin Quart J Med Sci 20; 169-172

Lax F, Horoupian D S, Tagaki H, Marmarou A (1979). Microvascular changes in infusion edema. J Neuropath exp Neurol 38; 328

Leao A A P (1944). Spreading depression of activity n the cerebral cortex, J Neurophysiol 7; 359-390

Leao A A P (1986). Spreading depression. Functional Neurol 1; 363-366

Leenders K L, Beaney R P, Brooks D J, Lammertsma AA, Heather J D, McKenzie C G (1985). Dexamethasone treatment of brain tumour patients; effects on blood flow, blood volume and oxygen utilisation. Neurology 35; 1610-15

Lemon R (1984). Methods for neuronal recording in conscious animals. John Wiley & Sons, Chichester, pp162

Lerch K D, von Wild K (1983). (Influence of alpha methyl prednisolone on perifocal brain edema: CT observations in ten patients with circumscribed supratentorial brain tumours). Neurochirurgia (Stuttg) 26; 97-103.

Levy W J, McCaffrey M, York D M, Tanzer F (1984). Motor evoked potentials from transcranial stimulation of the motor coretex in cats. Neurosurgery 15; 214-27

Long D M (1970). Capillary ultrastructure and the blood brain barrier in human malignant glioma. J Neurosurg 32; 127-144

Long D M, Arce-Puyo C, Epstein M H, Aarabi B (1980). Role of dibutyrl cyclic adenosine monophosphate in the genesis of brain edema. Adv Neurology 28; 231-40

Luse S A, Harris B (1960). Electron microscopy of the brain in experimental oedema. J Neurosurg 17; 439- 447

McCormick C, Wallace I (1981). An investigation in vitro of the exocytosis of lysosomal enzymes from C6 glioma cells. Acta Neuropathol (Berl) 47; 85-87

McDermott J R, Gibson A M, Turner J D (1987). Involvement of endopeptidase 24.15 in the inactivation of bradykinin by rat brain slices. Biochem Biophys Res Commun 146; 154-8

MacDonald H L, Bell B A, Smith M A, Kean D M, Tocher J L, Douglas RHB, Miller J D, Best J J K (1986). Correlation of human NMR T_1 values measured in vivo and brain water content. Brit J Radiol 59; 355-357.

McKenzie E T, Scatton B (1987). Cerebral circulatory and metabolic effects of perivascular neurotransmitters. CRC Crit Rev Clin Neurobiol 2; 357-419

Maier-Hauff K, Baethmann A J, Lange M, Schurer L, Unterberg A. (1984a). The kallikrein-kinin system as a mediator in vasogenic brain edema Part II: Studies on kinin formation in focal and perifocal brain tissue. J Neurosurg 61; 97-106.

Marmarou A, Shulman K, LaMorgese J. (1975). Compartmental analysis of compliance and outflow resistance of the cerebrospinal fluid system. J Neurosurg 48; 523-534

Marmarou A, Shulman K, Shapiro K (1976). The time course of brain tissue pressure and local CBF in vasogenic edema. In Pappius H M, Feindel W (Ed's) Dynamics of brain edema. Springer-Verlag, Berlin/Heidelburg/New York 1976, pp 113-121.

Marmarou A, Poll W, Shulman K, Bhagavan H (1978). A simple gravimetric technique for measurement of cerebral edema. J Neurosurg 49; 530-537.

Marmarou A, Takagi H, Shulman K (1980). Biomechanics of brain edema and effects on local blood flow. Adv Neurol 28; 345-358.

Marmarou A, Tanaka K, Shulman K. (1982). An improved gravimetric measure of cerebral edema. J Neurosurg 56; 246-253.

Meinig G, Aulich A, Wende S, Reulen H J (1976). The effect of diuretics on peritumoural brain edema; comparative study of tissue water content and CT. In Pappius H M, Feindel W (Ed's) Dynamics of brain edema. Springer-Verlag, Berlin/Heidelburg/New York pp 113-121.

Miller J D (1979). The management of cerebral oedema. Br J Hosp Med 21; 152-165

Miller J D, Sakalas R, Ward J D, (1977). Methylprednisolone treatment of patients with brain tumours. Neurosurgery 1; 114-119

Mosmans P C M (1974). Regional cerebral blood flow in neurological patients. Van Gorcum & Co, Assen, Netherlands. pp62-71

Murota T, Nagoa S, Momma F, Nishiura T, Soga M (1988) . [The effect of lidocaine on brain edema and neuronal function]. No To Shinkei 39; 915-21

Nagata K, Gross L E, Kindt G W, Geier J M, Adey G R (1985). Topographic electroencephalographic study with power ratio index mapping in patients with malignant brain tumours. Neurosurgery 17; 613-619

Nakagawa H, Groothuis D, Owens E S, Fenstermacher J D, Patlak C S, Blasberg R G (1987). Dexamethasone effects in [$_{125}$I] albumin distribution in experimental RG-2 gliomas and adjacent brain. J CBF Metab 7; 687-701

Narayan R K, Heydorn W E, Creed G V (1986). Protein Patterns in various malignant brain tumours by 2 dimensional gel electrophoresis. Cancer Res 46; 4685-94

Naruse S, Horikawa Y, Tanaka C, Hirakawa K, Nishikawa H, Yoshikazi K (1982). Proton nuclear magnetic resonance studies in brain oedema. J Neurosurg 56; 747-752

Nelson S R., Mantz M L, Maxwell J A. (1971). Use of specific gravity in the measurement of cerebral edema. J Appl Physiol 30; 268-271

Oettinger W, Baethmann A, Rothenfusser W, George R, Mann K (1976). Tissue and plasma factors in cerebral edema. In Pappius H M, Feindel W, (Ed's) Dynamics of Brain Edema, Springer-Verlag, Berlin, 161-163

Ojemann R (1985). Comments on paper by Nagata et al (vide supra). Neurosurgery 17; 619

Olesen S P, Crone C (1986). Substances that rapidly augment ionic conductance of endothelium in cerebral venules. Acta Physiol Scand 127; 233-41

Osterholm J L, Bell J, Meyer R, Ryenson J (1969). Experimental effects of free serotonin on the brain and its relation to injury. J Neurosurg 31; 408-421

Osugi Y, Uchida S, Imaizumi T, Yoshida N (1986). Bradykinin induced intracellular Ca^{2+} elevation in neuroblastoma x glioma hybrid NG108-15 cells; relationship to the action of inositol phospholipid metabolites. Brain Res 379; 84-9

Passerini P, Ferini Strambi L, Sbacchi M, Pezzoli G (1983). EEG pattern in cerebral tumours with and without cerebral edema. Electroencephal clin Neurophysiol 23; 117-122

Pasztor E, Symon L, Dorsch N W C, Branston N M. (1973). The hydrogen clearance method in assessment of blood flow in cortex, white matter and deep nuclei of baboons. Stroke 4; 556-567

Patton H D, Amassian V E (1954). Single multiple unit analysis of cortical stage of pyramidal activation. J Neurophysiol 17; 345-357

Palvolgyi R (1969). Regional cerebral blood flow in patients with intracranial tumours. J Neurosurg 31; 149-163

Paxinos G, Watson C (1982). The rat brain in stereotaxic coordinates. Acad Press, Sydney.

Penfield W, Buckley A (1928). Punctures of the brain. Arch Neurol Psychiat (Chic) 20; 1 - 13.

Penfield W, Cone W (1926). Acute swelling of the oligodendroglia. Arch Neurol Psychiatr (Chic) 16; 131-153.

Penn R D (1980). Cerebral edema and neurological function in human beings. Neurosurgery 6; 249-254

Perret G E, Kernohan J W (1943). Histopathological changes of the brain caused by intracranial tumours. J Neuropath Exp Neurol 2; 341-352

Persson L, Hillered L, Ponten U, Ungerstadt U (1989). Intracerebral microdialysis for continous metabolic monitoring of neurosurgical patients. J CBF Metab 9(Suppl 1); S584

Philippon J, Foncin J F, Grob R et al. (1984). Cerebral edema associated with meningiomas: possible roles of a secretory-excretory phenomenon. Neurosurgery 14; 295-301

Picozzi P., Todd N V, Crockard A E (1985). The role of cerebral blood volume changes in brain specific gravity. J Neurosurg 62; 704-710

Pirola C J, Balda M S, Alvarez A, Finkelman S, Nahmod V (1986). Interaction between acetylcholine and bradykinin in the lateral septal area of rat brain; Involvement of muscarinic receptors in the cardiovascular response. Neuropharmacol 25; 1387-93

Podulso S E, Miller K, Jang Y (1983). Comparison of lipids and lipid metabolism in human glioma cell line , its clone and oligodendroglioma. Cancer Res 43; 1014-18

Poliakova A G (1972). Origin of early component of thye evoked response in the association cortex of the cat. Electroencephal clin Neurophysiol 32; 129-138

Prados M, Strowger B, Feindel W H (1945). Studies on cerebral oedema I. Reaction of brain to air exposure. Pathological changes. Arch Neurol Psychiat 54; 163-174.

Quindlen E A, Bucher A P. (1987). Correlation of tumor plasminogen activator with peritumoral cerebral edema. J

Neurosurg 66; 729-733.

Rao P J, Bhattacharya S K (1988). Hyperthermic effects of centrally administered bradykinin in the rat; role of prostaglandin and serotonin. Int J Hyperthermia 4; 183-9

Regoli D (1986). Kinins, receptors and antagonists. Adv Exp Med Biol 198; 549-58

Regoli D, Barabe J. (1980). The pharmacology of bradykinin and related kinins. Pharm Rev 32; 1-47

Reichardt M (1905). Zur Entstehung des Hirndrucks bei Hirngeschwulsten und anderen Hirnkrankheiten und uber eine bei diesen zu beobachtende besondere Art der Hirnschwellung. Dtsch Nervenheilk 28; 306-355

Reiser G, Hamprecht B (1982). Bradykinin induces hyperpolerization in rat glioma cells and neuroblastoma x glioma hybrid cells. Brain Res 239; 191-9

Reiser G, Hamprecht B (1985). Bradykinin causes a transient rise of intracellular Ca^{2+} activity in cultured neuronal cells. Pflugers Arch 405; 260-4

Reiser G, Walter U, Hamprecht B (1984). Bradykinin regulates the level of guanosine 3',5' cyclic monophosphate in neural cell lines. Brain Res 290; 367-71

Reulen H J, Graham R, Spatz M, Klatzo I (1977). Role of pressure gradients and bulk flow in dyanmics of vasogenic brain edema. J Neurosurg 46; 24-35

Reulen H J, Tsuyumu M, Prioleau G (1980). Further results concerning the resolution of vasogenic brain edema. Adv Neurol 28; 375-382

Reynolds J R (1855). The diagnosis of diseases of the brain, spinal cord and nerves and their appendages. John Churchill, London, pp 251

Rosenblum W I (1988). Loss of endothelial relaxation in mouse cerebral microvessels may be rapidly reversible. Microvasc Res 35; 132-138.

Rostan L L (1823).Recherches sur le ramollisement du cerveaux. Bechet-Jeune, Paris, Ed 2.

Russell D, Rubenstein L J (1989). Pathology of tumours of the central nervous system. 4th Edition,

Ryan B, Joiner B L, Ryan T A (1985). MINITAB. Duxbury Press, Boston, Mass. pp 379

Sawaya R, Highsmith R (1988). Plasminogen activator activity and molecular weight patterns in human brain tumours. J

Neurosurg 68; 73-79

Scalabrino G, Ferioli M E, Luccarelli G (1985). Polyamine biosyntheis in primary tumours of the human central nervous system: Review of current knowledge. Prog Neurobiol 25; 289-95

Schaul N, Ball K, Gloor P, Pappius H (1976). The EEG in cverebral edema. In Pappius H, Feindel M (Ed's), Dynamics of brain edema. Springer, Berlin, 144-149

Scheinker I M (1941). Cerebral swelling and edema associated with cerebral tumour. Arch Neurol Psychiat 45; 117-129.

Scheinker I M (1947). Histopathology, classification and clinical significance of brain oedema. J Neurosurg 4; 255-275

Schwarz R D, Skolnick P, Paul S M (1988). Regulation of gamma aminobutyric acid/barbiturate receptor gated chloride ion flux in brain vesicles by phospholipase A2: possible role of oxygen radicles. J Neurochem 50; 565-71

Seitz R J, Wechsler W (1987). Immunohistochemical demonstration of serum proteins in human cerebral gliomas. Acta Neuropatol (Berl) 73; 145-152

Shibasaki H, Yamashita Y, Tsuji S (1977). Somatosensory evoked potentials. Diagnostic criteria and abnormalities with cerebral lesions. J Neurol Sci 34; 427-39

Shinonaga M, Chang CC, Suzuki N, Sato N, Kuwabara T (1988). Immunohistological evaluation of macrophage infiltrates in brain tumours. J Neurosurg 68; 259-265

Shimizu J, Ktayama Y, Minamisawa H, Sugimoto S, Suzuki S, Teashi A (1987). [Involvement of arachidonic acid cascade in brain oedema and cerebral energy metabolism after reperfusion]. No To Shinkei 39; 355-360

Shitara N, McKeever P E, Smith B H (1983). Products of cultured neuroglial cells. III. Release of an 85,000 molecular weight glycoprotein by C6 glioma cells in vitro. J Neurochem 39; 948-953

Smith R R, White H B, Jackson M (1968). Neutral lipid patterns of normal and pathological nervous tissues. Arch Neurol 19; 54-59

Snider R S, Niemer W T (1962). Stereotactic atlas of the cat brain. Uni of Chicago Press, Chicago.

Solly S (1847). The human brain. Its structure physiology and diseases with a description of the typical forms of brains in the animal kingdom. Longmans, London, Ed 2, p374

Spatz H (1929). Die Beduetung der "symptomatischen Hirnschwellung" fur die Hirntumoren und fur andere raumbeengende Prozesse in der Schadelgrube. Arch Psychiat Nervenkr 88; 790-794

Steudel W I,Beck V, Becker H, Hacker H, (1976). EEG in patients with tumours of the cerebral hemispheres. In Lanksch W, Kazner E (Ed's) Cranial computerized tomography, Springer, Berlin,p 188-200

Stewart P A, Hayakawa K, Farrell C I, del Maestro R F (1987) Quantitative study of microvessel ultrastructure in human peritumoural brain tissue. J Neurosurg 67; 697-705

Stewart-Wallace A M (1939). A biochemical study of cerebral tissue and changes in cerebral oedema. Brain 62; 426-438

Stohr M, Dichgans S J, Voigt K, Buttner W (1983). The significance of somatosensory evoked potentials for localization of unilateral lesions within the cerebral hemispheres. J Neurol Sci 61; 49-63

Sullivan H G, Miller J D, Griffith R L, Emgr D (1979). Bolus versus steady state infusion for determination of the CSF outflow resistance. Ann Neurol 5; 228-238.

Sutton L N, Bruce D A, Welsh F A, Jaggi J L (1980). Metabolic and electrophysiological consequences of vasogenic brain edema. Adv Neurol 28; 241-254

Sutton L N, Frewen T, Marsh R, Jaggi J, Bruce D A (1982). The effects of deep barbiturate coma on multimodality evoked potentials. J Neurosurg 57; 178-185

Szymas J, Hossmann K A (1984). Immunofluorescent investigation of extravasated serum proteins in human brain tumour and adjacent structures. Acta Neurochir (Wien) 71; 229-241

Takagi H, Shapiro K, Marmarou A, Wisoff H. (1981). Microgravimetric analysis of human brain tissue. Correlation with computerized tomography. J Neurosurg 54; 797-801.

Takizawa H, Gabra-Sanders T, Miller J D (1985). Validity of measurement of CSF outflow resistance estimated by the bolus injection method. Neurosurgery 17; 63-66

Takizawa H, Gabra-Sanders T, Miller J D (1986a). Analysis of changes in ICP and PVI at different locations in the craniospinal axis. Neurosurgery 19; 1-8

Takizawa H, Gabra-Sanders T, Miller J D (1986b). Variations in PVI and CSF outflow resistance at different locations in the feline craniospinal axis. J Neurosurg 64; 298-303

Tanaka K, Marmarou A, Nishimura S (1983). Electro-

physiological and regional cerebral blood flow changes associated with direct infusion edema. In Ishii S, Nagai H, Brock M (Ed's). Intracranial Pressure V, Springer, Berlin. pp 413-418

Terplan K L (1937). Histopathological changes in marked swelling of the brain. Am J Path 13; 664-667

Torack R M, Alcala H, Gado M, Burton R (1976). Correlative assay of computerized cranial tomography (CCT), water content and specific gravity in normal and pathological postmortem brain. J Neuropath Exp Neurol.35; 385-392.

Towe A L, Patton H D, Kennedy T T (1964). Response of neurons in the pericruciate cortex of the cat following electrical stimulation of the appendages. Exp Neurol 10; 325-344.

Tsubokawa T, Doi N, Ohata H, Kondo T (1983). The effects of brain edema fluid on cerebral blood flow in tissue infusion model. In Ishii S, Nagai H, Brock M (Ed's). Intracranial Pressure V, Springer, Berlin. pp 419-423

Unterberg A, Baethmann A. (1984). The kallikrein-kinin system as a mediator in vasogenic brain edema Part 1: Cerebral exposure to bradykinin and plasma. J Neurosurg 61; 87-96.

Unterberg A, Wahl M, Baethmann A (1984). Effects of bradykinin on permeability and diameter of pial vessels in vivo. J CBF Metab 4; 574-85

Unterberg A, Dautermann C, Baethmann A, Muller-Esterl W (1986). The kallikrein-kinin system as mediators in vasogenic brain edema; Part 3, Inhibition of kallikrein-kinin system in traumatic brain swelling. J Neurosurg 64; 269-76

Unterberg A, Schmidt W, Polk T, Wahl M, Ellis E, Marmarou A. Baethmann A (1987a). Evidence against leukotrienes as mediators of brain edema. J CBF Metab 7(Suppl 1); s625

Unterberg A, Wahl M, Hammersen F, Baethmannn A (1987b) Permeabilty and vasomotor response of cerebral vessels during exposure to arachidonic acid. Acta Neuropathol (Berl) 73; 209-219

Wahl M, Lauritzen M, Schilling L (1987). Change of cerebrovascular reactivity after cortical spreading depression in cats and rats. Brain Res 411; 72-80

Wahl M, Unterberg A, Baethmann A (1988). Mediators of blood brain barrier dysfunction and formation of vasogenic brain oedema. J CBF Metab 8; 621-634

Walker V, Pickard J. (1985). Prostaglandins, thromboxane,

leukotrienes and the cerebral circulation in health and disease. Adv Tech Standards In Neurosurg 16, 5-87.

Walstra G, Takagi H, Marmarou A, Shapiro K, Schulman K (1980). The time course of brain tissue compliance and resistance in a controlled model of brain oedema. In Schulman K, Marmarou A, Miller J D, Becker D, Hochwald G Brock M, Intracranial Pressure IV, Springer, Berlin. p253-6

Watanabe M, Rosenblum W I (1987). In vivo studies of pial vascular permeability to sodium fluorescein; absence of alterations by bradykinin, histamine, serotonin or arachidonic acid. Stroke 18; 1157-9

Weller R O, Foy M, Cox S (1977). The development and ultrastructure of the microvasculature in malignant gliomas. Neuropath Appl Neurobiol 3;307-322

Wei E P, Ellison M B, Kontos H A, Povlishock J T (1986). Oxygen radicals in arachidonate induced increased blood brain barrier permeability to proteins. Am J Physiol 251; H693-9

Westcott J Y, Murphy R C, Stenmark K (1987). Eicosanoids in human ventriculer CSF following severe brain injury. Prostaglandins 34; 877-87

Westergaard E (1975). Enhanced vesicular transport of exogenous peroxidase across cerebral vessels induced by serotonin. Acta Neuropathol (Berl) 39, 181-187

Whittle I R, Besser M, Johnstone I H (1987). Short latency somatosensory evoked potentials in children. Part 4; Findings with cerebral lesions. Surg Neurol 27; 37-43.

Wiederholt W G, Iragui-Madoz V J (1977). Far field somatosensory potentials in the rat. EEG clin Neurophysiol 42;456-65

Wohlwill F (1914). Uber amoeboide Glia. Virchows Arch 216; 468-499

Wolfe L S (1982). Eicosanoids: prostaglandins, thromboxanes, leucotrienes and other derivatives of carbon 20 unsaturated fatty acids. J Neurochem 38; 1-14

Yamada K, Bremer A M, West C R (1979). Effects of dexamethasone on tumour induced brain oedema and its distribution in the monkey. J Neurosurg 50; 361-367.

Yamakazi H, Tsukhara T, Uki J, Malsuzaki S (1986). Elevated levels of free putrescine and N-acetyl spermidine in cyst fluids of malignant barin tumours. J Neurol Neurosurg Psychiat 49; 209-210

Yanagahara T, Cummings J N (1968). Lipid metabolism in

cerebral oedema associated with human brain tumours. Arch Neurol 19; 241-247.

Young W (1980). H2 clearance measurement of blood flow; A review of technique and polargraphic principles. Stroke 11; 552-564

York D H (1987). Review of descending motor pathways involved with transcranial stimulation. Neurosurgery 20; 70-73

Yu A C, Chan P H, Fishman R A (1986). Effects of arachidonic acid on glutamate and gamma aminobutyric acid uptake in primary cultures of rat cerebral cortical astrocytes and neurones. J Neurochem 47; 1181-9

APPENDIX 1

CONSTITUENTS OF THE 20% PROTEIN INFUSATE

75 ml sterile water

10 ml bovine serum

9 ml Eagles Media (Contains the following essential amino acids)

- Arginine 100 mg/l
- Histidine 42 mg/l
- L-Cystine 73 mg/l
- Phenyl alanine 33 mg/l
- Tyrosine 45 mg/l
- L-isoleucine 42 mg/ml
- Cystine 28 mg /l
- L-Glutamine 290 mg/l
- L-Methionine 15 mg/l
- Tryptophan 10 mg/l
- Valine 47mg/l
- L-leucine 52 mg/ml

3.3 ml $NaHCO_3$

1 ml 100mM pyruvate

1 ml Nonessential aminoacids

1 ml penicillin (100 U/ml)

1 ml streptomycin (100 ug/ml)

1 ml 200uM glutamate

APPENDIX 2

GLIOMA CYST FLUIDS

Biochemical composition

		EB-GBM	TF-Oligo	GD-EBM	JH-AA
Na	mmol/L	136	146	135	141
K	mmol/L	3.4	3.7	3.4	4.6
Cl	mmol/L	105	114	102	106
CO_2	mmol/L	18	21	18	15
Urea	mmol/L	7.4	6.7	5.1	8.4
Bili	mmol/L	12	9	10	-
Alk P	U/L	16	30	41	24
PO4	mmol/L	1.19	0.98	1.28	1.14
Ca	mmol/L	1.76	1.82	1.91	1.79
Prot	g/L	40	42	46	51
Alb	g/L	28	30	29	35
Creat	mmol/L	0.06	0.09	0.09	0.09
LD	U/L	1289	1275	5740	2720
Ast	U/L	40	70	135	60
IgA	IU/ml	31	31	49	44
IgG	IU/ml	56	50	66	53
IgM	IU/ml	69	32	60	122
TFN *	g/L	1.51	1.26	1.52	2.43
Mg	mmol/L	0.77	0.37	0.74	0.54
Chol	mmol/L	6.4	5.2	5.5	3.1

Electrophoretic Profiles

	%	g/dl	%	g/dl	%	g/dl	%	g/dl
Albumin	67	2.67	64	2.69	59	2.7	64	3.25
Alpha-1	4	.16	3	.11	3	.13	1	.05
Alpha-2	7	.28	7	.28	12	.55	6	.29
Beta	11	.42	12	.51	14	.64	20	.10
Gamma	12	.46	15	.62	13	.58	10	.52
Albumin/ Globulin ratio	2.1		1.77		1.41		1.75	

Preoperative Dexamethasone

Total	240 mg	0	104 mg	52 mg
Days	15	0	7	3

* Transferrin

APPENDIX 3

Variations of ICP with P_aCO_2 in the normal rat

The following data was obtained from two rats that were paralysed and ventilated. P_aCO_2 adjustments were produced by altering the tidal volume and respiratory rates of the ventilater. In all cases the P_aO_2 was above 100 mmHg

ICP (mmHg)	mean BP (mmHg)	P_aCO_2 (mmHg)	pH
6.5	100	42	7.30
4.0	135	32	7.43
4.5	100	29	7.38
7.5	170	48	7.26
6.0	150	39	7.35
4.5	120	32	7.43
5.0	108	30	7.39
8.0	105	50	7.25

Linear regression equation for the relationship between ICP and P_aCO_2

$$ICP = 0.173\ P_aCO_2 - 0.81$$
$$r = 0.96 \qquad p < 0.001$$

APPENDIX 4

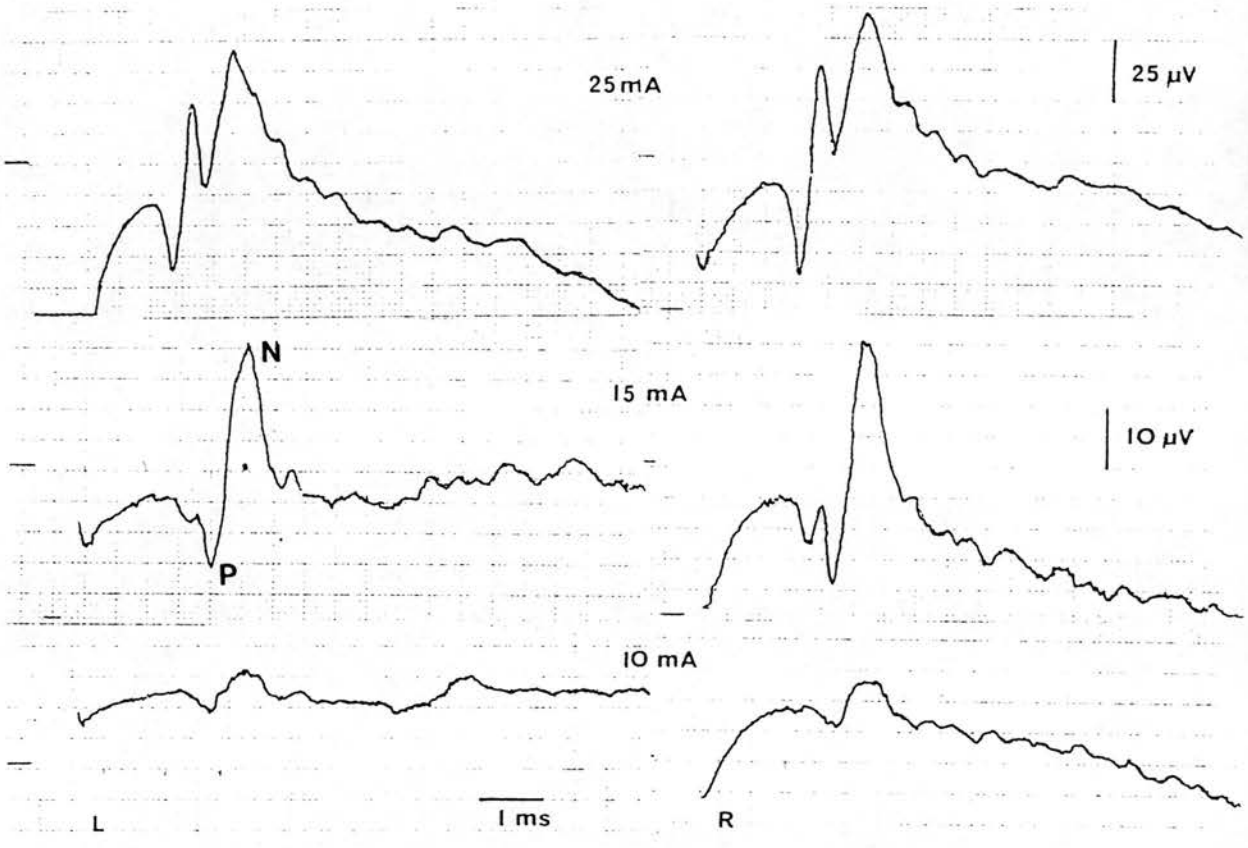

The morphology and amplitude of the spinal MEP waveform is directly related to stimulus intensity. At 10 mA stimulation of the motor cortex through a platinum iridium electrode a small negative (N) wave can be recorded from the low thoracic cord. At 15 mA stimulation a larger waveform is recorded and there is a negative subcomponent to the P wave. At 25 mA stimulus the waveform is of larger amplitude with two well defined negative peaks. R = waveform following right cortical stimulation, L that following left cortical stimulation.

APPENDIX 5

Differences in CBF (ml/100g/min) calculated using a 5 and 120 point analysis of the initial slope

CBF 5 point	CBF 120 point	Difference
43	47	-4
54	47	+8
45	45	0
45	45	0
35	47*	-12
45	53*	-8
42	47	-5
45	40	+5
49	60*	-11
47	54	-7
57	62	-5
55	55	0
24	25	-1
24	26	-2
27	29	-2
26	32	-6
30	33	-3
33	40	-7
37	50*	-13
52	53	-1
58	59	-1
35	51*	-16
42	46	-4
46	47	-1
20	21	-1
21	24	-3
23	25	-2
26	34*	-8
23	26	-3
35	41	-6

In these 30 comparative flow values the 5 point analysis was below the computerized 120 point analysis in 21 cases, the same in 3 and higher in 6 cases. Computerized analysis using videographics also enabled bi-exponential curves (*) to be readily detected. Nontheless the median error, assuming 120 point analysis is the most accurate method, was for the 5 point analyses to be 3 ml/100g brain/min low.

APPENDIX 6

TABLES

Table A.1: Rat Subcortical tissue specific gravity adjacent and contralateral to the site of intracerebral infusion. All data mean ± SD. P values refer to interhemispheric differences.

INFUSION TYPE	n	INFUSED (L) HEMISPHERE	CONTRALATERAL HEMISPHERE
Sham	5	1.0384 ± .0009 *	1.0387 ± .0015
Saline	5	1.0325 ± .0009**	1.0394 ± .0016
20% Protein	5	1.0332 ± .0021 **	1.0402 ± .0011

* $p = 0.69$ ** $p < .001$

Table A.2: Rat grey matter specific gravity adjacent and contralateral to the site of intracerebral infusion. There were no statistically significant differences between hemispheres with any infusate. All data mean ± SD.

INFUSION TYPE	n	INFUSED (L) HEMISPHERE	CONTRALATERAL HEMISPHERE
Sham	5	1.0417 ± .0009	1.0413 ± .0016
Saline	6	1.0423 ± .0016	1.0418 ± .0016
20% Protein	5	1.0429 ± .0022	1.0418 ± .0023

Table A.3: Brain water content determined using wet/dry weights of the infused and contralateral "control" hemisphere in the rat. All data mean ± SD.

INFUSION TYPE	n	INFUSED HEMISPHERE	CONTRALATERAL HEMISPHERE
Saline	15	77.5 ± 0.66%	77.3 ± 0.72% *
20% Protein	11	78.3 ± 0.29%	77.8 ± 0.65% **

* $p > 0.5$ ** $0.1 < p < 0.05$

Table A.4: ICP changes in the rat (n = 7) during intracerebral infusion with saline at 0.1 ml/hr. All data mean ± SD.

Time (min)	ICP (mmHg)	P_aCO_2 (mmHg)	BP (mmHg)
0	4.4 ± 1.6 *	34 ±2.4	94 ± 21
20	5.0 ± 1.5	36 ±2.9	95 ± 20
40	5.5 ± 1.6	36 ±1.7	89 ± 16
60	6.3 ±1.6 *	38 ±5.1	87 ± 16

* p = 0.04

Table A.5: ICP changes during intracerebral infusion in the rat (n = 7) with a 20% protein solution at 0.1 ml/hr. The difference between 0 and 60 min ICP is not significant. All data mean ± SD.

Time (min)	ICP (mmHg)	P_aCO_2 (mmHg)	BP (mmHg)
0	5.4 ± 1.2	31.4 ±3.2	92 ±21
20	5.7 ± 0.7	32.2 ±2.1	96 ±10
40	5.9 ± 1.2	33.3 ±2.7	88 ±9
60	6.2 ± 2.2	32.6 ±1.7	93 ±15

Table A.6: Infusion pressure, brain tissue hydraulic resistance (R_t) and brain tissue compliance (C_t) in the rat during intracerebral saline infusion at 0.1 ml/hr. Data are mean $\pm$ SD, n = 15.

TIME (min)	INFUSION PRESSURE (mmHg)	R_t ($\times 10^4$) (mmHg/ml/min)	C_t ($\times 10^{-3}$) (ml/mmHg)
Peak	38 $\pm$ 20 *	2.275 $\pm$ 1.10 *	0.22
20	24 $\pm$ 15 *	1.437 $\pm$ 0.89 *	1.38
40	23 $\pm$ 13	1.425 $\pm$ 0.81	2.81
60	21 $\pm$ 12	1.233 $\pm$ 0.77	4.85

* $p < .001$

Table A.7: Infusion pressure, brain tissue hydraulic resistance (R_t) and brain tissue compliance (C_t) in the rat during intracerebral 20% protein infusion at 0.1 ml/hr. Data are mean $\pm$ SD, n = 18.

TIME (min)	INFUSION PRESSURE (mmHg)	R_t ($\times 10^4$) (mmHg/ml/min)	C_t ($\times 10^{-3}$) (ml/mmHg)
Peak	43 $\pm$ 19 *	2.575 $\pm$ 1.14 *	0.19
20	23 $\pm$ 11 *	1.378 $\pm$ 0.66*	1.43
40	20 $\pm$ 9	1.198 $\pm$ 0.54	3.30
60	18 $\pm$ 9	1.078 $\pm$ 0.54	5.55

* $p < .001$

		P_6	N_{12}	P_{14}	N_{20}	P_{28}	MAP	P_aCO_2
0	L	5.9 ± 0.6	12.3 + 0.8	14.1 + 0.8	20.5 + 1.3	27.5 + 1.8	94 ± 15	40 ± 3.3
	R	6.1 ± 0.3	12.8 + 0.7	14.8 + 0.9	20.2 + 1.1	27.5 + 1.5		
20	L	5.6 ± 0.3	12.4 + 0.9	14.0 + 0.9	19.7 + 0.9	26.0 + 1.5	93 ± 7	34 ± 1.5
	R	5.7 ± 0.3	12.7 + 0.8	14.8 + 0.9	19.8 + 1.5	28.7 + 1.7		
40	L	5.7 ± 0.4	12.2 + 0.6	14.0 + 0.2	20.0 + 0.9	27.5 + 1.8	97 ± 9	34 ± 2.2
	R	5.8 ± 0.5	12.3 + 0.8	14.6 + 0.9	20.3 + 0.8	28.7 + 1.8		
60	L	5.7 ± 0.4	12.1 + 0.7	14.1 + 0.9	20.2 + 0.9	28.5 + 2.0	98 ± 12	36 ± 2.0
	R	5.4 ± 0.5	12.3 + 0.9	14.4 + 0.8	20.8 + 0.8	29.6 + 2.1		

Table A.8: Peak latencies (ms) of the five major cortical SEP waveform components obtained from the infused (left) and contralateral (right) hemispheres during intracerebral 0.1 ml saline infusion in the rat (n = 5) over one hour. Mean arterial pressure (MAP) in mmHg and P_aCO_2 are also listed. All data is mean ± SD.

		P_6	N_{12}	P_{14}	N_{20}	P_{28}	MAP	P_aCO_2
0	L	5.9 ± 0.7	12.2 + 0.6	13.7 + 1.2	19.9 + 1.7	25.5 + 1.5	84 ± 12	33 ± 3.1
	R	6.0 ± 0.9	12.6 + 1.3	14.4 + 1.3	20.0 + 1.5	26.5 + 1.7		
20	L	5.6 ± 0.5	12.3 + 0.9	13.8 + 0.8	19.9 + 1.7	26.5 + 1.5	81 ± 9	34 ± 3.3
	R	6.1 ± 0.9	12.5 + 0.6	14.0 + 0.6	19.6 + 1.8	28.5 + 1.0		
40	L	5.4 ± 0.6	12.0 + 0.6	14.0 + 0.5	19.9 + 1.7	26.7 + 2.2	83 ± 9	34 ± 3.4
	R	6.1 ± 1.0	12.5 + 0.4	13.6 + 0.4	20.1 + 1.4	28.5 + 1.3		
60	L	5.3 ± 0.5	12.0 + 0.5	13.5 + 0.2	19.8 + 1.8	27.5 + 2.5	79 ± 4	34 ± 3.5
	R	6.2 ± 0.9	12.4 + 0.4	13.8 + 0.3	19.6 + 1.1	29.5 + 1.5		

Table A.9: Peak latencies (ms) of the five major cortical SEP waveform components obtained from the infused (left) and contralateral (right) hemispheres during intracerebral 0.1 ml 20% protein infusion in the rat (n = 5) over one hour. Mean arterial pressure (MAP) in mmHg and P_aCO_2 are also listed. All data is mean ± SD.

Table A.10: CBF (ml /100 g brain/ minute) during the course of left frontal intracerebral saline infusion (0.1 ml/hr for 60 minutes) in the rat with corresponding mean arterial pressure (MAP) and P_aCO_2. Data expressed as mean ± SD.

	Baseline	20 min	45 min	70 min
Site	n = 10	n = 10	n = 10	n = 10
R Ant Parietal	40 ±14	41 ±11	46 ±16	37 ±17
L Ant Parietal	37 ±16	29 ±10	30 ±9	29 ±7
R Post Parietal	35 ±17	36 ±17	37 ±17	39 ±14
L Post Parietal	38 ±17	31 ±8	35 ±13	36 ±10
P_aCO_2(mmHg)	35.5 ±3.1	34 ±6.6	32.8 ±4	32.9 ±4
MAP(mmHg)	89 ±12.5	86 ±11.2	89 ±9.8	88 ±14.2

Table A.11: CBF (ml /100 g brain/ minute) during the course of left frontal intracerebral 20% protein infusion (0.1 ml/hr for 60 minutes) in the rat with corresponding mean arterial pressure (MAP) and P_aCO_2. All data mean ± SD.

	Baseline	20 min	45 min	70 min
Site	n = 10	n = 9	n = 9	n = 9
R Ant Parietal	45 ±17	37 ±12	42 ±18	46 ±16
L Ant Parietal	42 ±15	36 ±9	35 ±11	40 ±9
R Post Parietal	40 ±16	32 ±15	34 ±15	37 ±14
L Post Parietal	45 ±16	41 ±16	45 ±16	42 ±14
P_aCO_2(mmHg)	32.8 ±3.1	35 ±4.0	33.9 ±3.3	32.0 ±2.7
MAP(mmHg)	84 ±16	86 ±16.8	85 ±14	84 ±14.4

LOCATION	SALINE INFUSION	20% PROTEIN INFUSION
R Ant Parietal	CBF = 1.613 P_aCO_2 - 16.9 n = 49 r = 0.762	CBF = 1.17 P_aCO_2 + 3.4 n = 28 r = 0.72
L Ant Parietal	CBF = 1.58 P_aCO_2 - 5.2 n = 46 r = 0.75	CBF = 0.52 P_aCO_2 + 25.8 n = 36 r = 0.482
R Post Parietal	CBF = 1.433 P_aCO_2 - 12.9 n = 37 r = 0.762	CBF = 0.85 P_aCO_2 +2.9 n = 37 r = 0.53
L Post parietal	CBF = 1.51 P_aCO_2 - 12.8 n = 48 r = 0.774	CBF = 1.06 P_aCO_2 - 1.2 n = 29 r = 0.605

Table A.12; The regression equations, correlation coefficients (r) and levels of significance (p) for CBF CO_2 reactivity for each of the four cerebral locations tested following 0.1 ml left frontal intracerebral saline and 20% protein infusion. $p < 0.001$ for all locations except L anterior parietal, following protein infusion only, where $0.01 > p > 0.001$.

Table A.13; Specific gravity and water content (ml/100 gm tissue) of cat frontal cortex and white matter, sampled following sham infusion into the right centrum ovale. All data mean ± SD.

Tissue	n	H_2O content	SG
Cortex R	4	78.7 ± 0.9	1.0459 ± .0021
Cortex L	4	79.2 ± 0.7	1.0448 ± .0016
White R 5-7 mm	8	68.4 ± 1.0	1.0419 ± .0015
White L 5-7 mm	7	68.0 ± 0.9	1.0425 ± .0012

Table A.14: Specific gravity and water content (ml/100 gm tissue) of cat frontal cortex and white matter, sampled at 5-7 mm depth following 0.6 ml saline infusion into the right centrum ovale. All data mean ± SD.

Tissue	n	H_2O content	SG
Cortex R	5	80.1 ± 0.5	1.0430 ± .0010
Cortex L	4	79.4 ± 0.7	1.0444 ± .0017
White R 5-7 mm	5	78.8 ± 3.8 *	1.0277 ± .0052
White L 5-7 mm	3	67.2 ± 0.9 *	1.0436 ± .0013

* $p < .001$

Table A.15: Specific gravity and water content (ml/100 gm tissue) of cat frontal cortex and white matter, sampled at depth of 5-7 mm, following infusion of 0.6 ml of 20% protein solution into the right frontal centrum ovale. All data mean ± SD.

Tissue		H_2O content	SG
Cortex R	3	82.3 ± 0.3	1.0379 ± .0017
Cortex L	3	81.0 ± 0.3	1.0399 ± .0019
White R 5-7 mm	4	80.9 ± 0.4 *	1.0265 ± .0006
White L 5-7 mm	4	69.9 ± 0.3 *	1.0407 ± .0019

* $p < .001$

Table A.16; Specific gravity and water content (ml/100 gm tissue) of cat frontal cortex and white matter, sampled at variable depth, following infusion of 0.6 ml of 5000 ng/ml bradykinin solution (0.2 ml/hr for three hours) into the right frontal centrum ovale. All data mean ± SD.

Tissue	n	H_2O content	SG
Cortex R	9	80.1 ± 1.5	1.0430 ± .0034
Cortex L	8	78.5 ± 1.0	1.0465 ± .0021
White R 3 mm	6	77.7 ± 2.2	1.0292 ± .0029
White R 7 mm	8	79.8 ± 2.7 *	1.0264 ± .0036
White L 3 mm	5	69.3 ± 2.3	1.0407 ± .0034
White L 7 mm	6	69.4 ± 2.8 *	1.0406 ± .0038

* $p < .001$

Table A.17; Specific gravity and water content (ml/100 gm tissue) of cat frontal cortex and white matter, sampled at variable depth, following infusion of 0.6 ml of 150 ug/ml bradykinin solution into the right frontal centrum ovale. All data mean ± SD.

Tissue	n	H_2O content	SG
Cortex R	2	79.7 ± 0.4	1.0437 ± .0009
Cortex L	2	80.1 ± 0.3	1.0429 ± .0004
White R 3-7 mm	4	76.8 ± 2.7 *	1.0305 ± .0036
White L 3-7 mm	3	68.9 ± 1.2 *	1.0412 ± .0014

* $p < .01$

Table A.18: Specific gravity and water content (ml/100 gm tissue) of cat frontal cortex and white matter, sampled at variable depth, following infusion of 0.6 ml of arachidonic acid solution (2 - 15 mg/ml) into the right frontal centrum ovale. All data mean ± SD.

Tissue	n	H_2O content	SG
Cortex R	8	80.7 ± 1.4	1.0413 ± .0034
Cortex L	7	78.5 ± 1.0	1.0467 ± .0012
White R 5-7 mm	8	79.4 ± 2.2 *	1.0270 ± .0055
White L 5-7 mm	7	68.1 ± 1.2 *	1.0426 ± .0018

* $p < .001$

Table A.19: Specific gravity and water content (ml/100 gm tissue) of cat frontal cortex and white matter, sampled at variable depth, following infusion of 0.6 ml of human glioblastoma cyst fluid (GD) into the right frontal centrum ovale. All data mean ± SD.

Tissue	n	H_2O content	SG
Cortex R	4	80.1 ± 0.8	1.0429 ± .0017
Cortex L	4	78.6 ± 1.4	1.0463 ± .0031
White R 5-7 mm	6	80.3 ± 2.1 *	1.0337 ± .0014
White L 5-7 mm	5	68.1 ± 1.2 *	1.0423 ± .0017

* $p < .001$

Table A.20: Specific gravity and water content (ml/100 gm tissue) of cat frontal cortex and white matter, sampled at variable depth, following infusion of 0.6 ml of human anaplastic astrocytoma cyst fluid (JH) into the right frontal centrum ovale. All data mean ± SD.

Tissue	n	H_2O content	SG
Cortex R	3	79,9 ± 0.4	1.0432 ± .0009
Cortex L	3	79.5 ± 0.4	1.0442 ± .0008
White R 5-7 mm	6	80.3 ± 4.1 *	1.0335 ± .0030
White L 5-7 mm	3	68.8 ± 1.2 *	1.0417 ± .0014

* $p = .003$

Table A.21: Specific gravity and water content (ml/100 gm tissue) of cat frontal cortex and white matter, sampled at variable depth, following infusion of 0.6 ml of human glioblastoma cyst fluid (EB) into the right frontal centrum ovale. All data mean ± SD.

Tissue	n	H_2O content	SG
Cortex R	4	80.2 ± 1.4	1.0425 ± .0033
Cortex L	4	81.1 ± 0.7	1.0406 ± .0015
White R 5-7 mm	7	82.5 ± 4.7 *	1.0320 ± .0031
White L 5-7 mm	4	70.0 ± 2.0 *	1.0398 ± .0027

* $p = .001$

Table A.22: Specific gravity and water content (ml/100 gm tissue) of cat frontal cortex and white matter, sampled at variable depth, following infusion of 0.6 ml of human oligodendroglioma cyst fluid (TF) into the right frontal centrum ovale. All data mean ± SD.

Tissue	n	H_2O content	SG
Cortex R	2	80.5 ± 0.2	1.0419 ± .0004
Cortex L	2	80.7 ± 0.2	1.0414 ± .0004
White R 5-7 mm	2	78.9 ± 0.6 *	1.0350 ± .0004
White L 5-7 mm	2	68.1 ± 0.3 *	1.0424 ± .0004

* p = .002

Table A.23; Intraventricular pressure (ICP) recorded during 3 hour period of sham infusion in the cat with corresponding mean arterial pressures and P_aCO_2 levels (n = 3). All data mean + SD.

Time (min)	ICP (mmHg)	P_aCO_2 (mmHg)	BP (mmHg)
0	4.8 ± 1.0 *	32.6 ±3.0	110 ± 7
60	5.0 ± 2.6	35.6 ±0.6	120 ± 20
120	7.3 ± 4.9	37.0 ±4.0	120
180	7.8 ± 6.2 *	35.2 ±1.0	123 ± 6
360	10.5± 3.5	46.5 ±1.4	122 ± 6

* p = 0.45

Table A.24; ICP changes in four cats having saline or saline/5% ether (*) infusion at either 0.2 or 0.3 ml/hr.

Volume/hr	n	Baseline	60 min	120 min	180 min
0.2 ml	2	4, 10	6, 20	4, 24	11, 23
0.2 ml *	1	2	7	14	15
0.3 ml	1	6	24	20	36

Table A.25; Intraventricular pressure (ICP) recorded during 20% protein intracerebral infusion at 0.2 ml/hr for three hours in the cat (n = 8), with corresponding mean arterial pressures and P_aCO_2 levels. All data mean ± SD.

Time (min)	ICP (mmHg)	P_aCO_2(mmHg)	BP (mmHg)
0	6.7 ± 3.8 *	31.9 ±2.28	135 ± 19
60	11.4 ± 7.6	32.8 ±2.29	137 ± 20
120	14.4 ± 9.1	33.9 ±2.97	132 ± 19
180	16.9 ± 9.4 *	34.8 ±3.11	136 ± 16
360	14.1 ± 2.8	36.8 ±6.0	110± 10

* p = 0.02

Table A.26: Intraventricular pressure (ICP) recorded during and after bradykinin infusion, at 5000 ng/ml (n = 7) and 150 ug/ml (n = 1), in the cat. The mean arterial pressures and P_aCO_2 levels are for the 5000 ng/ml infusion group. All data mean ± SD.

Time (min)	ICP 5000 ng/ml	ICP 150 ug/ml	P_aCO_2(mmHg)	BP (mmHg)
0	4.5 ± 2.5 *	9	31.9 ±2.28	135 ± 19
60	6.8 ± 3.2	15	32.8 ±2.29	137 ± 20
120	12.0 ± 5.1	27	33.9 ±2.97	132 ± 19
180	16.1 ± 5.8 *	23	34.8 ±3.11	136 ± 16
360	15.8 + 7.8	12	43.0 ±5.71	112 ± 7

* p = .003

Table A.27: Intraventricular pressure (ICP) recorded during arachidonic acid infusion, at doses ranging from 2 - 15 mg/ml, in the cat (n = 6), with corresponding mean arterial pressures and P_aCO_2 levels. All data mean ± SD.

Time	ICP (mmHg)	P_aCO_2 (mmHg)	BP (mmHg)
0	5.1 ± 2.4 *	34.4 ±3.0	122 ± 16
30	8.2 + 2.5	34.0 +3.7	128 + 12
60	8.0 ± 3.6	34.2 ±1.3	115 ± 19
90	10.0 + 3.9	34.2 +2.4	114 + 20
120	11.8 ± 3.2	34.8 ±2.0	122 ± 16
150	13.7 + 4.3	35.1 +3.2	115 + 23
180	14.0 ± 3.0 *	34.8 ±1.3	115 ± 25
360	8.2 ± 1.1	37.6 ±4.4	121 ± 13

* $p < .001$

Table A.28 Intraventricular pressure (ICP) recorded during 3 hour period of intracerebral infusion of 0,6 ml of human glioblastoma cyst fluid (GD) in the cat (n = 2), with corresponding mean arterial pressures and P_aCO_2 levels. All data mean ± SD.

Time	ICP (mmHg)	P_aCO_2 (mmHg)	BP (mmHg)
0	6.0 ± 3.5	34.0 ± 1.8	138 ± 3
60	11.0 ± 0.8	33.5 ± 2.8	130
120	15.8 ± 10	32.0 ± 1.7	120
180	21.3 ± 5.3	34.2 ± 1.7	110
360	12.8 ± 1	42.5 ± 4	115

Table A.29; Intraventricular pressure (ICP) recorded during 3 hour period of intracerebral infusion of 0,6 ml of human anaplastic astrocytoma cyst fluid (JH) in the cat ($n = 2$), with corresponding mean arterial pressures and P_aCO_2 levels. All data mean $\pm$ SD.

Time	ICP (mmHg)	P_aCO_2(mmHg)	BP (mmHg)
0	8.3 $\pm$ 1.7	34.3 $\pm$ 2.2	140 $\pm$ 6
60	13.8 $\pm$ 1.8	33.5 $\pm$ 0.8	125 $\pm$ 14
120	17.5 $\pm$ 3.5	33.0 $\pm$ 1.4	118 $\pm$ 11
180	22.0 $\pm$ 5.6	32.0 $\pm$ 1.4	118 $\pm$ 11
360	16.2 $\pm$ 3.2	34.0 $\pm$ 1.4	115

Table A.30; Intraventricular pressure (ICP) recorded during 3 hour period of intracerebral infusion of 0,6 ml of human glioblastoma cyst fluid (EB) in the cat ($n = 2$), with corresponding mean arterial pressures and P_aCO_2 levels. All data mean $\pm$ SD.

Time	ICP (mmHg)	P_aCO_2(mmHg)	BP (mmHg)
0	9.8 $\pm$ 3.2	34.3 $\pm$ 5.0	130 $\pm$ 11
60	12.3 $\pm$ 5.3	34.5 $\pm$ 2.1	132 $\pm$ 17
120	14.5 $\pm$ 7.2	33.8 $\pm$ 0.5	127 $\pm$ 11
180	19.0 $\pm$ 9.0	32.5 $\pm$ 3.5	135 $\pm$ 7
360	9.8 $\pm$ 3.3	37.0	135 $\pm$ 7

Table A.31; Intraventricular pressure (ICP) recorded during and after a 3 hour period of intracerebral infusion of 0,6 ml of human oligodendroglioma cyst fluid (TF) in one cat with corresponding mean arterial pressures and P_aCO_2 levels. All data mean $\pm$ SD.

Time	ICP (mmHg)	P_aCO_2(mmHg)	BP (mmHg)
0	3.0	33	120
60	9.5	35	130
120	14	30	130
180	13	32	125
300	13	35	100

TIME (min)	SHAM (n = 3)	SALINE (n = 3)	20% PROTEIN (n = 8)	BRADYKININ (n = 6)	ARACHIDONIC ACID (n = 5)
0	0.411 ± .048	0.379 ±.114	0.529 ± .193	0.444 ± .169	0.343 ± .102
60	0.367 ± .110	0.460 ±.160	0.517 ± .173	0.437 ± .150	0.350 ± .070
120	0.342 ± .128	0.499 ±.048	0.545 ± .170	0.483 ± .108	0.323 ± .083
180	0.335 ± .133	0.436 ±.040	0.515 ± .078	0.456 ± .108	0.304 ± .068
360	0.408	NA	0.445 ± .119	0.398 ± .122	0.326 ± .068
	p = 0.23	p = 0.55	p = 0.63	p = 0.62	p = 0.73

Table A.32: The intracranial pressure volume index (PVI) in ml calculated following an intraventricular 0.1 ml saline bolus during intracerebral infusion for three hours at a rate of 0.2 ml/hr with saline, 20% protein and bradykinin 5000 ng/ml solutions. All data is mean ± SD. P values refer to differences between baseline (0) and 180 min PVI values.

TIME (min)	EB-GBM (n = 2)	JH-AA (n = 2)	GD-GBM (n = 2)	TF-OLigo (n = 1)
0	0.538 ± .069	0.417 ±.034	0.361 ± .107	0.371
60	0.400 ± .051	0.418 ±.016	0.352 ± .043	0.504
120	0.398 ± .095	0.428 ±.044	0.315 ± .143	0.509
180	0.462 ± .183	0.464 ±.058	0.316 ± .053	0.386
360	0.462	0.490 ±.035	0.332	0.480

Table A.33: The intracranial pressure volume index (PVI) in ml calculated following an intraventricular 0.1 ml saline bolus during intracerebral infusion for three hours at a rate of 0.2 ml/hr with various human glioma cyst fluids. All data is mean ± SD.

TIME (min)	SHAM (n = 3)	SALINE (n = 3)	20% PROTEIN (n = 8)	BRADYKININ (n = 6)	ARACHIDONIC ACID (n = 6)
0	70 ± 31	120 ± 95	88 ± 57	70 ± 31	99 ± 65
60	84 ± 47	137 ± 99	139 ± 91	103 ± 93	166 ± 112
120	173 ± 85	125 ± 87	138 ± 113	133 ± 113	230 ± 106
180	149 ± 104	205 ± 96	128 ± 106	189 ± 96	437 ± 298
360	130	NA	152 + 73	136 ± 138	188 ± 79
	p = 0.15	p = 0.22	p = 0.32	p = 0.015	p= 0.045

Table A.34; CSF outflow resistance (R_o) in mmHg/ml/min before and at 60 minute intervals during intracerebral infusion calulated one minute after an intraventricular injection of 0.1 ml bolus of saline. All data is mean ± SD. P values refer to differences between baseline (0) and 180 min values.

TIME (min)	EB-GBM (n = 2)	JH-AA (n = 2)	GD-GBM (n = 2)	TF-OLIGO (n = 1)
0	170 + 53	78 ± 22	89 ± 24	50
60	137 + 89	140 ± 6	241 ± 97	140
120	260 + 48	240 ± 74	195 ± 67	184
180	252 + 28	269 ± 74	457 ± 154	183
360	224	325 ±	430 + 205	88

Table A.35: CSF outflow resistance (mmHg/ml/min) measured before and at 60 minute intervals during intracerebral infusion with various human glioma cyst fluids one minute after an intraventricular injection of 0.1 ml bolus of saline. All data mean ± SD.

TIME	SHAM (n = 3)	SALINE (n = 3)	20% PROTEIN (n = 8)	BRADYKININ (n = 6)	ARACHIDONIC ACID (n = 5)
0	.042 ± .008	.039 ±.018	.039 ±.011	.040 ±.019	.035 ± .022
60	.036 ± .016	.026 ±.020	.023 ±.013	.028 ±.019	.019 ± .007
120	.024 ± .013	.019 ±.018	.015 ±.008	.023 ±.019	.012 ± .004
180	.024 ± .013	.012 ±.005	.014 ±.009	.014 ±.007	.010 ± .003
360	.012	NA	.015 ± .003	.012 +.009	.017 ± .003
	p = 0.11	p = 0.013	p = 0.03	p = 0.01	p = 0.016

Table A.36: Lumped craniospinal compliance (ml/mmHg) measured before and at 60 minute intervals during intracerebral infusion following intraventricular injection of 0.1 ml of saline. All data mean ± SD. p values refer to difference in compliance between baseline (0) and 180 minute values.

TIME (min)	EB-GBM (n = 2)	JH-AA (n = 2)	GD-GBM (n = 2)	TF-OLIGO (n = 1)
0	0.029 ± .013	0.022 ±.013	0.031 ± .011	0.047
60	0.016 ± .004	0.013 ±.001	0.014 ± .001	0.023
120	0.015 ± .002	0.011 ±.001	0.010 ± .002	0.016
180	0.008	0.009 ±.001	0.008 ± .001	0.012
360	0.022	0.011 ±.004	0.011	-

Table A.37: Lumped craniospinal compliance (ml/mmHg) recorded following intraventricular bolus injection of 0.1 ml of saline before, during and after intracerebral infusion with glioma cyst fluid. All data mean ± SD.

Table A.38: Infusion pressure (P_{inf}) and ICP (both in mmHg) at specific times (min) during intracerebral infusion in 8 cats. Brain tissue hydraulic resistance (R_t) is in mmHg/ml/min x 10^3. Cat 1 protein infusion, cat 2 saline infusion, cats 3-8 bradykinin infusion. No ICP data available for cats 1 and 5. Mean ± SD for each parameter at each time point is listed in the last three rows.

		Time (min)				
Cat		2 - 3	10	60	120	180
1	P_{inf}	34	18	12	13	14
	ICP	-	-	-	-	-
2	P_{inf}	42	18	15	12	15
	ICP	8	8	8	12	13
3	P_{inf}	30	15	15	25	30
	ICP	10	12	12	22	25
4	P_{inf}	32	10	10	10	12
	ICP	6	6	8	12	14
5	P_{inf}	42	20	20	25	30
	ICP	-	-	-	-	-
6	P_{inf}	14	11	13	12	13
	ICP	3	3	3	4	10
7	P_{inf}	22	11	12	17	25
	ICP	9	8	10	15	22
8	P_{inf}	43	12	10	10	14
	ICP	7	8	8	9	14
P_{inf}		32 ±10 *	14 ± 4 *	13 ± 3	15 ± 6	19 ± 8
ICP		7 ±3	8 ± 3	8 ± 3	14 ± 8	15 ± 6
R_t		9.8 ±3.0 *	4.3 ±1.2 *	4.1 ±1.0	4.7 ±1.9	6.0 ±2.4

* $p < .001$

TIME (min)	LOCUS	SEP LATENCIES				
		N_6	P_{10}	N_{17}	P_{28}	N_{47}
Base	R	5.6	9.2 ± 1.1	16.2 ± 1.3	29.5± 0.7	49 ± 4.2
	L	5.9 ± 0.2	9.2 ± 0.4	16.0 ± 1.7	28	37
60	R	5.3 ± 0.2	8.9 ± 1.2	16.5 ± 1.6	29.5 ± 2.1	43 ± 6.3
	L	5.9 ± 0.2	9.1 ± 0.6	15.4 ± 2.2	29	36
120	R	5.5 ± 0.2	8.8 ± 1.2	15.7 ± 1.8	29.7 ± 1.4	44 ± 2,8
	L	6.1 ± 0.1	9.2 ± 0.7	15.3 ± 2.0	33	39
180	R	5.6	8.7 ± 1.0	16.2 ± 1.9	28.5 ± 2.1	46 ± 0.7
	L	6.0 ± 0.4	9.2 ± 0.8	16.2 ± 2.7	30	39
360	R	5.5 ± 0.2	8.8 ± 1.2	15.4 ± 1.6	29.5 ± 0.7	47 ± 1.4
	L	5.9 ± 0.2	9.2 ± 0.7	16.5 ± 1.5	33	38

Table A.39; Short and long latency components (ms) of the cat cortical SEP following forepaw stimulation during and after sham right intracerebral infusion for three hours (n = 3). Intertrial amplitude of P_{10} - N_{17} component varied between 4 and 10 uV. All data mean ± SD.

TIME (min)	LOCUS	SEP LATENCIES				
		N_6	P_{10}	N_{17}	P_{28}	N_{47}
Base	R	6.2 ± 0.6	10.0 ± 0.8	16.3 ± 1.6	30.5± 1.0	50
	L	5.9 ± 0.8	10.0 ± 0.8	16.1 ± 2.3	29.5 ± 1.0	47
60	R	6.5 ± 1.1	10.6 ± 1.0	18.5 ± 3.6	33.3 ± 2.8	46
	L	6.6 ± 0.8	10.5 ± 1.2	17.6 ± 2.9	30.3 ± 2.6	43
120	R	6.6 ± 1.1	10.8 ± 1.2	18.9 ± 3.4	31.7 ± 1.5	54
	L	6.7 ± 1.3	10.6 ± 1.4	18.8 ± 4.0	31.0 ± 2.6	48
180	R	6.7 ± 1.3	10.7 ± 1.3	19.5 ± 3.9	32.7 ± 2.5	46
	L	6.6 ± 1.5	10.6 ± 1.3	19.0 ± 3.9	30.8 ± 2.2	48
360	R	7.0 ± 1.4	10.3 ± 1.0	18.7 ± 3.2	31.5 ± 0.7	50
	L	6.8 ± 1.7	10.1 ± 1.3	17.9 ± 4.3	30.5 ± 3.5	46

Table A.40; Short and long latency components (ms) of the cat cortical SEP following forepaw stimulation during and after right intracerebral infusion with saline at 0.2 ml/hr for three hours (n = 4). Intertrial variation in P_{10}-N_{17} amplitude was 8 to 20 uV. All data mean ± SD.

TIME (min)	LOCUS	SEP LATENCIES				
		N_6	P_{10}	N_{17}	P_{28}	N_{47}
Base	R	5.7 ± 0.2	9.8 ± 0.9	16.3 ± 0.8	30.8± 2.7	46.5 ± 3.5
	L	5.5 ± 0.5	9.8 ± 0.5	16.5 ± 1.4	30.6 ± 1.6	45.5 ± 3.5
60	R	5.5 ± 0.2	10.5 ± 0.8	17.1 ± 2.4	30.3 ± 4.0	42.6 ± 5.5
	L	5.6 ± 0.4	10.2 ± 0.8	16.8 ± 3.0	30.3 ± 3.8	42.3 ± 3.8
120	R	5.7 ± 0.2	10.5 ± 1.3	16.4 ± 2.3	29.3 ± 4.9	41.0 ± 5.0
	L	5.4 ± 0.3	9.9 ± 0.9	16.1 ± 2.7	29.6 ± 4.7	45.6 ± 4.9
180	R	6.4 ± 1.4	10.8 ± 1.4	18.6 ± 3.3	30.6 ± 4.6	41.6 ± 5.6
	L	5.7 ± 0.2	10.4 ± 1.2	17.4 ± 2.6	31.5 ± 4.9	38
360	R	6.0 ± 0.4	10.0 ± 0.8	16.6 ± 1.4	26.5 ± 0.7	39
	L	6.4 ± 0.6	9.8 ± 0.2	15.8 ± 1.8	30.5 ± 1.4	42

Table A.41; Short and long latency components (ms) of the cat cortical SEP following forepaw stimulation during and after right intracerebral infusion with 20% protein solution at 0.2 ml/hr for three hours (n = 3). Intertrial variation in P_{10}-N_{17} amplitude was 5 to 15 uV. All data mean ± SD

TIME (min)	LOCUS	SEP LATENCIES				
		N_6	P_{10}	N_{17}	P_{28}	N_{47}
Base	R	6.0 ± 0.5	10.3 ± 1.2	16.6 ± 2.2	27.6± 2.9	47 ± 9.0
	L	6.0 ± 0.6	10.2 ± 0.9	16.5 ± 1.8	30.6 ± 4.6	50 ± 1.7
60	R	6.2 ± 0.5	10.6 ± 1.3	17.0 ± 2.0	27.3 ± 4.2	43 ± 4.9
	L	6.0 ± 0.4	10.6 ± 0.7	17.1 ± 1.2	29.3 ± 2.5	46 ± 2.1
120	R	6.1 ± 0.5	10.3 ± 1.2	16.3 ± 2.2	27.0 ± 3.6	44 ± 2.5
	L	6.1 ± 0.4	10.3 ± 0.6	16.4 ± 1.2	29.0 ± 2.0	45 ± 1.7
180	R	6.1 ± 0.5	10.3 ± 1.1	16.4 ± 1.5	27.0 ± 2.0	44 ± 7.6
	L	6.1 ± 0.5	10.3 ± 0.7	16.4 ± 0.9	28.7 ± 2.1	46 ± 1.0
360	R	6.0 ± 0.6	10.0 ± 1.0	15.9 ± 1.9	25.5 ± 1.9	47 ± 10
	L	6.1 ± 0.7	10.2 ± 1.3	16.0 ± 2.0	26.0 ± 1.4	44 ± 4 3

Table A.42; Short and long latency components (ms) of the cat cortical SEP following forepaw stimulation during right intracerebral infusion with 5000 ng/ml bradykinin solution for three hours at 0.2 ml/hr and at six hours after commencement of the infusion (n = 6). All data mean ± SD.

TIME (min)	LOCUS	SEP LATENCIES				
		N_6	P_{10}	N_{17}	P_{28}	N_{47}
Base	R	6.0 ± 0.6	10.2 ± 1.2	16.2 ± 1.8	28.5± 4.7	43 ± 5.8
	L	6.0 ± 0.3	9.8 ± 1.3	16.2 ± 2.4	28.0 ± 1.6	48 ± 4.3
60	R	5.7 ± 0.3	10.3 ± 1.6	16.8 ± 2.9	29.5 ± 2.4	47 ± 7.9
	L	5.7 ± 0.2	9.6 ± 1.1	16.0 ± 2.1	29.7 ± 2.9	47 ± 8.4
120	R	5.8 ± 0.5	9.9 ± 1.2	16.3 ± 2.5	28.8 ± 3.5	49 ± 5.9
	L	5.8 ± 0.3	9.5 ± 1.0	15.6 ± 2.1	29.7 ± 3.8	47 ± 7.6
180	R	5.6 ± 0.3	9.8 ± 1.2	16.2 ± 2.3	26.7 ± 3.5	43 ± 3.0
	L	6.1 ± 0.6	9.6 ± 1.1	15.7 ± 2.2	28.8 ± 3.8	49 ± 5.2
360	R	5.7 ± 0.3	10.1 ± 1.2	16.6 ± 2.6	29.0 ± 2.8	47 ± 8.1
	L	5.8 ± 0.6	9.5 ± 1.2	15.6 ± 2.3	28.0 ± 2.2	48 ± 1.3

Table A.43; Short and long latency components (ms) of the cat cortical SEP following forepaw stimulation during right intracerebral infusion with arachidonic acid solution (2 - 15 mg/ml) mg/ml) for three hours at 0.2 ml/hr and at six hours after commencement of the infusion (n = 6). All data mean ± SD

TIME (min)	LOCUS	SEP LATENCIES					
		N_6	P_{10}	N_{17}	P_{28}	N_{47}	P_{60}
Base	R	5.2	10.0	16.0	29.0	42	-
	L	5.2	9.6	16.0	29.0	45	60
60	R	5.2	8.4	14.8	28.5	43	64
	L	4.8	8.4	14.6	27.7	44	-
120	R	4.4	8.8	14.4	26.8	38	54
	L	5.2	9.2	14.4	25.7	46	-
180	R	4.8	8.8	14.8	25.5	39	59
	L	5.2	8.8	14.4	25.8	45	51
360	R	4.8	8.8	14.6	24.0	36	57
	L	4.8	8.4	12.8	25.0	-	-

Table A.44: Short and long latency components (ms) of the cat cortical SEP following forepaw stimulation during right intracerebral infusion with oligodendroglioma cyst fluid for three hours at 0.2 ml/hr and at six hours after commencement of the infusion (n = 1).

TIME (min)	LOCUS	SEP LATENCIES				
		N_6	P_{10}	N_{17}	P_{28}	N_{47}
Base	R	5.6	9.6 ± 0.6	16.8	29.5 ± 0.7	58
	L	5.6	9.4 ± 0.3	16.8 ± 0.6	29.7 ± 0.7	50
60	R	6.1 ± 0.4	10.0	16,6 ± 0.3	29.5 ± 2.1	-
	L	5.8 ± 0.3	9.8 ± 0.3	17.2 ± 0.6	30.3 ± 0.7	45
120	R	5.4 ± 0.7	9.6	16.2 ± 0.3	31.0 ± 2.1	50
	L	5.4 ± 0.3	9.4 ± 0.3	16.0	30.0	46
180	R	5.6	9.8 ± 0.3	17.0 ± 0.8	30.0 ± 0.7	48
	L	5.4 ± 0.3	9.4 ± 0.3	16.6 ± 0.3	31.0 ± 0.7	48
360	R	6.0	10.8	18.6 ± 0.3	31.5 ± 2.1	52
	L	5.5 ± 0.1	9.9 ± 0.4	16.0 ± 1.1	31.5 ± 2.1	52 + 5

Table A.45: Short and long latency components (ms) of the cat cortical SEP following forepaw stimulation during right intracerebral infusion with anaplastic astrocytoma cyst fluid (JH) for three hours at 0.2 ml/hr and at six hours after commencement of the infusion (n = 2). Data ± SD.

TIME (min)	LOCUS	SEP LATENCIES				
		N_6	P_{10}	N_{17}	P_{28}	N_{47}
Base	R	5.8 ± 0.3	10.0 ± 1.7	17.4 ± 1.7	27.6 ± 0.7	38
	L	6.4 ± 0.6	10.2 ± 1.4	17.6 ± 1.4	28.5 ± 0.8	45
60	R	5.6	10.2 ± 0.3	16.4	27.2 ± 1.4	39
	L	6.2 ± 0.3	10.0 ± 0.6	16.6 ± 0.3	30.0 ± 1.6	41 ± 4
120	R	5.4 ± 0.3	10.0 ± 0.6	15.6 ± 0.6	25.5 ± 2.1	40 ± 2
	L	5.6	9.6 ± 0.6	15.8 ± 0.8	28.5 ± 2.8	40 ± 3
180	R	5.6	10.0 ± 0.6	15.8 ± 0.8	26.0 ± 2.7	50 ± 3
	L	5.6 ± 0.6	9.4 ± 0.3	15.2	27.0 ± 1.6	38
360	R	6.2 ± 0.3	10.0 ± 0.6	16.4 ± 1.7	26.5 ± 1.5	40 ± 2
	L	5.8 ± 0.3	10.2 ± 0.8	17.0 ± 0.6	30.5 ± 0.8	42

Table A.46: Short and long latency components (ms) of the cat cortical SEP following forepaw stimulation during right intracerebral infusion with glioblastoma cyst fluid (GD) for three hours at 0.2 ml/hr and at six hours after commencement of the infusion (n = 2). Data ± SD.

TIME (min)	LOCUS	SEP LATENCIES				
		N_6	P_{10}	N_{17}	P_{28}	N_{47}
Base	R	5.2 ± 0.6	9.0 ± 0.8	14.7 ± 0.3	27.0 ± 1.4	48 ± 4
	L	5.4 ± 0.3	9.0 ± 0.3	15.2 ± 1.7	29.0 ± 1.4	48 ± 7
60	R	5.2 ± 0.6	9.2 ± 0.8	15.2	28.0	47 ± 6
	L	6.2 ± 0.8	9.8 ± 1.7	15.7 ± 0.1	30.0	47 ± 6
120	R	5.6	9.5 ± 0.6	14.5 ± 0.4	29.0 ± 2.8	49
	L	5.6	9.5 ± 0.1	14.9 ± 0.1	29.0 ± 1.4	48
180	R	5.2	9.4 ± 0.3	15.6	27.5 ± 0.2	48 ± 6
	L	5.4 ± 0.3	9.7 ± 0.1	14.4 ± 0.6	28.5 ± 4.2	48
360	R	5.0 ± 0.8	9.0 ± 2.0	15.4 ± 2.5	29.0	50 ± 4
	L	6.1 ± 0.7	9.2 ± 1.1	15.2 ± 1.7	27.5 ± 2.0	51 ± 4

Table A.47: Short and long latency components (ms) of the cat cortical SEP following forepaw stimulation during right intracerebral infusion with glioblastoma cyst fluid (EB) for three hours at 0.2 ml/hr and at six hours after commencement of the infusion ($n = 2$). Data ± SD.

Table A.48: Latencies (ms) and amplitudes (uV) of the major components of the MEP recorded in the low thoracic region following unilateral transcranial stimulation three hours after completion of sham infusion into the right frontal centrum ovale. The amplitude is derived from the N_1-P_1 component.

Cat	Side	N_1	N_2	N_3	Amplitude
1	R	2.80	3.28	3.76	120
	L	2.80	3.32	3.84	120
2	R	2.76	3.56	5.76	35
	L	2.86	3.60	5.24	12

Table A.49; Latencies (ms) and amplitudes (uV) of the major components of the MEP recorded in the low thoracic region following unilateral transcranial stimulation three hours after completion of saline infusion into the right frontal centrum ovale. The amplitude is derived from the N_1-P_1 component.

Cat	Side	N_1	N_2	P_2	N_3	Amplitude
1	R	3.16	3.36	3.64	4.68	20
	L	3.16	3.32	3.56	4.64	6
2	R	2.60	3.28	4.32		12
	L	2.56	3.40	4.24		10

Table A.50: Latencies (ms) and amplitudes (uV) of the major components of the MEP recorded in the low thoracic region following unilateral transcranial stimulation three hours after completion of 20% protein infusion into the right frontal centrum ovale. The N_1 amplitude is derived from the N_1-P_1 component.

Cat	Side	N_1	P_1	N_2	N_3	N_4	Amp
1	R	2.48	2.76	3.20	4.32	6.44	75
	L	2.52	2.76	3.16	4.36	6.60	75
2	R	2.60	2.92	3.28	-	-	15
	L	2.56	2.84	3.40	-	-	15

Table A.51: Latencies (ms) and amplitudes (uV) of the major components of the MEP recorded in the low thoracic region following unilateral transcranial stimulation three hours after completion of bradykinin infusion into the right frontal centrum ovale. The N_1 amplitude is derived from the N_1-P_1 component. Cats 1 - 4 bradykinin 5000 ng /ml infusion, cat 5 bradykinin 150 ug/ml infusion.

Cat	Side	N_1	P_1	N_2	N_3	N_4	Amp
1	R	2.95	3.23	3.60	4.05	4.65	8
	L	2.95	3.20	3.60	-	4.70	8
2	R	2.88	3.08	4.00	-	-	7
	L	2.88	3.12	4.30	-	-	7
3	R	2.40	2.60	2.80	3.20	3.64	30
	L	2.40	2.68	2.80	3.40	3.80	30
4	R	2.60	2.92	3.28	4.68	6.36	25
	L	2.56	2.84	3.40	4.92	6.88	25
5	R	2.52	2.72	3.28	4.36	6.56	100
	L	2.52	2.76	3.28	4.24	6.60	90

Table A.52: Latencies (ms) and amplitudes (uV) of the major components of the MEP recorded in the low thoracic region following unilateral transcranial stimulation three hours after completion of arachidonic acid infusion into the right frontal centrum ovale. The N_1 amplitude is derived from the P_1-N_1 component. Cats 1 - 3 arachidonic acid 10 mg/ml infusion, cat 4 arachidonic acid 15 mg/ml infusion.

Cat	Side	N_1	P_1	N_2	N_3	N_4	Amp
1	R	2.40	2.80	3.16	3.64	4.68	60
	L	2.36	2.72	3.16	3.68	5.04	60
2	R	2.16	2.32	2.60	2.80	-	40
	L	2.16	2.32	2.56	2.76	-	40
3	R	2.36	2.76	3.12	3.64	-	8
	L	2.32	2.72	3.12	3.52	-	8
4	R	2.24	2.52	2.70	3.08	3.56	50
	L	2.24	2.52	2.76	3.08	3.56	50

Table A.53: Latencies (ms) and amplitudes (uV) of the major components of the MEP recorded in the low thoracic region following unilateral transcranial stimulation three hours after completion of human glioma cyst fluid infusion into the right frontal centrum ovale. The N_1 amplitude is derived from the P_1-N_1 component. Cat prefix refers to tumour type and patient from which extracted. Cat JH-AA * MEP recorded from T_6 region.

Cat	Side	N_1	P_1	N_2	N_3	N_4	Amp
GBM-GD	R	2.64	3.16	-	-	-	8
	L	2.44	2.76	-	-	-	8
GBM-GD	R	2.92	3.40	3.72	4.04	4.92	50
	L	2.80	3.08	3.40	4.28	4.76	50
JH-AA	R	2.52	-	3.08	3.36	3.92	100
	L	2.52	-	3.12	3.40	4.00	100
JH-AA*	R	2.12	2.84	3.56	6.08	-	40
	L	2.12	2.84	3.56	6.08	-	40
GBM-EB	R	2.80	-	-	-	6.16	300
	L	2.80	-	-	-	6.16	300
GBM-EB	R	2.88	-	3.20	-	5.64	200
	L	2.84	-	3.24	-	5.72	200
TF-OLI	R	2.28	2.64	3.04	3.44	3.68	60
	L	2.28	2.60	3.04	3.44	3.68	200

Table 3.54: rCBF (ml/100 g brain/min) before and during the course of sham infusion with corresponding P_aCO_2 values (n = 3). All data mean + SD.

TIME (min)		INFUSED (R) HEMISPHERE	CONTROL (L) HEMISPHERE	P_aCO_2 (mmHg)
0	Frontal	26 ± 6	28 ± 5	32.6 ± 3.0
	Parietal	36 ± 5	38 ± 18	
60	Frontal	32 ± 6	31 ± 11	35.6 ± 0.6
	Parietal	50 ± 8	42 ± 17	
120	Frontal	28 ± 6	32 ± 6	37.0 ± 4.0
	Parietal	46 ± 6	44 ± 6	
180	Frontal	29 ± 10	29 ± 7	35.2 ± 1.0
	Parietal	43 ± 3	40 ± 12	

Table A.55: rCBF (ml/100 g brain/min) before and during R frontal 0.2 ml/hr saline infusion, with corresponding P_aCO_2 (n = 3). All data mean ± SD.

TIME (min)		INFUSED (R) HEMISPHERE	CONTROL (L) HEMISPHERE	P_aCO_2 (mmHg)
0	Frontal	38 ± 10	48 ± 10	32.0 ± 1.0
	Parietal	37 ± 12	44 ± 12	
60	Frontal	47 ± 11	42 ± 9	33.2 ± 2.0
	Parietal	48 ± 11	50 ± 7	
120	Frontal	38 ± 9	34 ± 9	34.6 ± 1.5
	Parietal	47 ± 3	43 ± 3	
180	Frontal	38 ± 10	35 ± 12	31.6 ± 1.5
	Parietal	42 ± 6	41 ± 9	

Table A.56: rCBF (ml/100 gm brain/min) during three hours of intracerebral infusion with 20% protein infusion at 0.2 ml/hr in the cat (n=7). All data mean ± SD.

TIME (min)		INFUSED (R) HEMISPHERE	CONTROL (L) HEMISPHERE	P_aCO_2 (mmHg)
0	Frontal	42 ± 16	38 ± 5	31 ± 3.6
	Parietal	47 ± 16	36 ± 10	
60	Frontal	49 ± 16	44 ± 14	32 ± 1.9
	Parietal	48 ± 11	45 ± 18	
120	Frontal	49 ± 12	48 ± 18	32 ± 3.2
	Parietal	53 ± 13	48 ± 19	
180	Frontal	46 ± 13	49 ± 18	34 ± 3.7
	Parietal	48 ± 12	48 ± 18	

Table A.57; rCBF (ml/100 g brain/min) during three hours of R frontal infusion with 5000 ng/ml bradykinin solution at an infusion rate of 0.2 ml/hr im the cat (n = 6). All data mean ± SD.

TIME (min)		INFUSED (R) HEMISPHERE	CONTROL (L) HEMISPHERE	P_aCO_2 (mmHg)
0	Frontal	43 ± 23	42 ± 22	34 ± 2.6
	Parietal	39 ± 15	52 ± 14	
60	Frontal	41 ± 16	39 ± 18	34 ± 1.9
	Parietal	36 ± 15	50 ± 15	
120	Frontal	44 ± 16	37 ± 16	35 ± 1.7
	Parietal	37 ± 10	53 ± 14	
180	Frontal	41 ± 13	40 ± 12	34 ± 1.4
	Parietal	35 ± 9	52 ± 18	

Table A.58: rCBF (ml/100 g brain/min) during three hours of intracerebral infusion with arachidonic acid solution (2-15 mg/ml) at an infusion rate of 0.2 ml/hr in the cat (n = 6). Mean BP ranged from 114 to 122 mmHg during the period of infusion. All data mean ± SD.

TIME (min)		INFUSED (R) HEMISPHERE	CONTROL (L) HEMISPHERE	P_aCO_2 (mmHg)
0	Frontal	48 ± 8	52 ± 22	34 ± 3.0
	Parietal	50 ± 17	51 ± 11	
60	Frontal	47 ± 14	45 ± 16	34 ± 1.3
	Parietal	55 ± 13	49 ± 13	
120	Frontal	55 ± 17	50 ± 20	35 ± 2.0
	Parietal	60 ± 16	50 ± 15	
180	Frontal	43 ± 10	43 ± 14	35 ± 1.3
	Parietal	54 ± 20	55 ± 16	

Table A.59: rCBF (ml/100 g brain/min) during three hours of intracerebral infusion with glioblastoma cyst fluid (GD) at an infusion rate of 0.2 ml/hr in the cat (n = 2). Mean BP ranged from 110 to 138 mmHg during the period of infusion. All data mean ± SD.

TIME (min)		INFUSED (R) HEMISPHERE	CONTROL (L) HEMISPHERE	P_aCO_2 (mmHg)
0	Frontal	49 ± 7 *	50 ± 14	34 ± 1.8
	Parietal	50 ± 17	-	
60	Frontal	45 ± 8	40 ± 9	34 ± 2.8
	Parietal	51 ± 16	-	
120	Frontal	39 ± 4	46 ± 20	32 ± 1.7
	Parietal	54 ± 28	-	
150	Frontal	26 + 3	41 + 14	32
	Parietal	31 + 15	-	
180	Frontal	19 ± 4 *	39 ± 15	34 ± 1.7
	Parietal	40 ± 19	-	

* $p < .001$

Table A.60: rCBF (ml/100 g brain/min) during three hours of intracerebral infusion with anaplastic astrocytoma cyst fluid (JH) at an infusion rate of 0.2 ml/hr in the cat (n = 2). Mean BP ranged from 110 to 150 mmHg during the period of infusion. All data mean ± SD

TIME (min)		INFUSED HEMISPHERE	CONTROL HEMISPHERE	P_aCO_2 (mmHg)
0	Frontal	39 ± 7	47 ± 5	35 ± 3.3
	Parietal	30 ± 7	37 ± 3	
60	Frontal	32 ± 12	41 ± 6	33 ± 1.4
	Parietal	25 ± 2	29	
120	Frontal	32 ± 8	48 ± 7	33 ± 1.4
	Parietal	32 ± 2	30	
180	Frontal	34 ± 2	63 ± 6	32 ± 1.7
	Parietal	34 ± 14	22	

Table A.61: rCBF (ml/100 g brain/min) during three hours of intracerebral infusion with anaplastic astrocytoma cyst fluid (EB) at an infusion rate of 0.2 ml/hr in the cat (n = 2). Mean BP ranged from 110 to 138 mmHg during the period of infusion. All data mean ± SD

TIME (min)		INFUSED HEMISPHERE	CONTROL HEMISPHERE	P_aCO_2 (mmHg)
0	Frontal	41 ± 6 *	43 ± 5 **	34 ± 1.8
	Parietal	41 ± 10	63 ± 9	
60	Frontal	32 ± 4	38 ± 7	34 ± 2.8
	Parietal	36 ± 12	55 ± 14	
120	Frontal	31 ± 1	30 ± 5	32 ± 1.7
	Parietal	36 ± 8	52 ± 12	
180	Frontal	30 ± 3 *	30 ± 11 **	34 ± 1.7
	Parietal	40 ± 4	57 ± 18	

* $p = 0.003$ ** $p = 0.018$

Table A.62: rCBF (ml/100 g brain/min) during three hours of intracerebral infusion with oligodendroglioma cyst fluid (TF) at an infusion rate of 0.2 ml/hr in the cat (n =1). Mean BP ranged from 110 to 138 mmHg during the period of infusion. All data mean ± SD.

TIME (min)		INFUSED HEMISPHERE	CONTROL HEMISPHERE	P_aCO_2 (mmHg)
0	Frontal	38 ± 9	40 ± 10	34 ± 1.8
	Parietal	44 ± 3	67 ± 5	
60	Frontal	66 ± 1	61 ± 16	35
	Parietal	90	78	
120	Frontal	69 ± 4	93 ± 20	30
	Parietal	89	101	
180	Frontal	38 ± 13	46 ± 19	32
	Parietal	59	77	

Table A.63; Frontal white matter CBF (ml/100g brain/min) during right intracerebral infusion with 20% protein solution at a rate of 0.2 ml/hr in the cat (n = 4). All data mean ± SD.

TIME (min)	INFUSED (R) HEMISPHERE	CONTROL (L) HEMISPHERE	P_aCO_2 (mmHg)
0	21 ±3.5	20 ±5.6	31 ± 3.6
60	21 ±2.1	17 ±3.6	32 ± 1.9
120	19 ±3.5	16 ±3.6	32 ± 3.2
180	17 ±3.9	18 ±3.1	34 ± 3.7

Table A.64; Frontal and parietal white matter CBF_w (ml/100 g brain/min) during intracerebral infusion with arachidonic acid solution (10 mg/ml) at a rate of 0.2 ml/hr in the cat (n = 5). All data mean ± SD

TIME (min)		INFUSED (R) HEMISPHERE	CONTROL (L) HEMISPHERE	P_aCO_2 (mmHg)
0	Frontal	17 ±4.0	19 ±2.8	34.4 ± 3.0
	Parietal	16 +1.4	17 +5.4	
60	Frontal	22 ±2.2	17 ±2.1	34.2 ± 1.3
	Parietal	14 +1.0	19	
120	Frontal	18 ±3.9	18 ±2.1	34.8 ± 2.0
	Parietal	14 +2.0	13	
180	Frontal	19 ±4.8	20 ±4.0	34.8 ± 1.3
	Parietal	15 +2.0	21	

Table A.65: CBF CO_2 reactivity following right frontal infusion with 0.6 ml of arachidonic acid solution (2.5 - 15 mg/ml) was expressed by the following equations (derived from linear regression analysis of CBF and CO_2 data). Correlation coefficients and levels of significance are also listed.

1 R Frontal	$CBF = 0.85\ P_aCO_2 + 9.2$	
	$n = 22$ $r = 0.58$	$0.01 > p > 0.001$
2 L Frontal	$CBF = 1.36\ P_aCO_2 - 1.9$	
	$n = 30$ $r = 0.60$	$p < 0.001$
3 R Parietal	$CBF = 1.01\ P_aCO_2 + 17.9$	
	$n = 18$ $r = 0.70$	$p < 0.001$
4 L Parietal	$CBF = 0.77\ P_aCO_2 + 26.1$	
	$n = 14$ $r = 0.75$	$p < 0.001$

Table A.66: CBF_w reactivity to changes in P_aCO_2 following right frontal intracerebral arachidonic acid infusion was expressed by the following equations and correlation coefficients (derived from linear regression analysis of CBF and CO_2 data).

1 R Frontal	$CBF_w = 0.31\ P_aCO_2 + 7.6$	
	$n = 22$ $r = 0.60$	$p < 0.001$
2 L Frontal	$CBF_w = 0.63\ P_aCO_2 + 1$	
	$n = 12$ $r = 0.77$	$0.01 > p > 0.001$
3 R Parietal	$CBF_w = 0.58\ P_aCO_2 + 5.2$	
	$n = 8$ $r = 0.87$	$0.01 > p > 0.001$
4 L Parietal	$CBF_w = 0.51\ P_aCO_2 - 0.2$	
	$n = 12$ $r = 0.79$	$0.01 > p > 0.001$

Table A.67: CBF CO_2 reactivity at four different loci, following right intracerebral 20% protein infusion was expressed by the following equations and correlation coefficients (derived from linear regression analysis).

1 R Frontal	$CBF = 0.571\ P_aCO_2 + 33.9$		
	$n = 30$	$r = 0.35$	$p = NS$
2 L Frontal	$CBF = 0.431\ P_aCO_2 + 32.8$		
	$n = 20$	$r = 0.32$	$p = NS$
3 R Parietal	$CBF = 0.42\ P_aCO_2 + 39.7$		
	$n = 17$	$r = 0.30$	$p = NS$
4 L Parietal	$CBF = 0.636\ P_aCO_2 + 29$		
	$n = 11$	$r = 0.34$	$p = NS$

Table A.68: CBF CO_2 reactivity at four different loci, following right frontal infusion with 0.6 ml of 5000 ng/ml bradykinin solution was expressed by the following equations and correlation coefficients (derived from linear regression analysis).

R Frontal	$CBF_g = 0.57\ P_aCO_2 + 13$	$n = 27$	$r = 0.33$	$0.1 > p > 0.05$
L Frontal	$CBF_g = 0.32\ P_aCO_2 + 29$	$n = 25$	$r = 0.14$	$p > 0.1$
R Parietal	$CBF_g = 0.005\ P_aCO_2 + 27$	$n = 24$	$r = 0.007$	$p > 0.1$
L Parietal	$CBF_g = 0.71\ P_aCO_2 + 23$	$n = 28$	$r = 0.32$	$p > 0.1$

Table A.69: CBF CO_2 reactivity, adjacent to and contralateral to the right frontal infusion site, following infusion of glioma cyst fluid was expressed by the following equations and correlation coefficients.

Tumour			
	RIGHT FRONTAL		
GD-GBM	$CBF = 0.29\ P_aCO_2 + 18$	$n = 13,$	$r = 0.24,$	$p =$ NS
EB-GBM	$CBF = 0.42\ P_aCO_2 + 11$	$n = 16,$	$r = 0.81,$	$p < 0.001$
JH-AA	$CBF = 0.13\ P_aCO_2 + 20$	$n = 16,$	$r = 0.14,$	$p =$ NS
TF-Oligo	$CBF = 2.25\ P_aCO_2 - 32$	$n = 9,$	$r = 0.96,$	$p < 0.001$
	LEFT FRONTAL		
GD-GBM	$CBF = 1.05\ P_aCO_2 + 3$	$n = 16,$	$r = 0.86,$	$p < 0.001$
EB-GBM	$CBF = 0.36\ P_aCO_2 + 12$	$n = 16,$	$r = 0.56.$	$p < 0.05$
JH-AA	$CBF = 2.34\ P_aCO_2 - 21$	$n = 10,$	$r = 0.97,$	$p < 0.001$
TF-Oligo	$CBF = 2.72\ P_aCO_2 - 33$	$n = 10,$	$r = 0.91,$	$p < 0.001$